EVALUATION OF INTERLOCKING CONCRETE BLOCK PAVEMENT WITH RECYCLED MATERIALS BASED ON EXPERIMENTAL AND FINITE ELEMENT ANALYSIS

By XINYUE NI, B.E.

A Thesis Submitted to the School of Graduate Studies in Partial Fulfilment of the Requirements for the Degree Master of Applied Science

INTERLOCKING CONCRETE PAVEMENT WITH RECYCLED MATERIALS

DESCRIPTIVE NOTE

McMaster University MASTER OF APPLIED SCIENCE (2022) Hamilton, Ontario (Civil Engineering)

TITLE: Evaluation of Interlocking Concrete Block Pavement with Recycled Materials Based on Experimental and Finite Element Analysis AUTHOR: Xinyue Ni, B. E. SUPERVISOR: Professor S.L. Tighe NUMBER OF PAGES: XIII, 101

ABSTRACT

To address the challenges associated with urban expansion and environmental changes, innovative interlocking concrete block pavement (ICBP) is being researched for usage in urban areas. The ICBP is designed to have higher durability and better long-term performance compared to traditional asphalt pavement. Using recycled concrete aggregates (RCA) and supplementary cementing materials (SCMs) can provide many environmental benefits. The objective of this research is to investigate the mechanical properties of concrete with recycled materials. This also involves the assessment of deflection and stresses associated with ICBP using the finite element method.

Four concrete mixtures with different RCA and SCMs contents were designed and cast. The RCA replacement levels were 20% and 40%, while slag and glass pozzolan were added to improve mechanical properties. The results showed that the use of RCA had adverse impacts on workability. The 28 days compressive strength of the Control Mix was 40 MPa. The compressive strength of Mix 3 was 40.5 MPa which was the highest strength among all mixtures. It demonstrated that 40% RCA replacement level could have non-negative effect on mechanical properties when the SCMs are added.

A three-dimensional pavement model was established using ABAQUS software. The orthogonal experimental design was used to evaluate the effects of the length/width ratio of blocks, the block thickness, the elastic modulus, and the laying pattern of blocks on the deflection and von Mises stress of all ICBP models under the vertical load. Considering the deflection of loading area, the length/width ratio had the greatest effect, then comes with thickness, elastic modulus, and laying pattern according to the Range Analysis. The bigger block size and higher elastic modulus of blocks could provide even better performance. Overall, the herringbone laying pattern is recommended as the optimum laying pattern with minimum deflection. It also contributes to better load spreading.

ACKNOWLEDGEMENTS

I would like to thank my supervisor, Professor Susan Tighe, for her unconditional support and love throughout my study. I highly appreciate the opportunity that she gave to me, which changed my entire life. She is not only a supervisor but also a mentor, and what I learned from her in the past three years will benefit me forever.

I would like to thank my thesis committee members: Professor Saiedeh Razavi and Professor Georgios Balomenos.

I would also like to thank the City of Toronto and SideWalk Lab company for funding this research project. Appreciation is also extended to The Miller Group and PSI Technologies for the supply of research materials and testing performance. Many thanks are also extended to Dr. Vimy Henderson, Dr. Daniel Pickel and Mathias Cawthra for their help and support.

I would also like to express my thanks to Dr. Hanaa Al-Bayati and Dr. Seyedata Nahidi for their guidance and unlimited help. I also want to thank my laboratory partner Shreenita Chhetri for working through this research project together.

I would like to thank Dr. Frank Yang Liu for his unconditional help, support, and advice throughout my study.

I would extend my appreciation to all my colleagues in CPATT for their kind support, Dr. Guangyuan Zhao, Dr. Fank Mi-Way Ni, Ali Qabur, Jonathan Zingaro, Tianshu Zhang, Peggie Danrong Wang, Rob Aurilio, Dandi Zhao, Abdulrahman Hamid, Tamanna Kabir, Abimbola Grace Oyeyi, Paula Barbi, Jessica Achebe, Hui Liao, Haya Almutairi, Shenglin Wang, and Saeid Salehiashani.

I would also like to express thanks to my friends, Erin Edward, Brittney Lato and Alexis Lato for their consistent trust, support, and company in the past two and half years. Many thanks are also extended to Margarete Wei and Yuqi Tang for supporting me all the time.

Finally, I would like to thank my parents, my grandparents and my big family for their love and support. Being apart from them for three years was hard and I miss them so much.

CONTENTS

LIST OF FIGURES

LIST OF TABLES

LIST OF ABBREVIATIONS

AASHTO………….. American Association of State Highway and Transportation Officials
ACI…………………………………………………………American Concrete Institute
ASCE…………………………………….…………American Society for Civil Engineers
ASTM ……………………………………………American Society for Testing Materials
BPN ………………………………………………………British Pendulum Number
CRA…………………………………….…………………Coarse Recycled Aggregates
CSA……………………………………………….………Canadian Standard Association
FEA ……………………………………….…...……………Finite Element Analysis
FEM…………………………………………….………...…….. Finite Element Method
FWD …………………………………………………….……..Falling Weight Deflectometer
GUL…………………………………………….….……….....General Use Limestone
HIE…………………………………………..………………..... Heat Island Effects
ICBP ………………………………………………Interlocking Concrete Block Pavement
ICPI………………………………………….. Interlocking Concrete Pavement Institute
IEA …………………………………………………………..International Energy Agency
IEEE …………………………………the Institute of Electrical and Electronics Engineers
IHCB…………………………………………….....Interlocking Hollow Concrete Block
LCC …………………………………………………..……………Life Cycle Cost
ITZ…………………………………………………….…. Interfacial Transition Zone
LTE……………………………………………………..…..Load Transfer Efficiency
LWD ………………………………………………………Light Weight Deflectometer
MTO ………………………………………………..Ministry of Transportation of Ontario
NRN…………………………………………………..………National Road Network
OA……………………………………………….………...………. Orthogonal Array
OPSS…………………………………………Ontario Provincial Standard Specification
RCA…………………………………………………….……Recycled Concrete Aggregates
SCMs……………………...……………………Supplementary Cementing Materials
TSMA…………………………………………...……Two-Stage Mixing Approach

DECLARATION OF ACADEMIC ACHIEVEMENT

I declare that I am the sole author of this thesis. This is a true copy of the thesis, including any required final revisions, as accepted by my examiners.

I understand that my thesis may be made electronically available to the public.

Chapter 1 INTRODUCTION

1.1 Background

With the rapid rate of global urbanization, there are not only economic development challenges but also socioeconomic issues, such as profound social instability, disease spreading, potential water crises, and risks to critical urban infrastructure, resulting from the increased population (World Economic Forum 2018). In this regard, the development of urban infrastructure should be consistent with both functionality and sustainability with the increased demand and need to design to mitigate environmental damage.

In cities, roads are the major mode of transportation for bicyclists and vehicular traffic. Urban road infrastructure provides adequate service levels to road users and covers 10% to 20% surface of the city area and even 40% in city centers (Marović et al. 2018). According to the National Road Network (NRN), there are more than 1.23 million kilometres of roads including 38,000 kilometres of highways in Canada by the end of 2017 (NRN 2022). As an integral part of urban infrastructure, pavements are expected to become multi-role assets to meet future requirements. However, most conventional asphalt pavement in cities is significantly affected by environmental and traffic factors. The consequential changes like increased maximum temperature, increased frequency and intensity of rainfall, and higher solar radiation caused by climate change tend to accelerate flexible pavement deterioration (Dawson 2014). Qiao et al. reported that a 5% in temperature and temperature variation would result in a 20% reduction in regard to longitudinal cracking and rutting of asphalt pavement (Qiao et al. 2013). Furthermore, the performance deterioration will result in increased maintenance costs and even affect total Life Cycle Costs (LCC). The dark heat-absorbent surface of asphalt pavement is also a critical factor contributing to Heat Island Effects (HIE) in cities. The surface temperature of asphalt pavement in a summer climate can be upwards of 60°C, which facilitates heat transfer from the ground to the air (Mohajerani, Bakaric, and Jeffrey-Bailey 2017).

To address the challenges associated with urban expansion and environmental changes, the interlocking concrete block pavement system is being researched for urban road infrastructure. In the early 1970s, concrete pavers came to North America from Europe. The total sales of segmental concrete paver products were 749 million square feet in North America in 2019 according to the Interlocking Concrete Pavement Institute (ICPI) (ICPI 2020a). The concrete pavers are less sensitive to temperature, moisture, and other environmental factors, thus the Interlocking Concrete Block Pavement (ICBP) has higher durability and better long-term performance. However, it is notable that they are primarily used for low-volume roads. Also worth noting is that the ICBP has high resistance to freeze-thaw which is a critical property when this technology is applied in the Canadian weather context. The maintenance and repair of ICBP are efficient and low-cost for some applications.

At the same time, materials consumption in pavement construction and the carbon emission from cement are other two important environmental issues. Over the past 20 years, 3.4 billion tonnes of aggregate have been consumed in Ontario, Canada. It is expected that the average consumption of aggregate will increase to around 192 million tonnes per year, 13% higher than the past in the next 20 years. Roads, both new and repair work, account for the biggest consumption of aggregate in construction work. According to the Ministry of Transportation (MTO), 20 million tonnes of aggregate will be needed for construction projects (Ministry of Natural Resources 2016). Additionally, the manufacturing of concrete is responsible for air pollution because of cement production. The carbon emission from cement production makes up 8% of the world's emissions (Lehne and Preston 2018).

To alleviate these issues, recycled materials, recycled concrete aggregates (RCA) and supplementary cementing materials (SCMs), are proposed in the work. RCA is a product recycled from construction, and demolition waste. The use of RCA can reduce both the consumption of natural aggregates and the landfill problems. The SCMs, such as fly ash, slag, silica fume, and glass pozzolan, are commonly used to replace cement in concrete production. Using these industry by-products helps to reduce the cement consumption, hence, the air pollution from that.

However, limited research has been done to incorporate recycled materials with newly designed ICBP for use in Canada. Like other pavements, the evaluation of ICBP involves laboratory and field tests. This research focused on evaluating laboratory performance followed by numerical modelling of different concrete block layer designs. The numerical simulation analysis is an evaluation method to understand ICBP's mechanical behaviour before launching a field study. The finite element method (FEM) allows the realistic simulation of ICBP's discontinuous surface and the nonlinearity of materials behaviour. The mechanical behaviour of ICBP with recycled materials was evaluated based on both experimental and finite element analysis in this study.

1.2 Research Objectives

The overall objective of this proposed research is to investigate the effects of using the RCA and SCMs to replace natural aggregates and cement on concrete properties and evaluate the mechanical performance of ICBP with different block layer designs. The main objectives of this research are as follows:

- Develop the concrete mix design with different RCA replacement levels (0%, 20%, 40%) and different SCMs content (Slag: 0%, 20%; Glass Pozzolan: 0%, 10%).
- Determine the effects of using the RCA and SCMs on concrete properties which include fresh properties (slump, air content, density), compressive strength and modulus of elasticity.
- Use the orthogonal experimental design to evaluate the effects of the length/width ratio of rectangular concrete blocks, the block thickness, the elastic modulus, and the laying pattern of blocks on the mechanical performance of ICBP.
- Develop the ICBP models with different block layer designs according to Ontario Provincial Standard Specification in ABAQUS.
- Investigate the effects of four factors based on the deflection and von Mises Stress of all ICBP models under the vertical load in ABAQUS.

1.3 Significance of Research

The development of an urban pavement system is critical to addressing the challenges of global urbanization. The use of ICBP in the southern Canadian environment brings potential sustainability, durability, and economical benefits. The sustainability of ICBP can be improved by applying recycled materials. Using recycled materials in concrete production helps to reduce material consumption, landfill problems, and carbon emissions.

However, ICBP is not commonly applied for traffic roads even though it can be seen in parking lots, parks, and sidewalks in cities. With the special structure, the evaluation of this type of pavement is complicated when various traffic loads are applied. Similar to flexible and rigid pavements, laboratory tests, fieldwork and construction practices are needed. As a part of the project collaborated with the SideWalk Lab company and the City of Toronto, this research includes some laboratory tests and numerical simulation analysis.

This research combined the ICBP context with recycled materials for the traffic road application. The significance comes from the concrete mix design development, the use of RCA and SCMs, and evaluations of machinal performances with different ICBP structural designs.

1.4 Thesis Arrangement

This thesis is organized into six chapters with the following contents:

Chapter 1: This chapter introduces the background of ICBP, the objectives, and the significance of this research.

Chapter 2: This chapter provides a comprehensive review of the ICBP system, current applications in Canada, concrete compressive performance, numerical analysis, and sustainability of ICBP. It also illustrated research gaps in the literature.

Chapter 3: This chapter presents the materials, concrete production, experimental programs, finite element method, and orthogonal experimental design used for this research.

Chapter 4: This chapter presents the experimental results and discussion of the proposed green concrete.

Chapter 5: This chapter presents the modelling process, numerical simulation, results, and discussion of the three-dimensional FEM models of ICBP.

Chapter 6: This chapter presents the conclusions obtained from this research and recommendations for future work.

Chapter 2 LITERATURE REVIEW

2.1 Interlocking Concrete Block Pavement System

Back in ancient Rome, the segmental paving systems were introduced around 500 BC. Before the invention of concrete, hexagon paving stones were applied on the surface of the pavement, especially for the main roads. With the development of technologies, the interlocking concrete block pavement is the product of this idea in a modern context (Garilli, Autelitano, and Giuliani 2017).

With the worldwide challenges, such as the shortage of natural resources, climate change, and urban heat island effects, the pavement design and construction should consider not only the structural performance but also environmental benefits. The ICBP is considered an alternative road form because of its sustainability and ability to reduce urban heat island effects (Jamshidi et al. 2019). Compared to asphalt pavement and conventional concrete pavement, the ICBP also has other advantages. The concrete pavers are normally precast in factories, which ensures high strength and consistent quality. The pavers will not be damaged by high temperature, moisture, and other environmental conditions, thus the ICBP has high durability and long-term performance. The construction can be conducted all year round, and there is less heavy equipment required and no curing time required after the construction. The maintenance and repair are simple and with low cost, which results in a low life cycle cost (UNILOCK 2019).

2.1.1 Structural components of ICBP

The typical structure of ICBP includes seven components: concrete pavers, jointing sand, bedding sand, base, sub-base, subgrade, and the edge restraint, as shown in Figure 2-1.

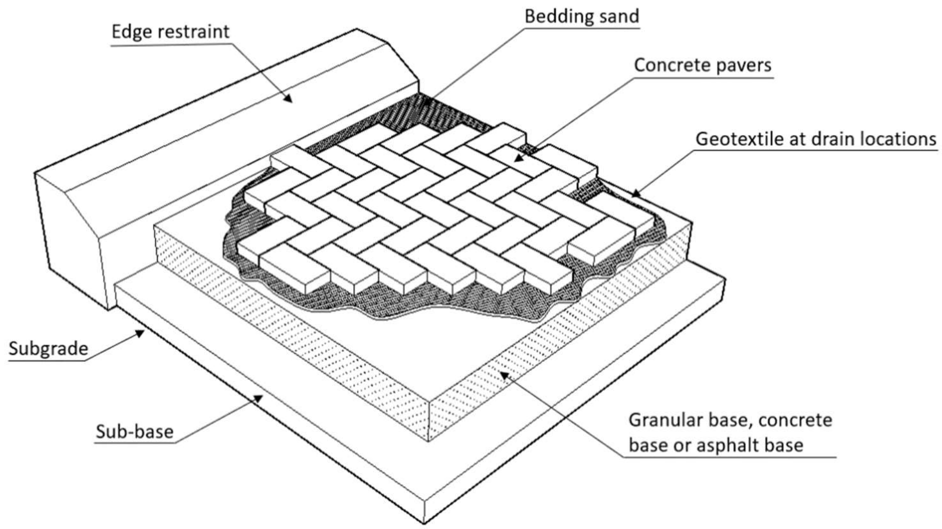

Figure 2-1 The Typical Structure of ICBP (Noda, Kasahara, and Yaginuma 2009)

The paver blocks can be manufactured in different shapes, thicknesses, and sizes, and these parameters affect the load-spreading mechanism and even the pavement performance. Rectangular, hexagon and unipaver, and dumble are the most common block shapes. The jointing sand shall be as dry as possible to easily complete filling. The bedding sand layer shall be spread uniformly to ensure the flatness of the surface, and the quality of sand is important for good performance.

According to Ontario Provincial Standard Specification (OPSS), the material properties of concrete pavers and other structural components are listed in Table 2-1.

Table 2-1 Standard Requirements of ICBP's Components in Ontario, Canada

(Ontario Provincial Standard Specification 2020)

Components	Material	Specification	Requirements
Concrete blocks	Precast concrete pavers	CSA-A231.2	- A face area ≤ 0.09 m^2 - An aspect ratio* ≤ 4 for pedestrian applications, and ≤ 3 for vehicular applications - A minimum thickness of 60mm - Compressive strength of individual pavers ≥ 40 MPa

Components	Material	Specification	Requirements
Jointing sand	Fine and dry sand	OPSS 1004	- The gradation shall meet mortar sand requirements - The normal joint width of 2 to 5 mm
Bedding sand	A layer of uncompacted moist sand	OPSS 1002	- The percent passing the 75 μm sieve shall be < 1% - Sufficient depth to achieve the final compacted thickness of 20 to 30 mm
Base	Granular base	OPSS 314	- The selected base form should suit traffic and environmental conditions - Shall be compacted according to OPSS 501
	Concrete base	OPSS 350	
	Asphalt base	OPSS 313	
Sub-base	Granular B	OPSS 1010	Shall be compacted according to OPSS 501
Subgrade	Soil	OPSS 206	Preparation shall be according to OPSS 206

* The aspect ratio is the overall length divided by pavers' thickness.

The preparation of subgrade, compaction of subbase, and base shall be according to OPSS 206 and OPSS 501, separately. The bedding sand shall be screeded after the placement, and concrete blocks will be placed on loose bedding sand in a certain pattern. The compaction has three steps: initial compaction, joint sand compaction, and final compaction. The final compacted thickness of bedding sand should be between 20 to 30 mm after at least three passes of a plate compactor. Joint sand shall fill the space between each paver after initial compaction. Sweeping sand and compaction shall be applied at the same time, and the excess sand shall be swept when the joints are filled. A least ten passes of a pneumatic-tired roller shall be applied to the surface during final compaction for vehicular applications. All loose, broken, or damaged concrete blocks during the installation shall be replaced by new ones (Ontario Provincial Standard Specification 2020).

2.1.2 Laying patterns of the concrete blocks

The concrete blocks are laid in certain patterns, and the jointing sand is the filler between each block. When the load applies to the pavement surface, the blocks transfer the load to lower layers and determine the bearing capacity. The common laying patterns of ICBP are herringbone, stretcher, and basket weave, as shown in Figure 2-2.

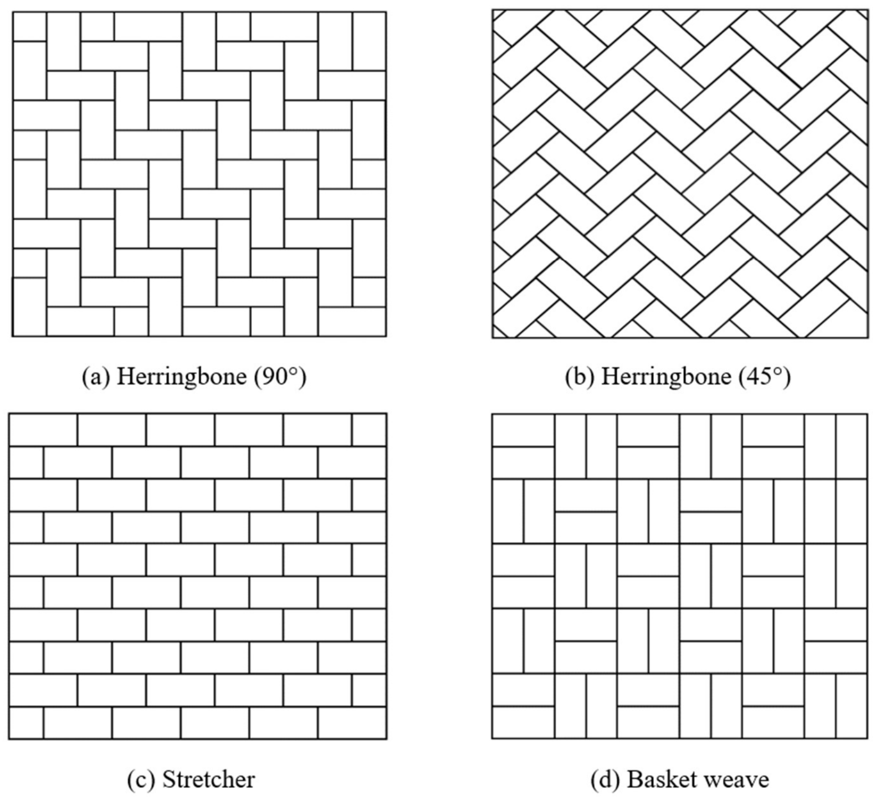

Figure 2-2 Rectangular Blocks in Different Laying Patterns (Rada et al. 1991)

Panda and Ghosh investigated the effect of different patterns on load deflection of ICBP and the results showed the laying pattern did not relate to the load-deflection path (Panda and Ghosh 2002). However, this conclusion is not consistent with research conducted by others (Miura, Takaura, and Tsuda 1984). The laying pattern has been proved to have influenced the mechanical performances of ICBP according to the modelling analysis as mentioned in Section 2.3.3.

2.1.3 Performances of ICBP

The structural behaviour of ICBP is like flexible pavements because of the interlocked nature. The discontinuity of the concrete pavers results in a lower chance of cracking even with the settlement of lower layers. The surface also provides durability, driving comfort, resistance to extreme environmental conditions, and slip and skid resistance.

Interlock mechanism is defined as the inability of a concrete paver to move within the whole paver structure, and it allows the ICBP to be considered a flexible pavement in terms of structural characteristics (Knapton and Barber 1982). The interlock shall be achieved in three directions: vertical, rotational, and horizontal, as shown in Figures 2-3.

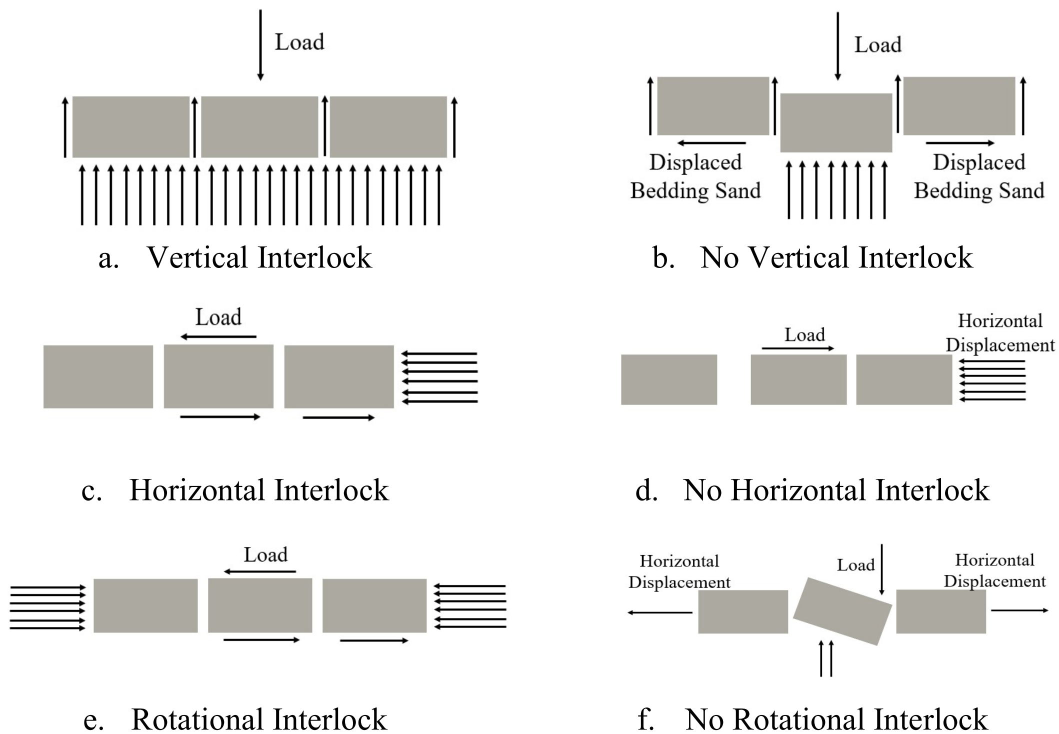

Figure 2-3 Vertical, Horizontal and Rotational Interlock (ICPI 2006)

The jointing sand between the blocks, compactions during the construction, and the support from the bedding layer contribute together to the vertical interlock. When a vertical load is applied to an individual block, the load is transferred to its neighbours through the jointing sand, and the shear transfer happens through the jointing sand. The rotation of a single block happens when the vertical load is applied to the block edges and there is the horizontal displacement of neighbour blocks, as explained in Figure 2-3. Therefore, the rotational interlock is achieved by the edge restraint, block thickness, and construction quality. The horizontal interlock is maintained by the laying pattern and stable edge restraints. In 1979, the creep phenomenon was observed from rectangular blocks in the stretcher laying pattern. The horizontal displacement of blocks was along the line of the road and traffic direction (Knapton and Barber 1982). A special block shape and other laying patterns can prevent or reduce the creep, and a herringbone laying pattern is recommended to resist the lateral movement in the literature (ICPI 2006).

In 1984, Miura et al. concluded that the load transferring ability improved when the applied load increased (Miura, Takaura, and Tsuda 1984). The mechanical performances of ICBP increase over time after the installation as the ‘lockup’ phenomenon will appear after receiving the traffic compaction. The elastic modulus of ICBP’s surface layer increased from 100 MPa to 620 MPa over years according to falling weight deflectometer (FWD) results (Kasahara and Matsuno 1987). The structural performances under traffic loading also relate to base materials. However, rigid layers can result in block damage because of the high local stress. The material quality and gradation of bedding and base layers shall be selected based on traffic and environmental conditions.

Besides the FWD method, the plate loading test, the Benkelman beam, the Light Weight Deflectometer (LWD), GeoGauge, and the push-in loading test are usually used to evaluate the load-deflection, stress distribution, and stiffness of ICBP. The elastic modulus can be calculated by experimental data through various formulas. Arjun Siva Rathan et al. investigated the correlation relationship between the test modulus by the plate loading test, LWD modulus, and geogauge modulus, and the correlation equations were developed. The statistical results showed there was a more significant correlation between the plate loading test and the LWD method, and the relationship of measured deflection value from these two experiments showed the best fit with an R^2 value of 0.915 (Arjun Siva Rathan, Sunitha, and Anusudha 2021).

The term load transfer efficiency (LTE) or “joint efficiency” is defined as the ability to transfer partial load from the loaded concrete slabs to its neighbours (Ioannides and Korovesis 1992). The LTE can be calculated by different formulas to provide quantitative measures of pavement-system response, and the most common definition adopted by the AASHTO is shown in Equation 2-1.

$$LTE_{\delta} = \frac{d_u}{d_l} \quad \text{Equation 2-1}$$

Where d_u is the deflection on the unloaded slabs or blocks, and d_l is the deflection on the loaded slabs or blocks. The LTE is highly related to the concrete block geometry and reflects the interlocking level. The ratio of the side area to the surface area of concrete pavers has a linear relationship with the LTE, as shown in Figure 2-4. Concrete blocks have a larger side area/surface area ratio and higher LTE, which means the applied load can be naturally transferred between blocks. Therefore, the ICBP has a better interlocking level than common jointed concrete pavements, and the ability to be adapted under heavy traffic conditions.

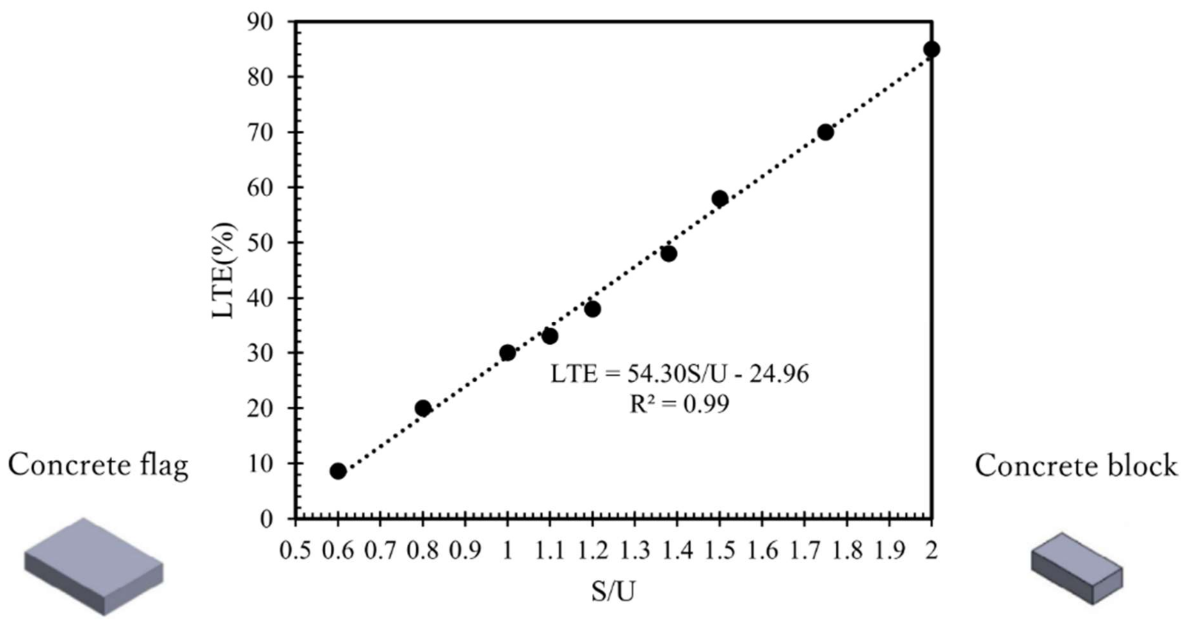

Figure 2-4 The Linear Relationship between LTE and Side Area/Surface Area Ratio (Jamshidi et al. 2019; Noda, Kasahara, and Yaginuma 2009)

The horizontal force test is commonly used to evaluate the horizontal shifting resistance of ICBP. It is often observed permanent shifting of concrete blocks due to horizontal load from dynamic heavy traffic. The block shapes, thickness, laying patterns and other parameters of ICBP will affect the horizontal shifting resistance, in another word, the rotational and horizontal interlock. Mudiyono investigated the effects of block shape, block thickness, joint width, and laying pattern on the horizontal performance, and the horizontal force testing installation and the typical failure pattern are shown in Figure 2-5. The results showed the direction of the horizontal force also influenced the horizontal mechanical behaviour besides other parameters.

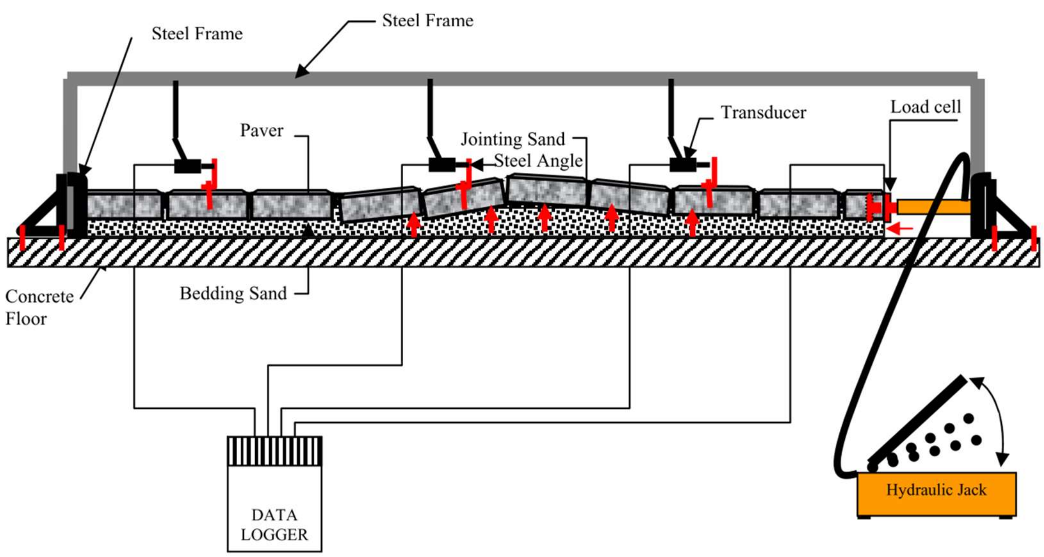

Figure 2-5 Horizontal Force Testing Installation and Typical Failure after Testing

(Mudiyono 2006)

The concrete block pavement shows better mechanical performance than asphalt pavement at high temperatures because of the material characteristic of concrete. The permanent deformation will happen on the ICBP like asphalt pavement. Therefore, the depth of rutting is considered the typical damage when the pavement is designed. The durability of ICBP including rutting, load resistance, and freeze-thaw resistance shall be considered through the service life.

The slip resistance for pedestrians and skid resistance for vehicles are critical to the safety of ICBP. The tribometer is typically used to measure slip resistance, however, this method cannot predict the likelihood of a pedestrian slipping. All testing methods measure the surface when it is found slippery. Many factors influence slip resistance of ICBP, such as surface conditions, wet or icing pavement, shoe sole material, and the style and speed of walking. The skid resistance should be measured under both static and dynamic conditions. The British Pendulum Tester is the most common static measuring device, which does not involve the use of a tire. The friction between the rubber shoe and the pavement is measured at low speed, which is influenced by the microtexture of the surface. ASTM E274, Standard Test Method for Skid Resistance of Paved Surfaces Using a Full-Scale Tire, is applied to measure dynamic skid resistance in North America. Both static and dynamic measurements are performed on the wet pavement to preset a more realistic frictional resistance. Like slip resistance, skid resistance is influenced by internal and external factors which include pavement texture, the speed and axle load of the vehicle, tire type, tire tread, and the environmental condition (ICPI 2020b). A British Pendulum Number (BPN) value of 45 is the minimum requirement; a value above 55 indicates acceptable skid resistance in general conditions, and a value above 65 indicates good skid resistance even under harsh environmental conditions. From the literature, the BPN values of ICBP ranged from 44 to 81 throughout the service life (Shackel 1986)(Mavin 1984)(Domenichini et al. 1998). The results from the ASTM E274 test were also acceptable at different testing speeds (Dahir and Mullen 1971). It is noted that the friction of the ICBP's surface may reduce when surface sealers are applied.

2.1.4 Typical Failures and Maintenance

Proper and timely maintenance is essential to provide durable and safe pavement. Common failures that the ICBP might experience are rutting, horizontal creep, settlement, damaged or cracked pavers, joint sand loss, etc. The reasons and required maintenance of different failures are shown in Table 2-2.

Table 2-2 Typical Failures and Required Maintenance of ICBP

Failure type	Reasons	Required maintenance
Rutting	Settlement of lower layers, poor quality of bedding sand, approaching the end of design life	The removal of the pavers and bedding sand and reinstate the whole system
Depression	Settlement of subgrade and base course	The removal of the pavers and bedding sand in the affected areas, the addition of new base material, and the replacement of new pavers and bedding sand
Horizontal creep	Traffic loading, inappropriate laying pattern, ununiform support	The pavers and bedding sand in the affected areas should be removed and replaced, and the base should be levelled
Settlement	Settlement of subgrade and base course, crack in the rigid base, poor quality of bedding sand	The pavers and bedding sand in the affected areas should be removed and replaced, placing a strip or patch of geotextile above the base course
Damaged or cracked pavers	Low paver strength, traffic loading	Damaged or cracked units should be removed and replaced
Joint sand loss	Low quality of joint sand, inadequate compaction	Joint sand should be reinstated
Edge restraint damage	Inadequate horizontal force resistance	The edge restraint should be repaired or replaced

2.1.5 Current application in Canada

In the early 1970s, concrete pavers came to North America from Europe. The first concrete paver manufacturer in North America, Unilock, was set up in Barrie, Ontario in 1972 (Whitehouse 2021). Since then, the concrete pavers have been successfully applied for parks, driveways, sidewalks, parking lots, bus stations, and airport roads. In 2019, the total sales of segmental concrete paver products were 749 million square feet in Canada and the U.S reported by ICPI (ICPI 2020a).

There were four main design methods available for concrete block pavements, which include the design based on experience, mechanistic methods based on structural analyses, modification of conventional flexible pavement design, and empirical (B. Shackel 1981). In North America, the structural design of interlocking block pavements follows Standard ASCE/T&DI/ICPI 58-16, Structural Design of Interlocking Concrete Pavement for Municipal Streets and Roadways, which was edited in 2016 (ASCE 2016). Because of the similar characteristic of flexible pavement and ICBP, the design method is modified based on the mechanistic-empirical design methodology. The design procedure starts with the design life, reliability, and traffic, then subgrade soil strengthening assessment, determining materials and thickness of base and sub-base, and lastly the requirements of surface elements. ASTM C 936, Standard Specification for Solid Interlocking Concrete Paving Units, explains the material requirements of concrete pavers (ASTM 2001). All material and construction also shall meet CSA A231.2 Precast Concrete Pavers and OPSS 355 Construction Specification for the Installation of Interlocking Concrete Pavers in Ontario, Canada (CSA A231.1/A231.2 2018)(Ontario Provincial Standard Specification 2020). Besides these standards, other authorities and companies also developed construction guides and specifications in Canada. For example, the ICPI developed the ICPI Tech Spec Library which provides resources for design, construction, and maintenance guides about ICBP. The Unilock company published Design Considerations for Interlocking Concrete Pavements which is specifically suitable for North American cities (UNILOCK 2019).

The first downtown interlocking pavement project was conducted in North Bay, Ontario in 1982. It has been popular to use the ICBP in a residence, however, there are still challenges to applying this pavement form on the vehicle street, especially with repeated heavy traffic loads. Except for the vehicular traffic, urban ICBP are subjected to harsh winter conditions and the presence of deicers in Canada. The key activities when designing urban ICBP include:

- Larger pavers should be installed to ensure stability and durability.

- Permacon recommends that the strips of pavers should be perpendicular to the traffic flow (Permacon 2015).
- Uniformity should be ensured during the installation, and the subbase and the base course must provide uniform support.
- Thickness design should be conducted for different traffic levels (main streets and boulevards, secondary streets, and sidewalks).
- Concrete pavers should able to resistant to fuels, freeze-thaw cycles, and de-icing chemicals.
- The friction between the tire and pavement surface should be larger enough, especially when the ICBP is applied at airports.
- Monitor and maintenance should be planned out at the beginning of service life.

With the variety of colours, block shapes, and tail area laying patterns, the ICBP is popular among pedestrians, homeowners, and urban planners. The great potential of using by-products and waste materials, reducing the heat island effect, and environmental emissions brings high social acceptance to the ICBP.

Recently, the permeable products have drawn the attention of city planners as they realized that ground infiltration is the solution for cities. Permeable interlocking concrete pavement (PICP) has higher efficiency than porous asphalt pavement in terms of stormwater management. In December 2020, ICPI hosted a virtual symposium about PICP, and municipal staff, engineers, and researchers from Calgary AB and London ON attended this seminar. The city engineers and conservation authorities received a clear picture of the advantages of PICP.

2.2 Concrete Compressive Performance

Concrete is made to obtain its extraordinarily high compressive strength compared with other natural materials; the mechanism of cement concrete strength is originated from a series of chemical reactions among its mineral composition, namely tricalcium silicate $SiO_2 \cdot 3CaO$, dicalcium silicate $SiO_2 \cdot 2CaO$, tricalcium Aluminate $Al_2O_3 \cdot 3CaO$, and tetra calcium Ferroluminate $4CaO \cdot Al_2O_3 \cdot Fe_2O_3$ (Aïtcin and J.Flatt 2016). Cement is the binding material for concrete, which holds all the materials together and forms a mechanical strength, while aggregates are composed of geological materials such as sand, gravel, and crushed stone, they help to make concrete more compact and can also decrease the use of cement and water, thus to contribute to the compressive strength of the concrete (CEMEX 2022).

Research has been conducted to investigate the effect of different variables on the mechanical behaviour of concrete, the compressive strength of interlock concrete block was reported to be influenced by admixtures (Baruah, Basack, and Goswami 2020), water-cement ratio (Malahayati et al. 2020), curing methods (Atoyebi et al. 2020), the strength of masonry blocks containing recycled aggregates was evaluated and it was found that the compressive strength of which is comparable with that of those containing natural aggregates (Matar and El Dalati 2011).

2.3 Numerical Analysis

2.3.1 Introduction

ICBP is an efficient pavement form with high strength, environment friendly, and easy installation, and exhibition. It is considered an alternative pavement that could be applied for sidewalks, cycle paths, driveways, parking lots even roads in residential areas. The understanding of ICBP's mechanical behaviour is critical for the pavement design, service level, maintenance, rehabilitation and durability. Same as other kinds of pavements, the evaluation of ICBP involves laboratory and field tests, which include compressive test, flexural test, splitting tensile strength test, rut and permanent deformation test, Benkelman beam deflection test, falling weight deflectometer test, pull-out test and skid resistance test (Ling et al. 2009).

To easily evaluate the mechanical performance of ICBP without time, material, and financial cost, numerical simulation analysis is a feasible method with the development of computer techniques. There were three methods to analyze ICBP, layered elastic analysis (B Shackel 1988), modified slab analysis (ABBO 1985), and finite element analysis (Tabatabaie and Barenberg 1978)(Nishizawa, Matsuno, and Komura 1984), proposed by other researchers. Compared to asphalt and traditional concrete pavement, the surface layer of ICBP is not continuous and homogeneous because of the absence of concrete blocks, jointing sand, and bedding sand. Based on the discontinuities property, the modelling of ICBP's structural characters is more complicated.

The Finite Element Analysis (FEA) is the practical application of the finite element method (FEM) which breaks down a system into finite elements. It can transfer a continuum problem to an element problem with a finite number of parameters for 1D, 2D or 3D domains (G.P.Nikishkov 2004). The advantages of the FEM are easier modelling, high accuracy, a better insight into design and analysis results, and various boundary conditions (IEEE Innovation at Work 2020).

The FEM allows the realistic simulation of ICBP's surface with jointing and bedding sand and the linearity or nonlinearity of materials behaviour. An example of a 3D finite element model of ICBP is shown in Figure 2-6, which consists of concrete blocks, jointing sand, bedding sand, base, sub-base, and subgrade.

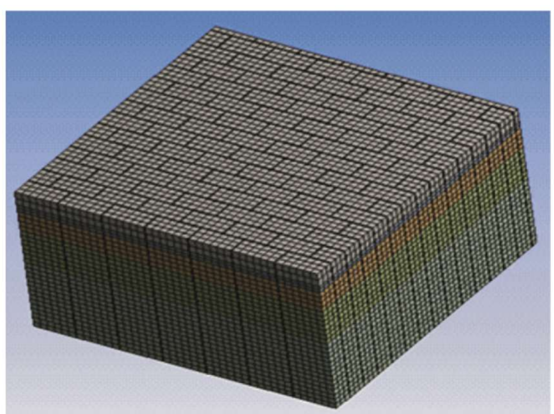

Figure 2-6 An Example of a 3D Finite Element Model of ICBP

(Di Mascio, Moretti, and Capannolo 2019)

2.3.2 Modeling of ICBP

ICBP is a multi-layer structural system, and the surface layer contains two different materials, concrete blocks, and jointing sand. To simulate the mechanical characteristic of

ICBP, the material properties and geometric description are both essential features to be defined.

Individual concrete block is precast by concrete companies, and the concrete mortar is a mix of aggregate, sand, cement, water, and some admixtures. The shape of concrete blocks is determined by the mould dimension, and the strength of concrete blocks is ensured by the proper curing process. Firstly, concrete blocks were considered to be elastic and the modulus of elasticity was around 2500 MPa and the Poisson's ratio was around 0.3 (Nejad 2003). In 2010, Khaki and Azadravesh used the concrete damage plasticity model to simulate concrete plastic behaviour under monotonic, cyclic, and dynamic loading. Compressive crushing and tensile cracking failure mechanisms were applied in this model (Khaki and Azadravesh 2010). The Drucker-Praguer material model and Willam-Warnke were used for compression and tension stresses separately in a combined mathematical model in another study (del Coz Díaz et al. 2011).

A lot of researchers treated jointing sand, bending sand layer, base, and sub-base as homogeneous and isotropic elastic materials (Hein 2016)(Lin et al. 2016)(Gunatilake and Mampearachchi 2019). Moreover, the subgrade was defined as a set of spring elements with the spring coefficient k (Lin et al. 2016). Table 2-3 shows the mechanical characteristics simulation of different layers of ICBP.

Table 2-3 Mechanical Characteristics Simulation of ICBP Materials

<table>
<tr><th>Layer</th><th>Material</th><th>Material Models</th><th>Property Parameters</th></tr>
<tr><td rowspan="2">Surface</td><td rowspan="2">Concrete blocks</td><td>Elastic behaviour</td><td>- Elasticity modulus E
- Poisson's ratio
- Density</td></tr>
<tr><td>The concrete damage plasticity model</td><td>- Elasticity modulus E
- Poisson's ratio
- Density
- Compression hardening and damage
- Tension stiffening and damage</td></tr>
</table>

<table>
<tr><th>Layer</th><th>Material</th><th>Material Models</th><th>Property Parameters</th></tr>
<tr><td></td><td>Jointing sand</td><td rowspan="4">Elastic behaviour</td><td rowspan="4">- Elasticity modulus E
- Poisson’s ratio
- Density</td></tr>
<tr><td>Bedding sand</td><td>Bedding sand</td></tr>
<tr><td>Base</td><td>Cement treated base
Asphalt treated</td></tr>
<tr><td>Sub-base</td><td>Granular layer</td></tr>
<tr><td>Subgrade</td><td>Soil</td><td>A set of springs</td><td>The spring coefficient k</td></tr>
</table>

As shown in Figure 2-6, the ICBP is usually modelled as a multi-layer cube with the actual size. FEM analysis is based on the discretization, nodes, and elements, and the element is comprised of nodes. Meshing is the process to break down all parts of a model into small solid elements, and the number of elements determines the accuracy of the simulation (Arjun Siva Rathan and Sunitha 2021). A smaller mesh size relates to more accurate analysis results; however, increased elements and nodes increase the computing analysis time. Taheri et al. investigated the impact of mesh size on ICBP behaviour analyzing results, and 5 cm particles were selected in the model (Taheri, Fakhri, and Hayati 2021). Another study chose a medium-mesh size based on the sensitivity analysis and analysis time reduction (Arjun Siva Rathan, Sunitha, and Anusudha 2021).

The interface between each layer is also a critical feature of the whole structure. The contact elements were used to represent the interface between concrete blocks and jointing sand. Fully boned contact was chosen for interfaces and no relative displacement would be detected (Shafabakhsh, Family, and Abad 2014). In 2018, Hengl et al. considered the disconnection between the surface layer and bedding sand, and a ‘hard’ contact was assumed in the vertical direction. Mohr-Coulomb model was applied in a tangential direction with a friction coefficient of 0.6 (Hengl et al. 2018). The boundary conditions are usually defined as fixed in X and Y directions, and the displacement can only happen in the Z direction, which is the loading direction.

2.3.3 Numerical Simulation of ICBP

Previous research has investigated the mechanical performances of the individual concrete blocks by using the FEM, which includes compressive behaviour, shear, and failure patterns under different loading conditions.

Three different types of interlocking hollow concrete blocks (HHIB) were developed with more vertical and horizontal ribs. The compressive strength of these HHIBs was investigated by the uniaxial compressive test and the failure patterns of the blocks were analyzed. A finite element model was proposed, and the model considered both material and structural properties. The effects of shape design on mechanical performance were investigated by experimental and numerical analyses. The simulated results were consistent with the experimental failure modes. Based on the finite element model results, a novel equation to predict the compressive strength of the HHIBs was developed, and the error rate was between 1.04% to 9.5% (Liu et al. 2019). Furukawa et al. conducted compression tests of the different interlocking blocks under two different support conditions. The effects of interlocking shapes and support conditions on the load-displacement relationship and the failure mechanism were examined. Furthermore, a 2D finite element model was designed, and it was concluded that the block shape will change the compressive strength. The finite element analysis kept high consistency with the compression test (Furukawa, Masuda, and Kiyono 2020). Tee et al. developed a green interlocking concrete block with fly ash, palm oil fuel ash, waste glass, and recycled concrete aggregate. The laboratory compressive test and FEM analysis were carried out to evaluate the damage characteristic of all mixes. FEM analysis provided the initial cracking and failure mechanism of blocks and the simulation results validated the experiment results (Tee, Agba, and Samad 2019).

Earlier studies have developed numerical models of ICBP to explore the effect of the material model properties, ICBP structures, and different loading conditions on the mechanical response of ICBP. Load transfer and deflection mechanism, stress-strain response, deformation, and subgrade settlement are commonly investigated in the literature. The summary of previous studies on ICBP simulation analysis using the FEM is shown in Table 2-4.

As important indexes of pavement model design, material model parameters determine the structural and mechanical characteristics. Taheri et al. investigated the effect of different Young's modulus of the concrete block layer on the load-deflection results. It was concluded that 2000 MPa resulted in close results compared with the experimental data (Taheri, Fakhri, and Hayati 2021). Surprisingly, Nejad and Shadravan concluded that the compressive strength of individual concrete blocks was independent of the load-deflection of ICBP (Moghadas Nejad and Shadravan 2010).

Pavement structure is the dominant factor influencing the performance and durability of ICBP. The thickness of the concrete block layer, bedding sand layer, and base layer has a big influence. Thicker concrete blocks, bedding sand, and base layer resulted in lower maximum load deflection (Di Mascio, Moretti, and Capannolo 2019). Lin et al. developed a deflection prediction model by both FEM analysis and LWD test results. The effect of block thickness is considered in the FEM model. The deflection prediction model was determined by the multi-regression analysis using PASW Statistics 18. Then, the deflection calculating equation was applied to a rut depth prediction model. The results showed thicker concrete blocks are the critical parameter to improve the rutting resistance ability of ICBPs (Lin, Cho, and Kim 2016). However, the layer structure design relates to the material consumption and construction time cost. Thicker layers result in better pavement performance and increased construction costs. The numerical analysis can be useful when there is a need to balance the required performance and cost.

The concrete block of ICBP has various shapes, sizes, and angles as mentioned in Section 2.1. Arjun et al. studied the effects of zigzag shape, I shape, and rectangle shape on load deflection, and the results showed the zigzag-shaped blocks had the minimum deflection (Arjun Siva Rathan and Sunitha 2021). The zigzag shape can change by using different angles, and it was conducted that 100°C and 110°C provide equivalent better performance (Gunatilake and Mampearachchi 2019). Similar to the thickness, the bigger block size could provide better performance of ICBP.

The jointing sand is another critical part of the surface layer, and it is the filling material between each block. The effect of jointing sand width has been studied in previous research, and the recommended width is between 2 mm to 4 mm (Moghadas Nejad and Shadravan 2010).

There are various ways to lay concrete blocks in construction practice, such as stretcher, herringbone, basketweave, and stack bond. The herringbone bond was verified, which could provide a better load spreading and better mechanical properties from the literature (Hengl et al. 2018).

ICBP bears different types of traffic loads when it is applied to different sites. For example, it needs to bear heavy and light vehicles when it is used on the ordinary road, and only pedestrians, bicycles, and wheelchairs will appear on a walkway. The simulation of loading conditions shall reflect the real traffic condition of ICBP in service. The most common method used by other researchers was applying a vertical distributed load in a rectangular or circular shape. A few studies simulated the moving load to analyze the mechanical response of ICBP. Moreover, the effect of loading positions on load deflection was evaluated as well. However, the failure developing mechanism should be paid more attention to when the load is applied to different locations of ICBP.

2.3.4 Software Application

According to the literature, it was found that researchers used various software to simulate load deflections, bearing capacity, and stress-strain condition of pavements by FEM, which includes MSC. Nastran, SAP, PLAXIS, ANSYS, EverFE, and ABAQUS (Guan et al. 2018)(Arjun Siva Rathan and Sunitha 2021)(Di Mascio, Moretti, and Capannolo 2019)(Shafabakhsh, Family, and Abad 2014)(Mampearachchi and Senadeera 2014)(Maske, Anandkumar, and Majumder 2013)(Šešlija, Radović, and Togo 2016)(Nagakumar, Ajay, and John 2022)(Sadiq, Hilal, and Fattah 2022).

Furukawa et al. used MSC.Nastran built a 2D finite element model and evaluated the effects of shapes and support conditions on the compressive strength of interlocking blocks (Furukawa, Masuda, and Kiyono 2020). Rachmat and Salsabilla used SAP and PLAXIS to build ICBP models with different paving shapes and concluded that hexagonal is the optimum shape by calculation results (Rachmat and Salsabilla 2019). Arjun Siva Rathan et al. simulated the plate load-deflection curve and shear stress-displacement of the previous ICBP by PLAXIS (Arjun Siva Rathan, V, and V 2021). The effects of bedding and jointing sand on shear-stress behaviour of ICBP were also evaluated (RT et al. 2020)(Raveendran Thulasibai et al. 2021). Moreover, the load-deflection prediction model of ICBP was developed based on the PLAXIS software and the model processed a 95% confidence level after the validation with experimental data (Arjun Siva Rathan and Sunitha 2021).

Gunatilake and Mampearachchi used SAP and ANSYS to build a three-dimensional model with a new block shape, and the effect of block angles on deflection and stress was analyzed (Gunatilake and Mampearachchi 2019). Di Mascio et al. simulated different vehicle types and traffic conditions in ANSYS and concluded the herringbone bond laying pattern connected with the best road performance and longer service life can be obtained from thicker blocks (Di Mascio, Moretti, and Capannolo 2019). The effects of joint width and block strength were analyzed in ANSYS by Moghadas Nejad and Shadravan. The results showed the joint width should be between 2 to 4 mm, and the strength of individual blocks is independent of the whole pavement performance (Moghadas Nejad and Shadravan 2010).

ABAQUS is software used for finite element modelling and analysis to solve complex engineering problems, which was released in 1978 (Wikipedia 2022). It was designed to address the non-linear analysis of engineering simulation. Among the existing software, ABAQUS is a professional, powerful, and accurate software application to conduct pavement analysis, which allows modelling 2D or 3D geometry, the application of non-linear behavioural models, various loading types, and clear visualization of analysis results (Jafaraghaei 2020). A finite element analysis in ABAQUS includes three individual steps: modelling, processing, and generating results.

ABAQUS has also been considered used when it comes to simulating and analyzing interlocking concrete block pavement. The stress, strain, and fatigue performance of ICBP were analyzed in a previous study (Shafabakhsh, Family, and Abad 2014)(Lin, Cho, and

Kim 2016)(Skar and Poulsen 2015)(Taheri, Fakhri, and Hayati 2021) (Hengl et al. 2018). In this research, ABAQUS is selected to conduct the numerical analysis because of its strong graphic tools, various meshing techniques, accurate analysis result, and the capability of providing a graphical display of the simulation results.

Table 2-4 A Summary of Previous Studies on ICBP Simulation Analysis Using FEM

Reference	Software	Type	Lab. tests	Source	Load type	Parameters	Performances	Major findings
(Rachmat and Salsabilla 2019)	SAP and PLAXIS	2D	No	Literature	Manual pavement road used Benkelman Beam Tool No.01/MN/BM/83	- Block shapes - Block thickness	-Deformation - Bending moment - Subgrade settlement	A hexagonal shape was recommended with minimum deformation, moment, and soil settlement
(Arjun Siva Rathan, V, and V 2021)	PLAXIS	3D	Yes	Experimental results	A circular (30 mm diameter) load up to 40 kN	NA	- Load deflection - Shear stress and strain	Used PLAXIS to simulate the plate load test and direct shear test of pervious ICBP
(RT et al. 2020)	PLAXIS	3D	Yes	Experimental results and literature	A uniformly distributed load between 50 to 125 kPa	With or without jointing sand	-Shear test result	The jointing sand is critical for the load transfer of ICBP
(Arjun Siva Rathan and Sunitha 2021)	PLAXIS	3D	Yes	Experimental results and literature	A square (150× 150 mm) load between 10 to 50 kN	- Block shapes - Block thickness - Laying patterns	-Load deflection	- The zigzag-shaped blocks had the minimum deflection - The thicker blocks and the herringbone pattern provided better performances - A deflection prediction model of ICBP was developed
(Mampearachchi and Gunarathna 2010)	SAP	3D	Yes	Experimental results	A rectangular (310 mm × 225mm) moving a vertical load of 50 kN	- Laying patterns - Loading positions	-Vertical and horizontal deflection	- The deflection at different loading points was investigated - A moving load was applied in two moving directions - The herringbone bond was determined

Reference	Software	Type	Lab. tests	Source	Load type	Parameters	Performances	Major findings
								as the optimum laying pattern under traffic loading
(Gunatilake and Mampearachchi 2019)	SAP and ANSYS	3D	Yes	Experimental results	A rectangular (310 mm × 225mm) load between 10 to 50 kN	- Block shapes - Block angles - Wheel wander	- Load deflection - Equivalent and shear stress	- A new block shape was suggested based on the lowest maximum load deflection and stress - The effect of block angles was investigated, and 100° and 110° were recommended
(Di Mascio, Moretti, and Capannolo 2019)	ANSYS	3D	No	Literature	Four different moving loads simulating different vehicle types	- Laying patterns - Loading positions - Block thickness - Bedding sand thickness	-Deformation under three different traffic levels - Stress-strain	- The herringbone bond contributes to a better load spreading - Thicker blocks provided longer service life
(Moghadas Nejad and Shadravan 2010)	ANSYS	3D	Yes	Experimental results and literature	A circular load between 10 to 50 kN	- Joint width - Block size - Block strength - Block thickness	-Load deflection	- The recommend joint width was between 2 to 4 mm - The bigger block size and thicker blocks could provide better performance - The block strength did not affect the whole pavement performance - The wedging action would result in horizontal forces between pavers

Reference	Software	Type	Lab. tests	Source	Load type	Parameters	Performances	Major findings
(Shafabakhsh, Family, and Abad 2014)	ABAQUS	3D	Yes	Experimental results and literature	A square (261× 261 mm) load of 41 kN	- Block thickness - Bedding sand thickness	Load deflection	- Thicker blocks provided better performance - The width of bedding sand should not be too thick
(Lin, Cho, and Kim 2016)	ABAQUS	3D	Yes	Experimental results and literature	A circular (300 mm diameter) load of 9, 18, and 32 kN	- Laying patterns - Block shapes - Block thickness - Base thickness	Load deflection	The rutting prediction model was developed, and thicker blocks, thicker base, and herringbone patterns resulted in lower rut depth
(Skar and Poulsen 2015)	ABAQUS	3D	No	Literature	A rectangular (178 mm × 162mm) load of 75 kN	Loading positions	Load deflection	Loading positions affected the cracking development
(Taheri, Fakhri, and Hayati 2021)	ABAQUS	3D	Yes	Experimental results and literature	A circular (300 mm diameter) load up to 2000 kPa	Elastic modulus of block paving	- Load deflection - Stress-strain	The recommended elastic modulus of ICBP and jointing sand was 2000 MPa in the 3D ABAQUS model
(Hengl et al. 2018)	ABAQUS	3D	Yes	Experimental results and literature	A standard vertical tire load of 57.5 kN	- Block shapes - Laying patterns	- Shear contact forces - Horizontal deformation	The herringbone bond pattern had the best performance

2.4 Sustainability

Sustainability in the construction industry has three aspects that are environmental, social, and economic requirements. In terms of pavement construction, the key parameters are natural resource consumption, greenhouse gas emissions, thermal performance, cost of construction and maintenance, service life, and durability. Concrete is widely used in pavement constructions because of its advantages of high hardness, high compressive strength, excellent durability, and long service life. Concrete benefits human civilization and world economic development, but the resources consumption and environmental impacts are inevitable. The total world cement production was 4.3 Gt in 2020 according to estimates by the IEA (IEA 2021). Meanwhile, the carbon emission from cement production makes up 8% of the world's emissions (Lehne and Preston 2018).

Clinker is the main ingredient of cement, and it is responsible for the carbon emissions generated in cement production. However, the clinker-to-cement ratio has increased by 1.6% per year worldwide from 2015 to 2020 (IEA 2021). To reduce the proportion of clinker, alternative materials should be considered in cement manufacturing, such as limestone and industry by-products. Portland-limestone cement is widely used for the rigid pavement construction, and there already are standards, like CSA A3001, CSA A23.1, ASTM C595, and ASTM C1157, for material requirements of Portland-limestone cement in North America. The percentage of limestone can be up to 15%, and an environmental product declaration for General Use (GU) and Portland-Limestone (GUL) Cements was developed by the Cement Association of Canada (CAC) in 2016. The life cycle assessment results showed that GUL can reduce 10% carbon emissions on average compared to GU cement (CAC 2016). The supplementary cementing materials (SCMs) can partially replace cement, which results in reducing the consumption of clinker as well. SCMs can strengthen the concrete through hydraulic and pozzolanic reactions. Many SCMs such as fly ash, slag, silica fume, and glass pozzolan are industry by-products. Using these materials reduces not only cement consumption but also landfill waste. It has been evaluated that SCMs have non-negative effects on the mechanical performance and durability of concrete.

Natural aggregates used in concrete production are from non-renewable natural resources. At the same time, construction, and demolition waste (C&D waste) is hard to dispose of and has potential environmental impacts. Because the lack of natural aggregates and the landfill problems have been increasingly concerned in recent years, replacing natural aggregates with recycled concrete aggregates (RCA) is considered an efficient solution to achieve sustainable development. The quality of RCA depends on the sources, separating, screening, and crushing processes. RCA normally is categorized into coarse recycled aggregates (CRA) and fine recycled aggregates (FRA) based on the particle size of 4.75 mm, and FRA is more harmful to the mechanical performance and durability of concrete (Xiao 2018). There are two additional components of RCA compared to natural aggregates, which are the old mortar and an interfacial transition zone (ITZ) between the original aggregate and old mortar as shown in Figure 2-7.

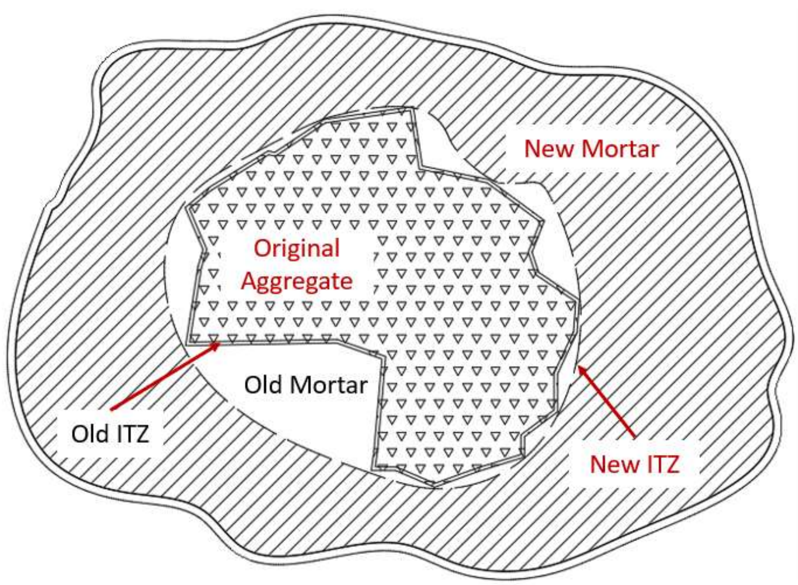

Figure 2-7 Schematic Diagram of RCA in New Concrete (Kisku et al. 2017)

The mortar content on the RCA surface results in low density, inadequate strength, and high-water absorption. The negative effects on concrete properties are from not only the characteristics of RCA but also the old and new ITZ. For construction applications, the general accepted replacement level of RCA is around 20% and the possibility of using 100% RCA has been proved on the laboratory scale (Klee 2009)(Anike et al. 2020).

There also is a tendency to use waste materials in the interlocking concrete blocks to meet the increasing requirements of the environment and urban sustainability. In 2016, Nishikant et al. partially replaced fine aggregates with waste glass to produce concrete pacing blocks. The use of wasters reduced the unit weight of blocks and increased the workability and durability of concrete. The compressive strength increased with increasing waste glass content in the range of 15 to 30 %. However, the waste glass hurt flexural strength. The results proved the possibility of using waste glass as fine aggregates in concrete paving blocks at a 30% replacement level and there are both environmental and economic benefits (Nishikant et al. 2016). Murugan et al. did similar research in the same year, which was using waste tire crumb rubber to partially replace fine aggregates in interlocking concrete blocks. The results showed the ICBP with waste rubber had a better-combined load-bearing mechanism even though the individual compressive strength of the concrete block decreased (Murugan, Natarajan, and Chen 2016). Sultan investigated the effect of RCA on ICBP based on fresh and hardened concrete tests, and deflection tests of ICBP. The compressive strength was between 37 to 47 MPa with 20%, 50%, 75%, and 100% RCA, when extra 20% cement kiln dust and superplasticizers were added. The workability was slightly reduced when the replacement level was 25% and 50%. The load capacity of the concrete block layer could be up to 230 kN according to the deflection results. However, the field study has not been conducted to investigate the industry application of waste materials in ICBP technology.

The special structure of ICBP already provides sustainable development as the paving units are reusable and broken blocks are easy to be recycled. Additionally, the ICBP can help to reduce heat island effects (HIE) compared to conventional concrete pavement and asphalt pavement. Figure 2-8 shows the surface temperature of ICBP, conventional concrete, and asphalt pavement under the same environmental condition. The temperature of ICBP is 13°C lower than it of asphalt pavement. Moreover, the application of PICP has more potential ability to solve the HIE problem because of the stormwater management of PICP.

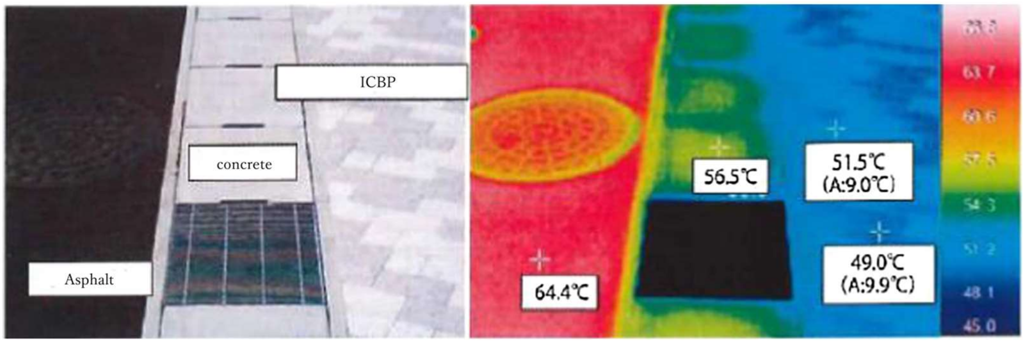

Figure 2-8 The Surface Temperature of ICBP, Conventional Concrete, and Asphalt Pavement (Japan Interlocking Pavement Engineering Association 2017)

2.5 Research Gaps

There are research gaps identified in the literature review as follows:

This ICBP design has not been used in Canadian urban areas, especially under various traffic conditions. Current applications are only for parking lots, bus stations, parks, household driveways, and sidewalks. The information on structural performance, service life, and benefits compared to conventional road forms are not enough for city planners to choose the ICBP. If there is more systematic research including laboratory tests, numerical analysis, and fieldwork, the understanding of ICBP would be more accurate and this could contribute to real construction practices. The fieldwork should be collaborated with concrete block producers to ensure the consistency of concrete blocks.

The ICBP is believed to be an environmental and social friendly pavement with high structural performance. This ideal pavement system is defined as post-modern pavement (Jamshidi et al. 2019). The sustainability of ICBP can be achieved by using waste materials, recycling broken blocks, reducing HIE, and managing stormwater. However, social acceptance must be improved among urban planners, environmental protection agencies, and pavement users. This means that successful design and construction projects of ICBP are needed. Many institutes such as ICPI have already increased the acceptance and applications of ICBP in North America. The challenges in design, construction, maintenance, and rehabilitation still need to be addressed and the responsibility should be taken by the government.

Research using FEM to investigate the influence of the geometric design of interlocking paver on the ICBP performance is mostly focused on the impact of a single factor. For example, the effect of block shape, thickness, and laying patterns on the mechanical behaviours of ICBP was conducted by many pavement engineers. Nonetheless, the reality of ICBP practice is always a combination of multiple factors. There is a lack of studies that considered the effect of multiple factors and their interaction with the performance of ICBP.

Above all, the first part of this study addresses the evaluation of mechanical performance for an interlocking concrete paver made of different proportions of recycled aggregates through a compressive strength test. The second part of the study used FEM software ABAQUS to analyze the effect of multiple geometric and mechanical variables as well as their interaction of the interlocking paver to the mechanical response of ICBP. Notably, the mechanical properties such as elastic modulus used in the FEM modelling are calculated from the indoor compressive tests in the first section of the study.

2.6 Summary

In this chapter, an overview literature review was provided. The topics include structural components, laying patterns, performances, typical failures, and maintenance of ICBP; current applications of ICBP in Canada; concrete compressive performance; modelling and numerical simulation of ICBP; and the sustainability of ICBP. The research gaps were identified based on the literature review and provide the base for this research.

Chapter 3 RESEARCH METHODOLOGY

The overall research methodology of this study consists of two major sections, one is the indoor laboratory experiments, and the other is FEM modelling, as shown in Figure 3-1. This chapter serves the purpose of elaborating the technical details of each section, namely, the material property, experimental method, and orthogonal experimental design.

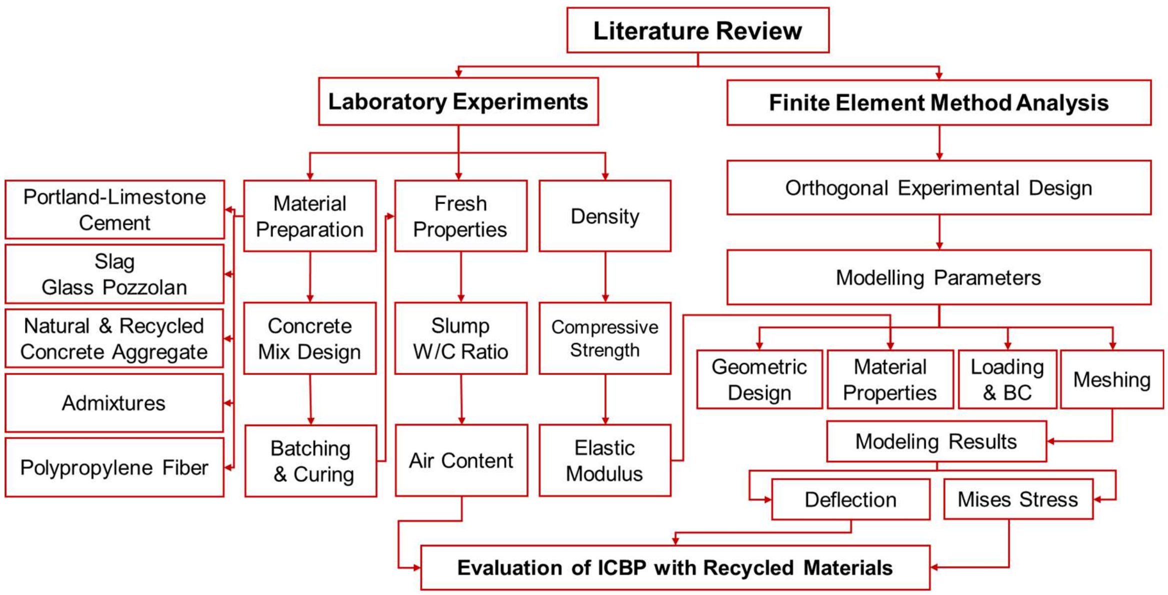

Figure 3-1 Research Methodology

3.1 Materials

3.1.1 Cement

Cement is an important ingredient in the concrete mixture. The chemical reaction between the cement and water creates hydration products that bind aggregates and sands together. It provides the strength to harden concrete. In CSA A 231.1, the hydraulic cement used for concrete pavers includes blended hydraulic cement, Portland cement, Portland-limestone cement, mortar cement, etc. The Portland-limestone or general use limestone (GUL) cement contains 5 to 15% limestone, which decreases CO_2 emissions by 10% on average by reducing clinker production (CAC 2016). The GUL cement produced by St. Mary's Cement in St. Mary's, Ontario, was used in this study, as shown in Figure 3-2. This type of cement is grey powder and contains 15% limestone. The pH value is between 12 to 13, and the relative density is 3.15 (water equals 1).

Figure 3-2 Portland-Limestone Cement Used in this Study

3.1.2 Supplementary Cementing Materials

Two types of SCMs were used in this study, ground granulated blast-furnace slag (GGBFS) and glass pozzolan. GGBFS is the by-products of iron and steel production, and it has been finely ground before using as the cementing material. Glass powders are widely used as pozzolans in concrete. The pozzolanic reaction occurs when the slag and glass pozzolans are added. The chemical compositions of these two materials are shown in Table 3-1.

Table 3-1 Chemical Compositions (%) of GGBFS and Glass Pozzolan

Cementing Material	CaO	SiO_2	Al_2O_3	Fe_2O_3	MgO	SO_3	Na_2O	K_2O
GGBFS	38.5	40.1	7.8	0.74	9.7	2.21	0.38	0.53
Glass Pozzolan	10.9	71	1.82	0.61	0.94	<0.1	13	0.52

3.1.3 Natural and Recycled Concrete Aggregate

Natural aggregates were provided by The Miller Group, a concrete construction company. The properties of natural aggregate are shown in Table 3-2. The gradation of coarse aggregate and fine aggregate are shown in Figure 3-3 and Figure 3-4, respectively.

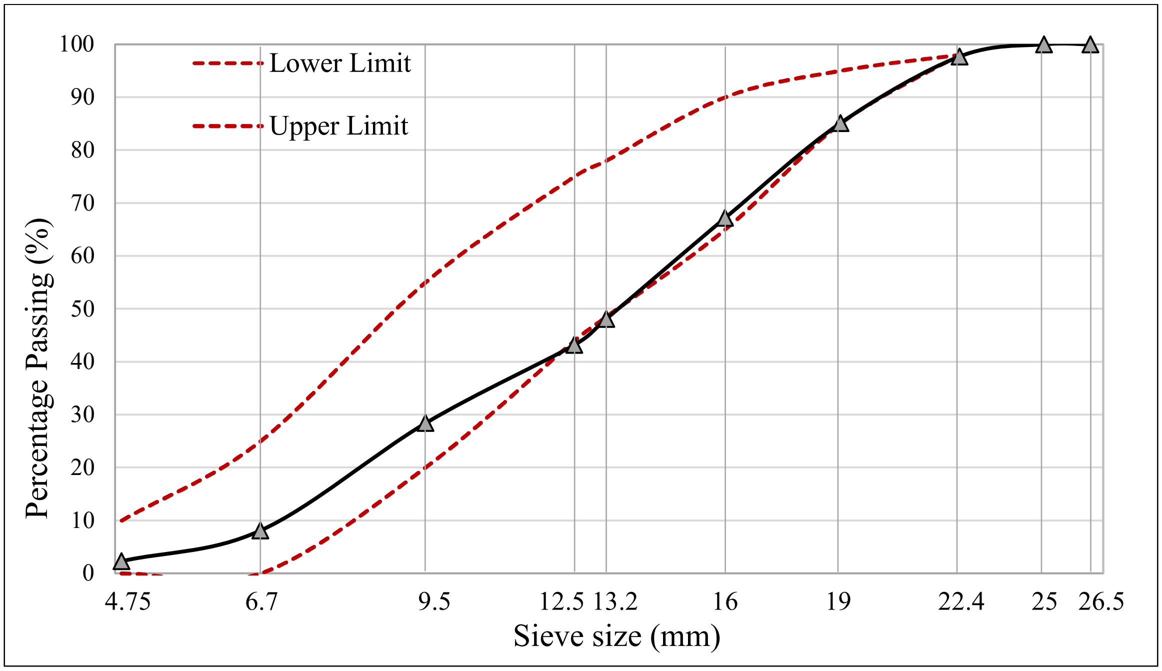

Figure 3-3 Gradation Curve of Coarse Aggregate

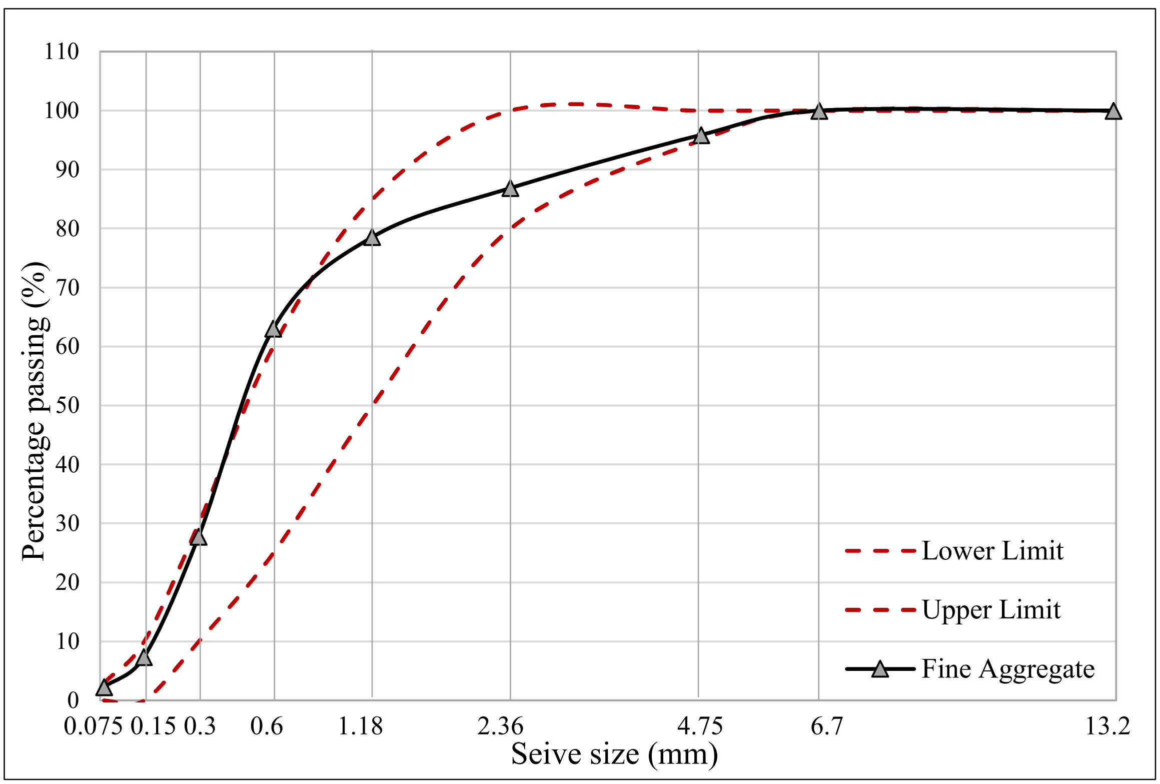

Figure 3-4 Gradation Curve of Fine Aggregate

The coarse RCA used in this study was crushed concrete obtained from a ready-mix concrete plant. The properties of RCA were tested by Hanaa Khaleel Alwan Al-Bayati in the University of Waterloo's CPATT laboratory, as shown in Table 3-2 (Al-bayati 2019). The gradation of coarse RCA is shown in Figure 3-5.

Table 3-2 Material Properties of Natural Aggregates and RCA (Al-bayati 2019)

Properties	Natural Aggregate	RCA
Apparent Specific Gravity	2.7	2.638
Absorption	0.66 %	5.91 %
Micro-Deval Abrasion Loss	12.58 %	23.57 %
Adhered Mortar Loss Percentage	-	3.02 %

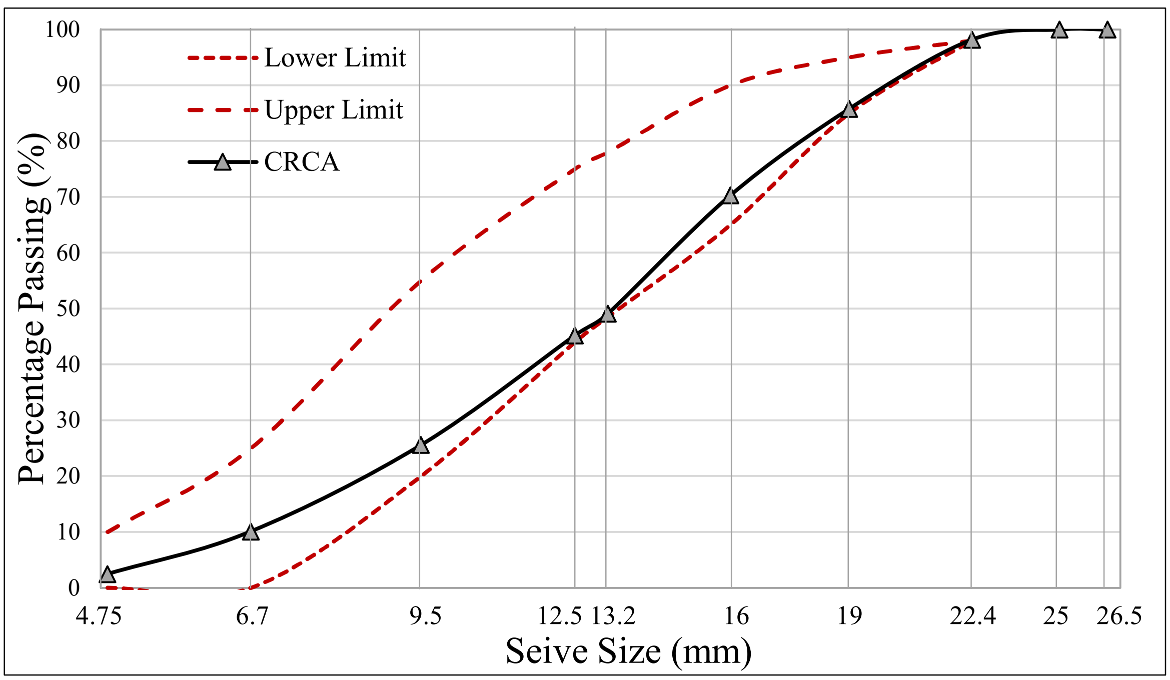

Figure 3-5 Gradation Curve of Coarse RCA

3.1.4 Admixtures

To improve the performance of concrete, water reducer and air entrainment were added to each concrete mixture. The water-cement ratio is a critical parameter in terms of the fresh and hardened properties of concrete. The higher absorption of RCA compared to natural aggregates results in a reduction in workability. The water reducer was added to enhance workability without increasing the water content in this study. Air entrainment was used to improve the freeze-thaw resistance and prevent segregation and bleeding of concrete. The quantities of water reducer and air entrainment were 76 g and 60 g separately in each concrete mixture.

3.1.5 Polypropylene Fiber

Polypropylene fibre is commonly used to reinforce concrete, and it controls cracking and reduces shrinkage. The crack will develop in the concrete when the tensile stress is larger than the tensile strength. The polypropylene fibre acts as crack arresters that can hold the mortar. The polypropylene fibre used in this study was MasterFiber F100, as shown in Figure 3-6. The physical properties of fibres are shown in Table 3-3. 160 g of 19 mm long polypropylene was added to each concrete mixture, separately. The addition of polypropylene fibres will not affect the mix design of the concrete mixture and there is no requirement for the slump modification.

Figure 3-6 Polypropylene Fibres with the Length of 19 mm

Table 3-3 Physical Properties of Polypropylene Fibre (MasterFiber 2021)

Length	19 mm
Specific gravity	0.91
Absorption	Nil
Alkali resistance	Excellent
Tensile strength	415 MPa
Modulus of Elasticity	5.52 GPa

3.2 Concrete Production

3.2.1 Aggregate Preparation

Before the concrete production, the RCA was washed with clean water to make sure that there was no dust, and particle from other wastes like wood, glass, plastic, metals etc. After the washing process, the RCA was put into the oven to be dried out at 110 ± 5 °C for 24 hours.

3.2.2 Concrete Mix Design

Four concrete mixtures were proposed based on mechanical performances and stability considerations. Except the Control Mix, other mixtures have different RCA replacement levels and different supplementary cementitious materials contents. The Control Mix only contained natural aggregates and was without slag and glass pozzolan. The coarse aggregates were replaced with coarse RCA at two different levels, 20% and 40% by mass. Mix 2 only used slag to partially replace limestone cement, and both slag and glass pozzolan was used to replace limestone cement in Mix 3. Table 3-4 outlines the designation of each concrete mixture.

Table 3-4 Concrete Mixture Summary

Concrete Mixture	Natural Aggregate (%)	Recycled Concrete Aggregates (%)	Portland Limestone Cement (%)	Slag (%)	Glass Pozzolan (%)
Control	100	0	100	0	0
Mix 1	80	20	100	0	0

Concrete Mixture	Natural Aggregate (%)	Recycled Concrete Aggregates (%)	Portland Limestone Cement (%)	Slag (%)	Glass Pozzolan (%)
Mix 2	80	20	80	20	0
Mix 3	60	40	70	20	10

3.2.3 Concrete Batching and Curing

A 3.5 cubic feet drum mixer was used to prepare all concrete mixture, as shown in Figure 3-7.

Figure 3-7 Concrete Mixer Used for Concrete Batching

There are different batching procedures developed for concrete mixing with RCA. A two-stage mixing approach (TSMA) was proposed by Tam et al. to reduce the impact of high-water absorption of RCA. The results showed that denser concrete and an improved ITZ were obtained from the TSMA resulting in increased compressive strength (Tam, Gao, and Tam 2005). Kong et al. proposed the triple mixing method to improve the microstructure of ITZ, strength, and durability of RCA (Kong et al. 2010). illustrates three different batching methods which were developed for RCA preparation.

For the normal mix procedure, the coarse aggregates are added with a small amount of water before running the mixer. Then, the fine aggregates, cement, and the rest of the water are added when the mixer is running. All ingredients are mixed for 180 seconds and resting for further 180 seconds. The fresh concrete shall be homogenous after a 120-second final mixing (ASTM 2002).

In the TSMA, the mixing procedure is divided into two stages and the water is added two times with an equal half amount. The first stage is to premix RCA and natural aggregates for 60 seconds, then the half of required water is added in following by a 60-second mixing. In the second stage, the cement is added, and the left half amount of water is added after a 30-second mixing. The fresh concrete mixture will be ready after another 120-second mixing of all added material and water (Tam, Gao, and Tam 2005).

The triple mixing method was developed based on the TSMA when there are admixtures, such as slag and fly ash, added to concrete mixtures. The natural aggregates and RCA are premixed for 15 seconds with a certain amount of water, then the admixture is added in followed by a 15-second mixing. The cement is then added to get the surface-coated aggregate with further 30-second mixing. The last step is to add the left water and the fresh mixture will be ready after the last 60-second mixing (Kong et al. 2010). The batching procedure of all mixtures in this study followed the TSMA as explained above, and all concrete mixture ingredients were measured by mass.

The cylinder moulds used in this study were 100×200 mm in diameter by length. Each mould was filled in three equal layers, and the fresh concrete should be distributed uniformly. The small steel tamping rod was used to consolidate the concrete by rodding 25 times for each layer. 25 strokes should be uniformly distributed across the layer surface. The air bubbles left by the tamping rod were released by tapping the sides of the mould 10 to 15 times with the rod. The third layer should be overfilled, and the top surface of the concrete was struck off with the tamping rod. After placing the lid on the mould, the specimens began the initial curing for 24 hours. All specimens were moist cured according to CSA A231.2-14 after the initial curing and demolding. All specimens were submerged in a saturated lime solution at temperatures around 23 ± 2 °C. The hydrated lime was used, and the moist curing was carried out in a water tank as shown in Figure 3-8.

a. Hydrated Lime b. Moist Curing of Cylinder Specimens

Figure 3-8 Hydrated Lime and Specimen Curing

3.2.4 Fresh Properties

Fresh properties of concrete control the long-term behaviour and performance of the concrete, which includes consistency, workability, segregation, bleeding, etc. Based on the CSA A23.1/23.2, the slump and air content of each fresh concrete mixture should be tested and meet the standard requirements.

The slump is a measure of consistency, and it also reflects the workability of fresh concrete. The higher slump means the higher workability of concrete. Each step of the slump testing should be performed properly as the result could vary to an improper procedure. The apparatuses include a cone shape test specimen with handles and foot pieces, around a straight tamping rod, a rigid, flat, and non-absorbent surface, or a base plate and a measuring tape. Due to the chemical reactions, the concrete mixture starts to change its state from fresh to hardened after mixing. Therefore, there is a time constraint for completing the test of a slump, which is within 10 minutes after obtaining the sample. The testing procedure contains preparation, first layer, the second layer, third layer, strike-off, mould removal, and slump measurement. The moist mould should be placed on the moist non-absorbent surface or a base plate resistant to vibration. After filling each layer, the tamping rod was used to rod 25 times uniformly distributing across the surface. There was excess concrete above the top of the mould after overfilling the third layer and rodding 25 times. Using the tamping rod to strike off the excess concrete, and spilled concrete on the plate should be removed. Raising the mould in around 5 seconds immediately after stepping off the foot pieces and placing the tamping rod on the top of the mould. The height difference between the rod bottom and concrete top was the slump number (CSA 2019c).

The pressure method is commonly used to measure air content within the concrete and the testing procedure is conducted according to CSA A23.2-4C. The apparatuses required in the air content test are similar to the apparatus used in the slump test, which includes a pressure vessel with the air meter and around a straight tamping rod, a rubber mallet, and a syringe, as shown in Figure 3-9.

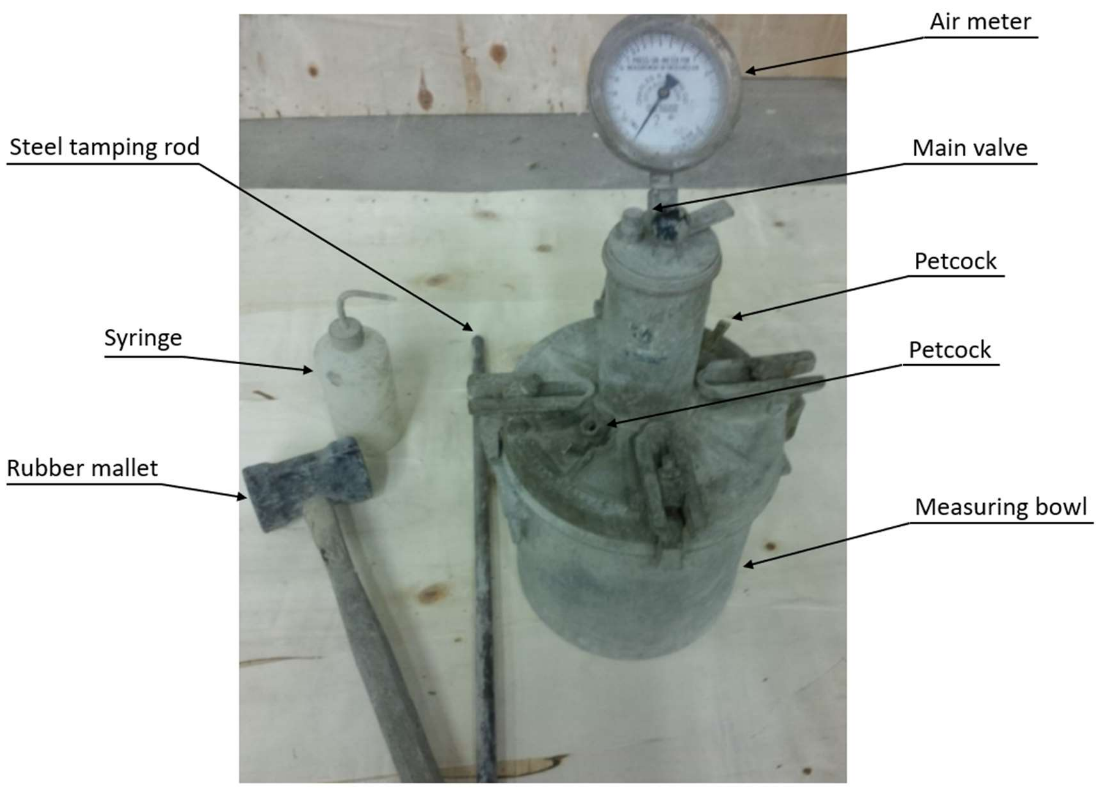

Figure 3-9 The Apparatuses Used in Air Content Test

The air content shall be measured after the slump test and the time constraint is within 10 minutes as well. The concrete was placed in three layers and rodded 25 times to consolidate each layer. After rodding, the bowl was tapped 10 times using the rubber head mallet to release air bubbles left within the concrete. The excess concrete was removed by the rod and the top surface must be levelled after this step. The edges of the bowl and the cover was cleaned properly without small pieces of material, like fine aggregate and sand, to ensure a pressure-tight seal. The gap between the cover and the top surface of the concrete was filled by water through the petcocks. Both petcocks were closed, and the air was released into the pressure vessel by opening the main valve. The percentage of air can be recorded from the air meter (CSA 2019b).

3.3 Compression Testing

3.3.1 Density

Before performing the compressive test, the density of concrete should be measured. The mass of each specimen was measured as shown in Figure 3-10. Therefore, the density was calculated by the volume and mass data, and the in-batch variability can be evaluated. The average result of three cylinders after curing for 28 days was the final density for each concrete mix.

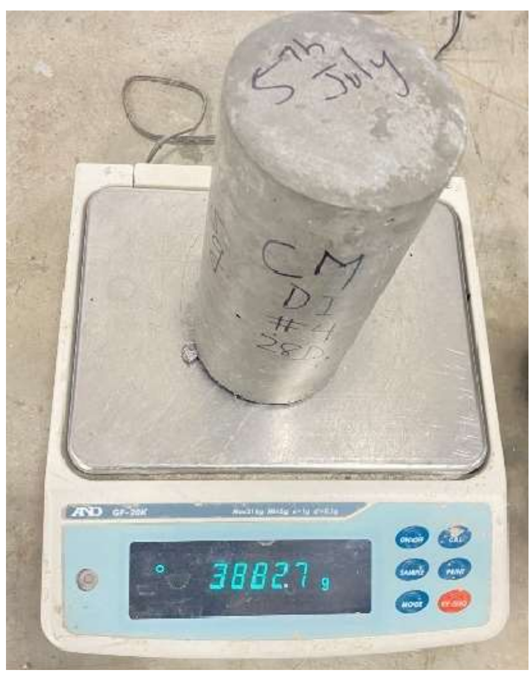

Figure 3-10 Measuring the Mass of Concrete Cylinder

3.3.2 Compression Testing

Compression testing of concrete cylinders was performed by CSA A23.1/23.2 (CSA 2019a). The cylinder samples were cast for standard size and tested on 1, 7, and 28 days after casting and curing. Testing was performed by the compression testing machine as shown in Figure 3-11. The numerical increment of this machine is 0.05% (1 KN). The loading pace rate is adjusted by the toolbar indicator, and the loading pace rate should be set around 0.15 to 0.35 MPa/sec before testing. Two steel spacers were used to hold the specimen, which ensures the uniformity of the cylinders and the contact of the entire surface area. Figure 3-11b shows a standard cylinder with compression load applied. The application of cylinders was to calculate the compression face area of the concrete. The peak force, peak stress, area of specimen, and loading pace rate will be recorded in the machine, and the real-time force-time graph is available when the machine is running. The average result of three cylinders was the final compressive strength for each concrete mix.

a. Compression Test Machine b. Testing Specimen

Figure 3-11 Concrete Compression Test

3.4 Finite Element Method

The Finite Element Method (FEM) is used in this study to analyze the overall mechanical response of interlocking concrete block pavement. A three-dimensional pavement model was established using FEM software ABAQUS, and the pavement layers included in the model are concrete blocks, bedding sand, cement-treated base, crushed aggregate base, and subbase. Many factors can contribute to the mechanical behavior of the pavement model, these factors include the shape of the block, the geometric design, the thickness of the block, elastic modulus, and the laying pattern of blocks. In this study, deflection and von Mises stress are the two major variables that were given special attention. Namely, this section of the study is seeking to find the effect of the ratio of length and width (rectangular blocks), thickness, elastic modulus, and the laying pattern on the deflection and von Mises stress of the interlocking concrete pavement.

3.5 Orthogonal Experimental Design

Orthogonal Experimental Design or Taguchi Orthogonal Array (OA), invented by Japanese Engineer Genichi Taguchi, is used for multi-factor and level experimental design. The Taguchi Array is balanced to ensure that all levels of all factors are considered equal. Therefore, the factors can be evaluated independently of each other despite the fractionality of the design (Weibull.com 2012). The biggest advantage of orthogonal experimental design is that it can significantly reduce the total number of tests. However, the limitation of this design method is that the optimum result is determined from selected combination, and it might not be the best result among all options. The interactions between the parameters should be considered when this method is applied.

In this study, four factors that were selected as the ICPB properties are the ratio between length and width of concrete blocks (rectangular blocks), the thickness, the elastic modulus, and the laying pattern of blocks. Each factor has three levels to investigate their impact on the deflection and load transfer efficiency of ICPB pavement. The levels for each factor are chosen according to the requirements in the specification of OPSS (Ontario Provincial

Standard Specification 2020). For example, the minimum thickness and aspect ratio are limited to ensure the ICPB meets the minimum functionality criteria.

The factors and levels of the selected design are shown in Table 3-5. The Orthogonal Array was obtained by an SPSS Orthogonal Array generator and is shown in Table 3-6, respectively.

Table 3-5 Factors and Levels of the Orthogonal Design

Levels	Factors			
	Length/Width[1] (N/A)	Thickness[2] (m)	Elastic Modulus (Pa)	Laying Pattern (N/A)
1	2:1	0.08	3.31E+10	Herringbone
2	3:1	0.10	3.30E+10	Stretcher
3	3:2	0.12	3.25E+10	Basket Weave

Note:

1. The length and width should align with the thickness level as the aspect ratio (Length/Thickness) ⩽ 4 for pedestrians and ⩽3 for vehicular application according to CSA-A231.2 of Ontario Provincial Standard Specification.
2. The thickness of the block should be greater than 60mm according to CSA-A231.2 of Ontario Provincial Standard Specification.

Table 3-6 Orthogonal Array for L9(3)

Model Number	R[1]	T[1]	P[1]	M[1]	Combination[2]
1	3	2	3	1	$R_3T_2P_3M_1$
2	3	3	1	2	$R_3T_3P_1M_2$
3	2	1	3	2	$R_2T_1P_3M_2$
4	2	3	2	1	$R_2T_3P_2M_1$
5	2	2	1	3	$R_2T_2P_1M_3$
6	1	3	3	3	$R_1T_3P_3M_3$
7	1	1	1	1	$R_1T_1P_1M_1$

8	3	1	2	3	$R_1T_1P_3M_1$
9	1	2	2	2	$R_2T_2P_3M_2$

Note:

1. R stands for Ratio of Length to Width; T stands for Thickness of blocks; P stands for Laying Pattern, and M stands for Modulus of Elastic.
2. The combination means the test model combination of factors and levels.

As the length/width are selected as one factor, the actual size of each geometric design is restricted by the aspect ratio, which is the ratio of length and thickness, to achieve two different usages of ICBP vehicular use or pedestrians. Therefore, the size of the block in each model is chosen to meet the requirements for such purposes. Furthermore, the change in the ratio of length to width can affect the display of each laying pattern, the typical laying pattern of interlocking paver (length/width=2:1) is presented in Figure 2-2. For the other ratio like 3:1 or 3:2, the display will be slightly different. The stretcher design will be the same regardless of the ratio of length and width, but for basket weave and herringbone, the laying pattern will be different, especially when the ratio of length and width is equal to 3:2, the basketweave is less like to achieve. The laying patterns of ICBP in different ratios of length and widths are shown in Figure 3-12.

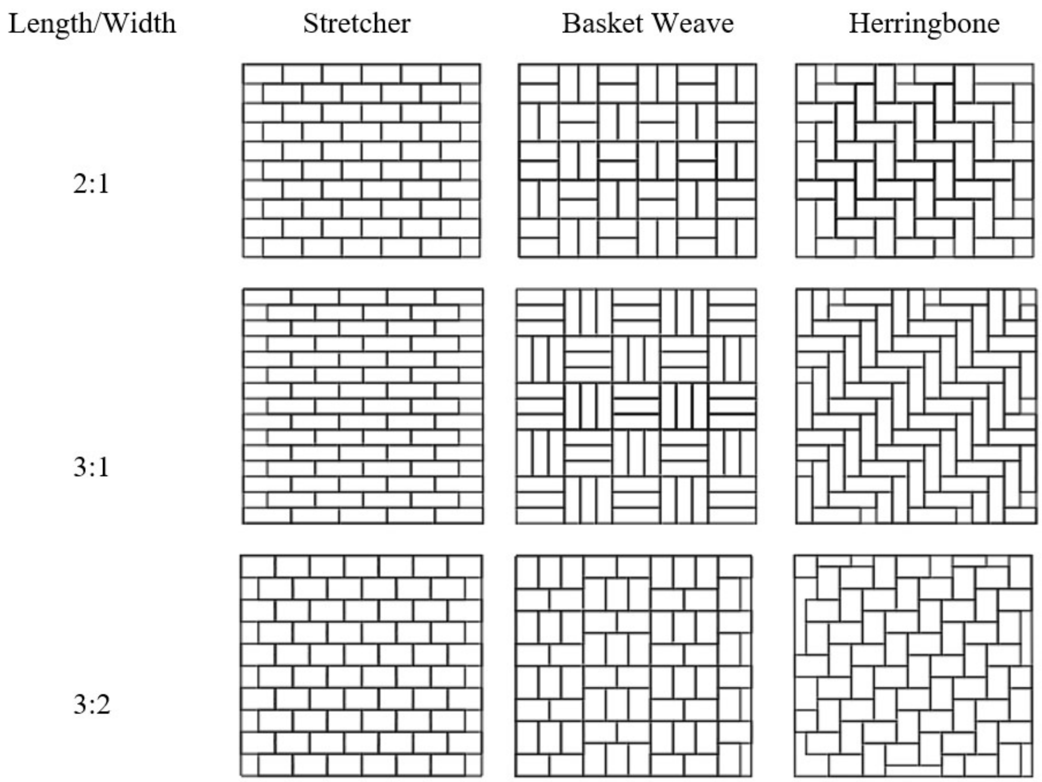

Figure 3-12 The Laying Pattern of Different Ratios of Length and Width

3.6 Summary

This chapter explained the research methods used in this thesis. The resources and properties of materials, concrete mix design, and batching method were introduced. The test procedures of fresh properties and compressive strength of concrete were briefly explained. The FEM technology was introduced as the main research tool for this research. The application of Orthogonal Experimental Design in the numerical analysis was explained as well.

Chapter 4 EXPERIMENTAL RESULTS AND DISCUSSION

4.1 Slump and Air Content

Because of the limited volume of the concrete mixer, each concrete mixture was prepared in two batches. The slump and air content tests were performed for each batch to ensure adequate concrete quality. The effects of different RCA replacement levels and the addition of SCMs on workability can be evaluated by the slump. Figure 4-1 illustrates the slump values for different RCA replacement levels and SCMs content, and the water-cement ratios are also shown in this figure.

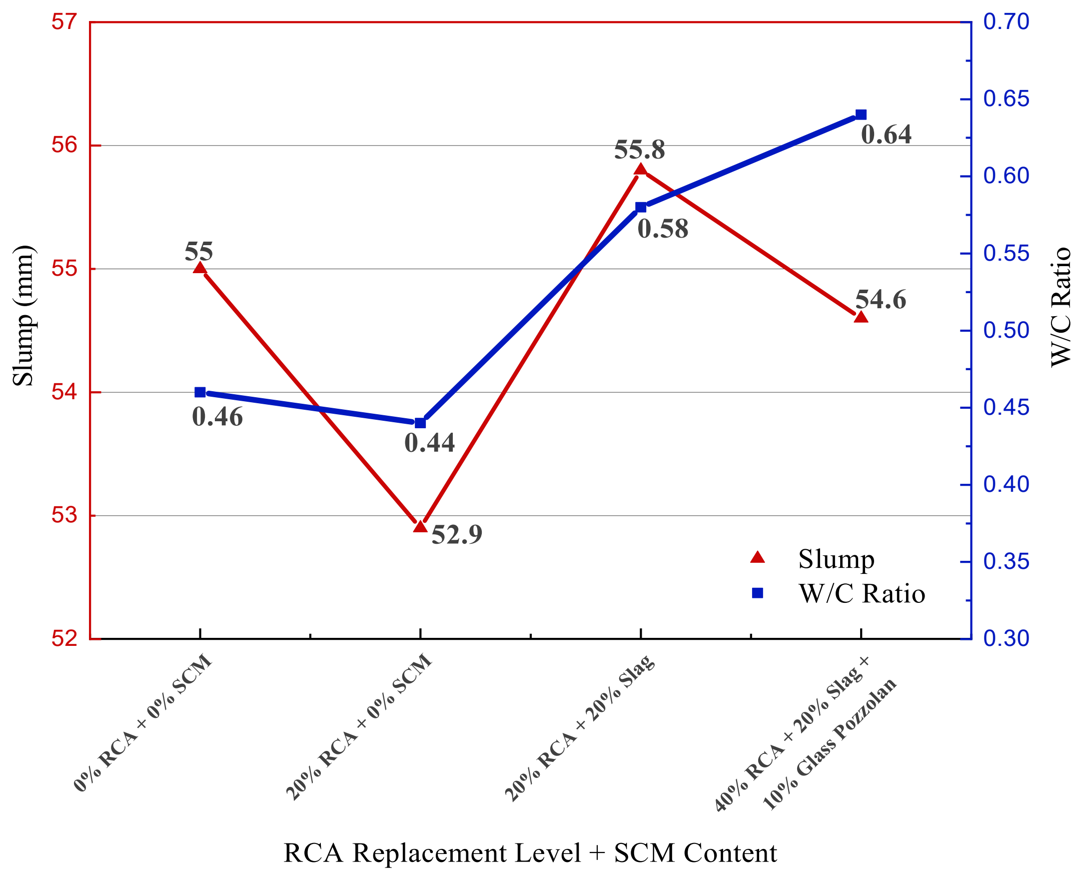

Figure 4-1 Slump and W/C Ratio for all Concrete Mixtures

All concrete mixtures exhibited slumps around 55 mm, and the variation was ± 5 mm. The replacement of RCA had two levels: 20%, and 40%. The slump value of Control Mix which did not contain RCA was 55 mm. Compared to the slump values between Control Mix and Mix 1, Mix 1 (20% RCA + 0% SCMs) had a lower slump value of 52.9 mm which was also the lowest value among all mixtures. When the RCA replacement level raised to 40 %, Mix 3 (40% RCA + 20% Slag + 10% Glass Pozzolan) had a lower slump value than Mix 2 (20% RCA + 20% Slag). It can be found that the higher RCA replacement level had adverse impacts on workability. However, the slump of Mix 3 was still higher than Mix 1 because of the addition of SCMs content. The water required to obtain adequate slump values also increased in general when the RCA replacement level increased. The main reason is that the residual mortar adhering to the RCA surface results in high water absorption of RCA. Additionally, the RCA used in this study was washed but did not get pre-treatments, such as microbial carbonate precipitation and carbonation, which can reduce the water absorption of treated RCA at different levels compared to untreated RCA (Danish and Mosaberpanah 2021). This results in a little amount of free water left in the fresh concrete mixture, which reflects on the slump values.

The air content tests were conducted according to CSA A23.2-4C (CSA 2019b). There was air entrainment used in all concrete mixtures to improve the freeze-thaw resistance and prevent segregation and bleeding of concrete. All mixtures had air contents from 4 to 7 %, as shown in Figure 4-2. For concrete indicated nominal maximum sizes of course aggregates in a range of 14 to 20 mm, the air content shall be between 4 to 7 % (CSA 2019b). The maximum size of course aggregates used in this study was 20 mm, therefore the entrapped air content fulfilled the requirement.

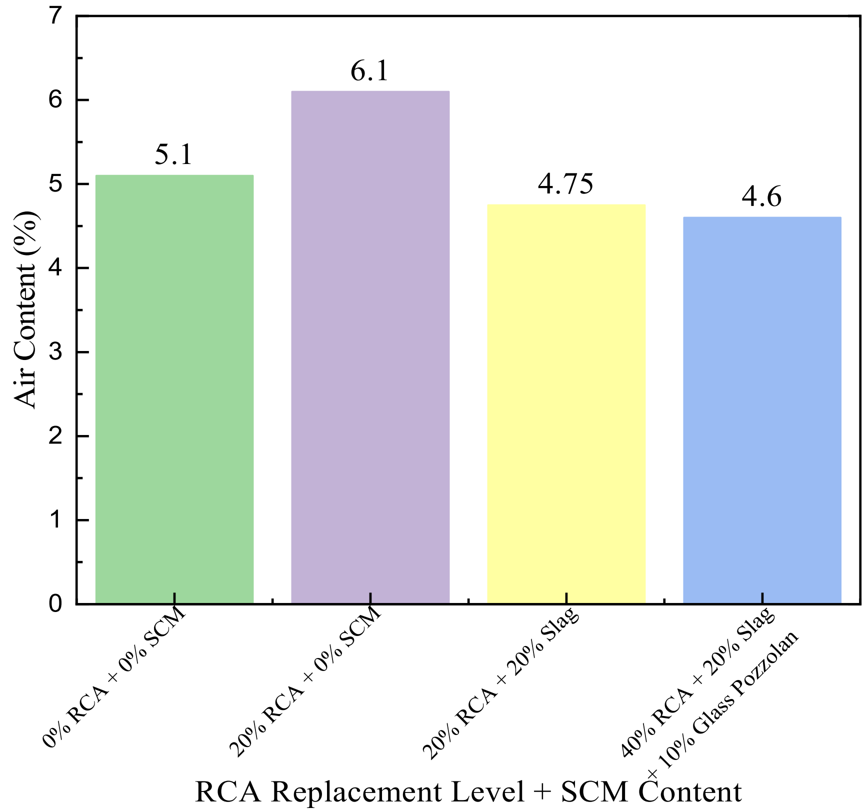

Figure 4-2 Air Contents for all Concrete Mixtures

Figure 4-2 showed that Mix 1 had the highest air content among all concrete mixtures because of the 20 % RCA. The porosity of RCA results in extra trapped air compared to natural aggregates. For Mix 2 and Mix 3, the addition of SCMs reduced the air voids of fresh concrete because of their fineness. All air content results were acceptable and reasonable for air-entrained concrete mixtures according to the CSA standard (CSA 2019b).

4.2 Density

The mass of concrete samples was measured before performing the compressive test after 1, 7, and 28 days of curing. Then, the density was calculated by the volume and mass data. In Figure 4-3, the variation of concrete density over 28 days from casting is shown. The Control Mix had the highest density among all mixtures throughout the whole time as the natural aggregates are denser than the RCA. The changes in the density of all mixtures had the same pattern. Their densities kept increasing while the concrete samples were moist cured. Concrete density can decrease under other curing conditions according to the literature (Ferreira, De Brito, and Saikia 2012). The density of Mix 1 (20% RCA + 0% SCMs) was much lower than Control Mix as Mix 1 had 20% RCA. However, Mix 2 was denser than Mix 1 as the slag is finer than cement, which is easy to fill the pores of RCA. The density of Mix 3 (40% RCA + 20% Slag + 10% Glass Pozzolan) was the lowest among all mixtures as Mix 3 had 40% RCA. The increasing density slopes of Mix 2 and Mix 3 between 7 to 28 days were larger than these of Control Mix and Mix 1. The reason was that the hydration of slag happened later than cement hydration and the hydraulic activity is lower as well. The hydration products of SCMs strengthened the concrete between 7 to 28 days. Meanwhile, the pozzolan reaction depends on calcium hydroxide, one of the cement hydration products, and the glass pozzolan reacts until there is no free water, calcium hydroxide, or space. The characteristics of SCM's hydration also affected the strength development as discussed in the below section.

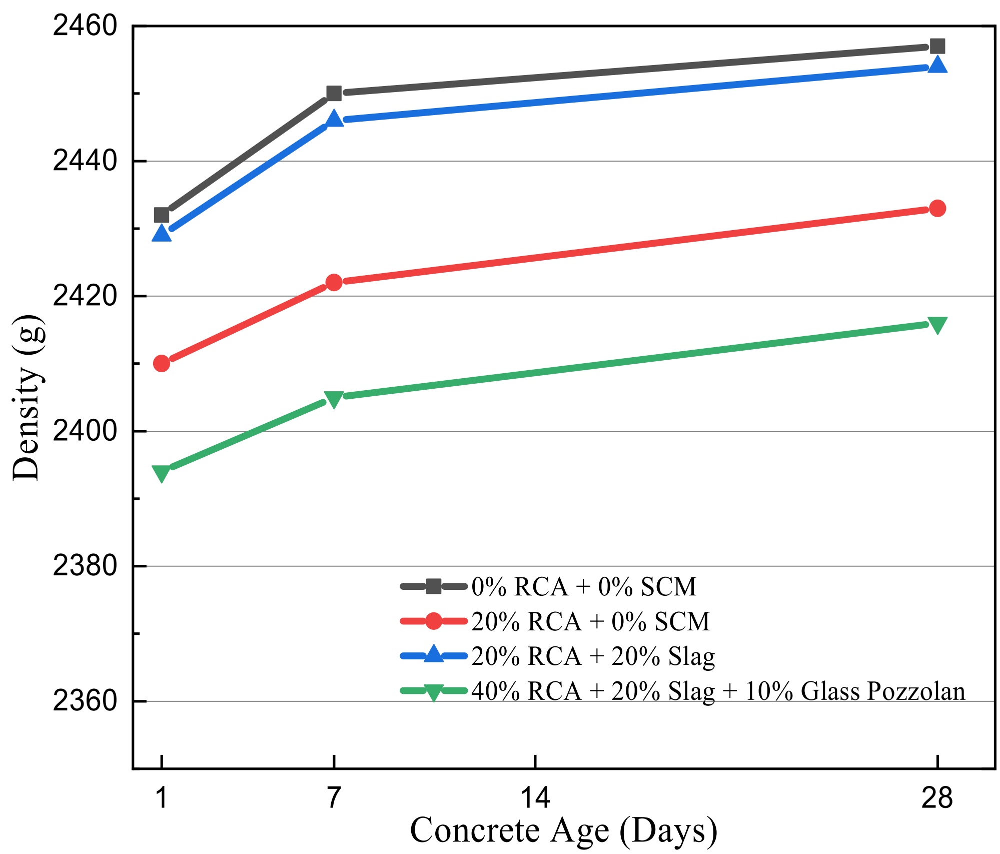

Figure 4-3 Density of all Mixtures Over 28 Days from Casting

4.3 Development of Compressive Strength

The compressive strength of each concrete mixture was tested on 1, 7, and 28 days after casting and curing, according to the procedure illustrated in Section 3.3.2. Figure 4-4 shows the compressive strength development for all concrete mixtures.

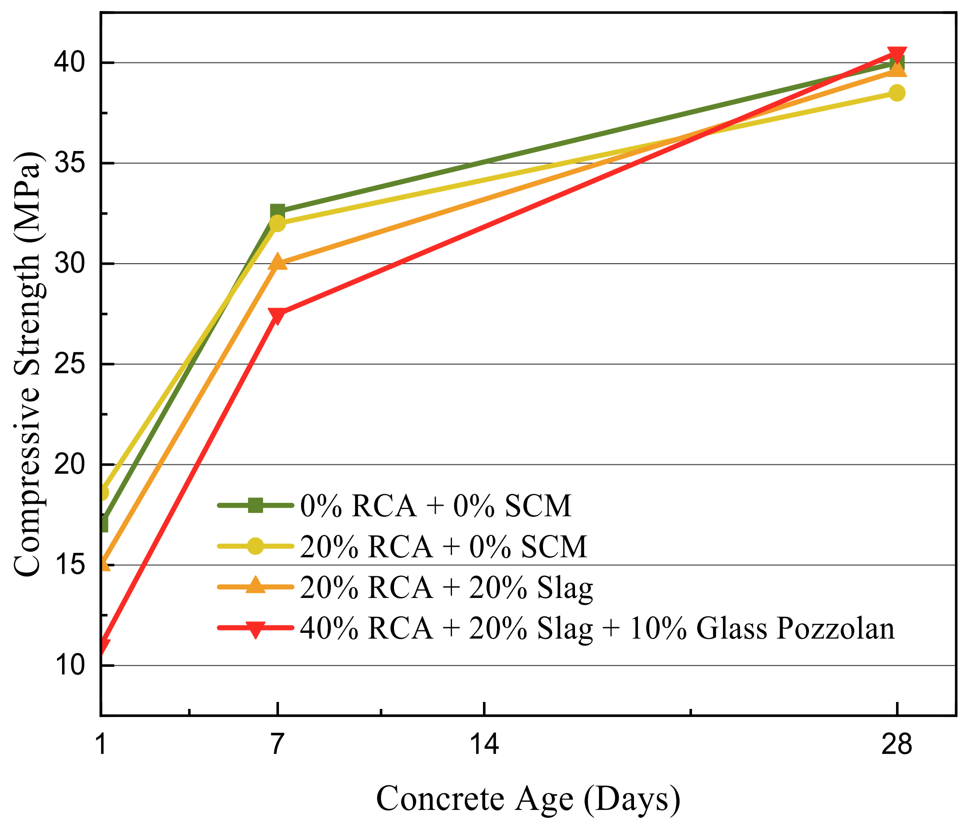

Figure 4-4 Compressive Strength Development for All Mixes Over 28 Days from Casting

The other three mixtures were designed based on Control Mix that only had natural aggregates and used 100% Portland-limestone cement. The 28 days compressive strength of the Control Mix was 40 MPa and it considerably increased from 17 MPa in 1 day. Predictably, the final compressive strength of Mix 1 (20% RCA + 0% SCMs) was lower than Control Mix because the 20% RCA affected the compressive performance. It also could be the consequence of the highest water/cement ratio of Mix 1 which was 6.1. The mix design of Mix 1 is unsatisfied if the 28 days compressive strength of Control Mix is considered as the design strength. The SCMs were used to improve the compressive performance of concrete with RCA as outlined in the research objectives. The 28-day compressive strength of Mix 2 (20% RCA + 20% Slag) was 39.6 MPa which was slightly lower than Control Mix. Compared to Mix 1, the addition of slag improved the final compressive strength, and the development of strength happened after 7 days of curing. The delayed strength development was more significant in Mix 3 (40% RCA + 20% Slag + 10% Glass Pozzolan). The compressive strength of Mix 3 increased from the lowest on 1 day, 11 MPa, to 40.5 MPa on 28 days, which was the highest strength among all mixtures. It was unpredictable as Mix 3 had 40% RCA even though the slag and glass pozzolan were added to improve the mechanical performance of concrete. Surprisingly, the 28 days compressive strength of Mix 3 even excessed that of Control Mix. The results proved the possibility to replace natural aggregates with RCA at a high replacement level when the SCMs are added.

4.4 Modulus of Elasticity

The modulus of elasticity is an important material property of hardened concrete. It is the ratio of the stress-strain curve of the concrete under applied loads. Normally, the modulus of elasticity of concrete can be determined by the compression test with the compressometer. Another method to determine the modulus of elasticity is calculating with formulas based on the compressive strength and unit weight of concrete. The design codes from ACI and CSA standards and their limitations are listed as below:

According to ACI 318-19, for normal-weight concrete:

$$E_c = 4700\sqrt{f_c'} \qquad \text{Equation 4-1}$$

According to CSA A23.3, for normal-weight concrete with the compressive strength between 20 to 40 MPa:

$$E_c = 4500\sqrt{f_c'} \qquad \text{Equation 4-2}$$

ACI and CSA also provided formulas for the modulus of elasticity considering the unit weight of concrete.

According to ACI 318-19, for concrete with a density between 1440 to 2560 kg/m^3:

$$E_c = 0.043 w_c^{1.5} \sqrt{f_c'} \qquad \text{Equation 4-3}$$

According to CSA A23.3, for high strength concrete with a density between 1500 to 2500 kg/m^3:

$$E_c = \left(3300\sqrt{f_c'} + 6900\right)\left(\frac{w_c}{2300}\right)^{1.5} \qquad \text{Equation 4-4}$$

Where:

E_c = Modulus of elasticity in MPa;

f_c' = Compressive strength of concrete in MPa;

w_c = Density of concrete in kg/m^3.

The estimated modulus of elasticity using formulas explained above of each concrete mixture in this study is shown in Table 4-1.

Table 4-1 The Estimated Elastic Modulus of Each Concrete Mixture Type (MPa)

Design Code	Control Mix	Mix 1	Mix 2	Mix 3
ACI 318-19	29719	29162	29600	29905
CSA A23.3	28454	27921	28341	28632
ACI 318-19 (Considering the density)	33129	32020	32976	32507
CSA A23.3 (Considering the density)	30671	29786	30560	30048

Equation 4-1 and Equation 4-2 are similar and only base on the compressive strength of concrete. The prediction results from Equation 4-2 are not considered as the compressive strength of Mix 3 was above 40 MPa. The prediction results from Equation 4-4 are not considered as it is applied for high strength concrete. Equation 4-3 consider both compressive strength and density of concrete. The calculated results from Equation 4-3 are used instead of Equation 4-1 in the finite element model because the use of RCA highly affected the density of concrete and this effect also showed in the compressive strength results.

4.5 Summary

In this chapter, the results of the laboratory tests were presented. The effects of concrete mixtures with different amounts of recycled materials on a slump, air content, density, and compressive strength were evaluated. The elastic modulus of all concrete mixtures was calculated according to the codes from standards, and the results calculated from ACI 318-19 based on both compressive strength and density were selected for the following modelling analysis.

Chapter 5 FINITE ELEMENT MODEL ANALYSIS

5.1 Introduction

The mechanical property of ICPB can be evaluated through various indoor laboratory tests, for example, the effect of different dosages of RCA on the elastic modulus of the concrete mixture was analyzed through the compressive test. However, for an interlocking paver, the mechanical behaviour of a single block is just one small component of the whole ICPB pavement, the performance of an interlocking concrete pavement is also related to the geometric design of the blocks such as the length/width ratio, the thickness, as well as the laying pattern. The impact of these factors on the overall performance of a pavement is unlikely to assess through simple indoor laboratory tests, but the Finite Element Method provides solutions for problems like this.

5.2 Modelling Parameters

The ABAQUS software was used in this study to investigate the effect of geometric and mechanical factors of ICPB on the overall performance of an interlocking pavement. The basic modelling parameters for the three-dimensional pavement model include geometric design, material properties, parts assembly, interaction property, loads and boundary conditions, and mesh techniques.

5.2.1 Geometric Design

The 3D ICPB pavement models were built through ABAQUS Standard/Explicit Model, the model design was based on CSA A231.2, OPSD 561.020, as shown in Figure 5-1, and AASHTO Pavement Design Guide. All models consist of five layers which are concrete blocks layer, bedding sand, cement-treated base, unbound dense-graded base, and subbase. The blocks with different sizes (0.3m×0.1m, 0.3m×0.15m, and 0.3m×0.2m) and thicknesses (0.08m, 0.1m, and 0.12m) in a rectangular shape were studied, and the dimensions of all blocks meet the standard requirements in CSA-A231.2 that the face area is less than 0.09 m^2 and the aspect ratio is less than 4. The detailed graphical design is presented in Figure 3-8 of Chapter 3.

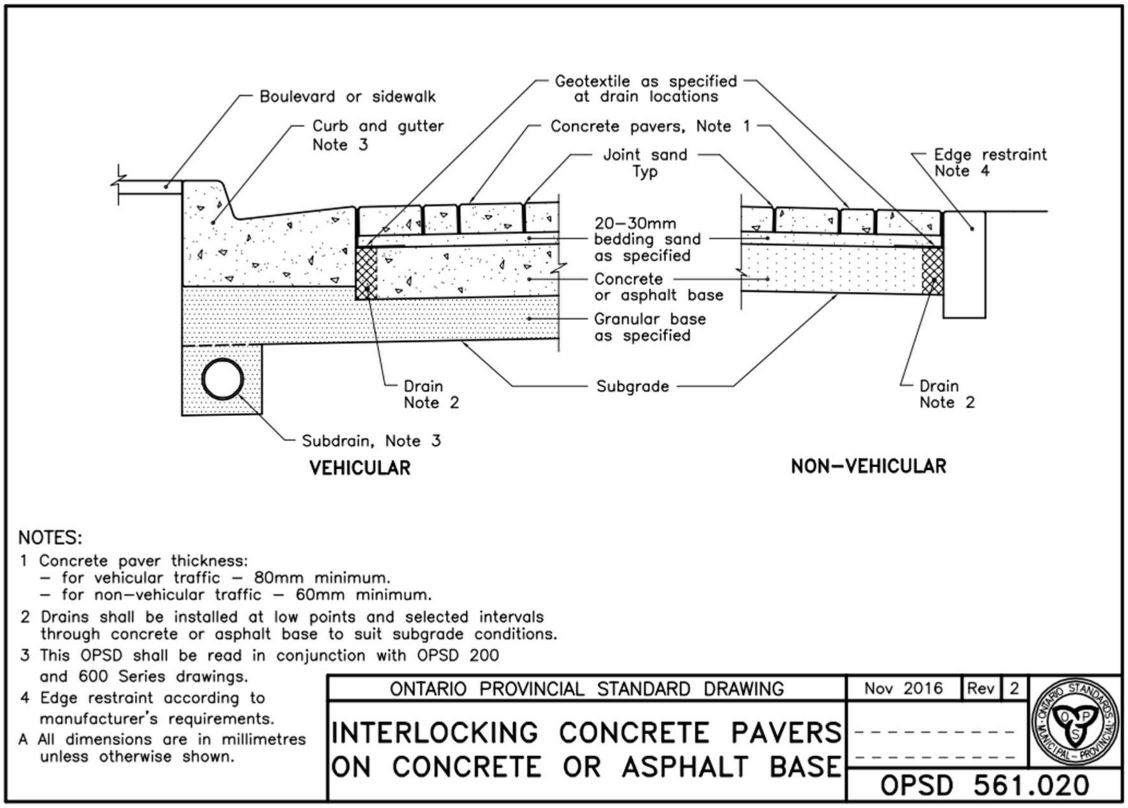

Figure 5-1 Interlocking Concrete Pavers on Concrete or Asphalt Base (OPSD 561.020)

The thicknesses of bedding sand, cement-treated base, unbound dense-graded base, and subbase were determined based on the design reliability, estimated traffic, service life, pavement drainage, subgrade, and base type (ICPI 2020c). In this study, models were designed with subgrade category 3, fair pavement drainage, 80% design reliability, lifetime traffic of 5,000,000 ESALs, and cement-treated base. An example of the geometric design of 3D ICBP models is displayed in Figure 5-2. The width and length of all models are 1.5m×1.5m considering the calculation time cost and accuracy requirement. The orthogonal design was carried out to evaluate the effects of concrete block size, block thickness, laying pattern, and concrete with recycled materials on the ICBP performances.

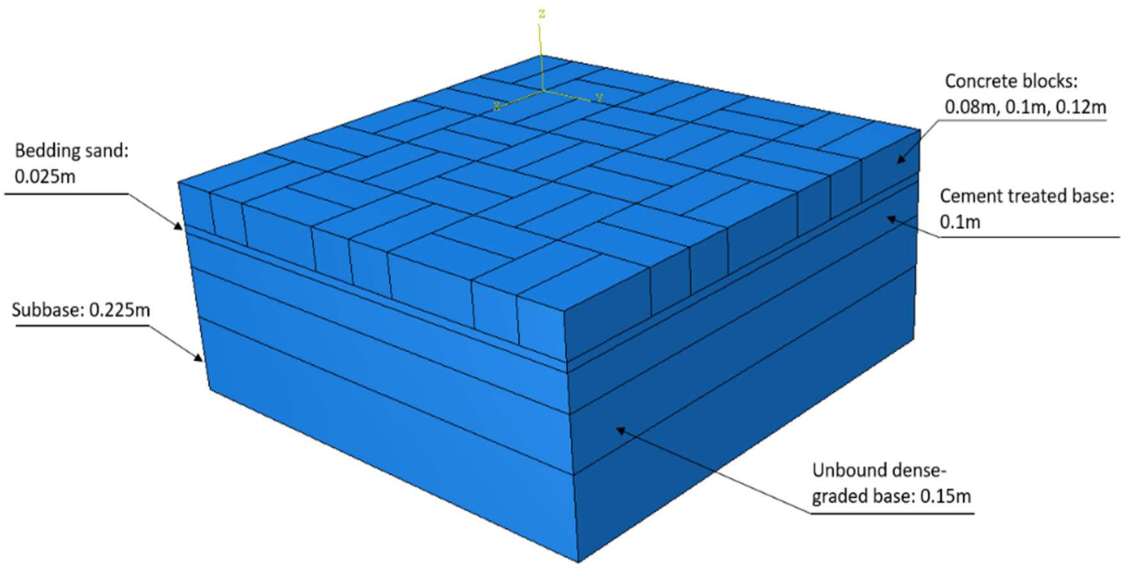

Figure 5-2 3D ICBP Model in Basket Weave Pattern

5.2.2 Material Property

The engineering property of each type of material and the simplification of their constitutive model are crucial for the accuracy of the results. In this study, all the materials are considered isotropic and homogenous. As the objective of this study is focused on the mechanical behaviour of interlocking concrete block layer, thus each material was assumed to be linear elastic, which is a reasonable and the most common assumption for brittle materials like concrete concrete, gravels, and other natural geotechnical materials (Raveendran Thulasibai et al. 2021)(Taheri, Fakhri, and Hayati 2021)(Gunatilake and Mampearachchi 2019).

In this research, the elastic modulus of concrete blocks was determined by the ACI 318-19 code based on the cylinder compressive strength and density. The calculated elastic modulus of Control Mix, Mix 2, and Mix 3 was used in finite element models to evaluate the possibility of using recycled materials in the ICBP. Density was obtained from the laboratory result, and Poisson's ratio was adopted as 0.3 for concrete blocks (Taheri, Fakhri, and Hayati 2021).

The bedding sand layer, cement-treated base, unbound dense-graded base, and subbase are homogeneous and isotropic elastic materials. The material properties were adopted from a study conducted by Taheri et al. (Taheri, Fakhri, and Hayati 2021). All the parameters defined in finite element models are shown in Table 5-1.

Table 5-1 Engineering Properties of Materials in Different Layers

Layer Materials \ Engineering Property (Unit)	Density (kg/m^3)	Elastic Modulus (Pa)	Poisson's Ratio (v)
Concrete Blocks Layer	2450	3.2507E+10	0.30
		3.2976E+10	
		3.3129E+10	
Bedding Sand	1735	7.00E+07	0.35
Cement Treated Base	2240	1.27E+10	0.20
Crushed Aggregate Base	2337	9.72E+08	0.30
Subbase	2210	6.22E+08	0.30

5.2.3 Contact and Interaction

Defining the contact condition and interaction properties for the connected surface in ABAQUS is important for a realistic simulation and accurate calculation results. However, this process can be extremely complex and sometimes hard to obtain the results one needed. Therefore, in this study, all the connected surfaces including block to block, block to bedding sand, and other contacted surfaces are assumed to have a friction coefficient of 0.3 to simplify the model calculation (Taheri, Fakhri, and Hayati 2021). It is worth mentioning that the contact between blocks is much more complex than other connected surfaces as the gap between blocks is filled with bedding sand, and these sands are not uniformly distributed due to the connection condition.

5.2.4 Loads and Boundary Conditions

A load of interlocking pavement includes traffic load and pedestrian load. For the simplicity of the modelling, a quarter of the traffic loads (1 ESAL = 80kN) are assumed to be uniformly distributed as a pressure in a shape of 0.3 m×0.3 m square (Figure 5-3), so the pressure of the loading area is 222222 Pa and the direction points downwards perpendicular to the pavement surface. It is worth noting that at least two elements of such assumptions are different from the reality: one is the actual shape of the vehicle tire and pavement are closer to an ellipse, not square, and the other is that the actual tire pressure distribution is non-uniform within the contacting area. However, an elliptical load will lead to a much more complex meshing issue and might cause a non-convergence issue, and the objective of the orthogonal experiment is to evaluate the effect of different factors on the overall mechanical behaviour for ICBP, therefore, the same loading quantity and area for all models can meet this need regardless of the actual loading condition.

The boundary conditions of the model consist of two parts, the sides, and the bottom. The bottom boundary condition is set as ENCASTRE, which means the bottom is fully restricted to have any form of movement. For the two sides of the x-plane, the boundary condition was set to XSYMM (U1=UR2=UR3=0), which restricts the translation of the direction of the x-axis and the rotation around the y-axis and z-axis. Correspondingly, For the two sides on the y-place, the boundary condition was set to YSYMM (U2=UR1=UR3=0).

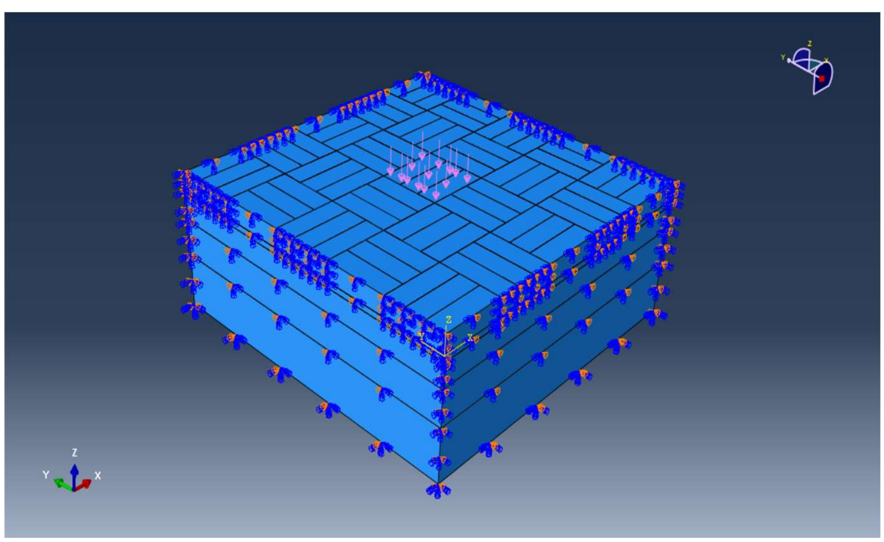

Figure 5-3 Load and Boundary Conditions

5.2.5 Mesh Techniques

The meshing of a model is directly related to the accuracy of the simulation results, sometimes, the poor quality of a meshed model can cause non-convergence issues and the calculation process cannot be completed. In this study, two element types were selected to compare the calculation accuracy: hexahedral element and tetrahedral element. Global seed size of 0.05 m was selected for the hexahedral mesh models and 0.06 m for tetrahedral element models. This study focuses on the mechanical behaviour of the interlocking block layer; therefore, a finer mesh seed was applied for the interlocking paver layer, but it caused a non-convergence error for some models due to the complex contact condition. Thus, the separate mesh seed density method for different layers of ICBP was abandoned in this study.

For the hexahedral element models, the structural hexahedral unit was set as the mesh control and mesh elements were determined as C3D8R: an eight-node brick element, as shown in Figure 5-4a. For the tetrahedral models, the free tetrahedral unit was the mesh control method, and the element type was C3D10: a 10-node quadratic tetrahedron, as shown in Figure 5-4b. Particularly, the mesh layout of the interlocking block layer in the tetrahedral element could be affected by the laying pattern and loading surface partition. Some irregular meshed areas appeared where loading applies as shown in Figures 5-5a, b, and h. However, a similar situation did not appear in hexahedral element-based models (Figure 5-4a), this might be the result of the 0.05 m seed size, which is the common divisor of all the possible interlocking blocks dimension (0.3m, 0.1m, 0.15m, 0.2m) and model size (1.5 m*1.5 m).

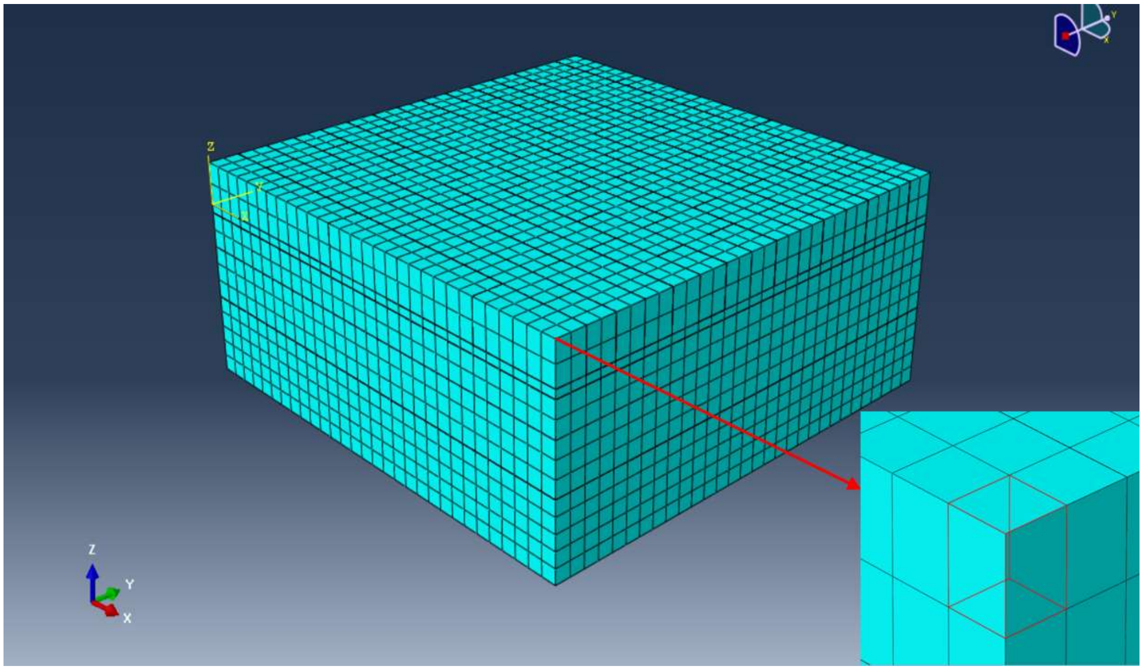

a. Hexahedral Mesh and C3D8R Element

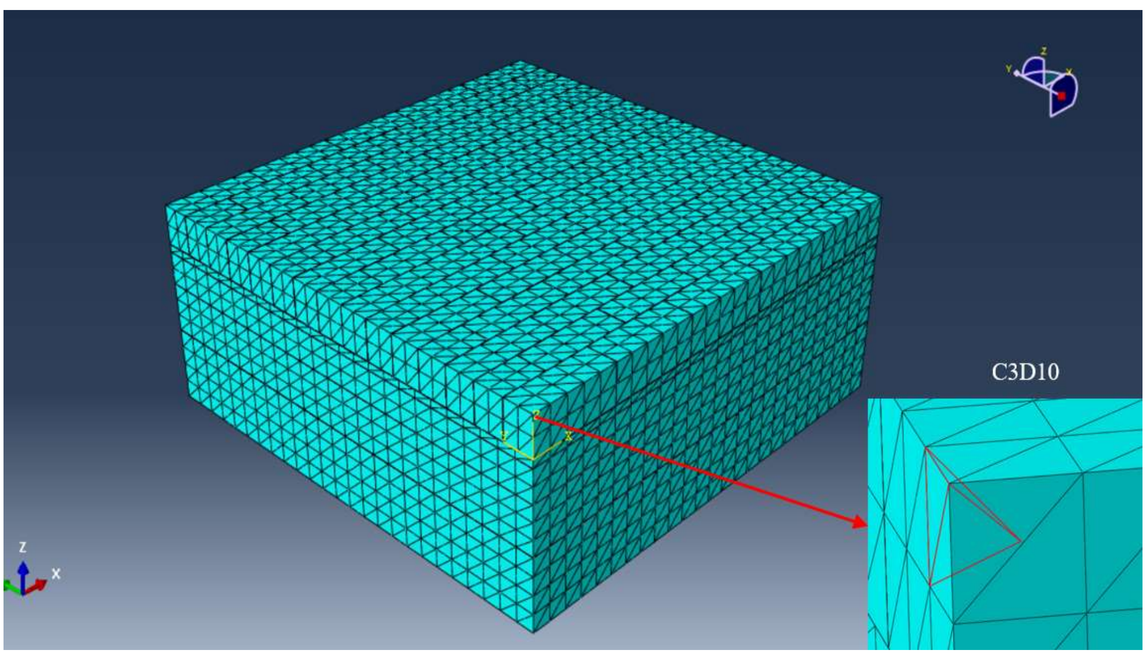

b. Tetrahedral Mesh and C3D10

Figure 5-4 Mesh Types for ICBP

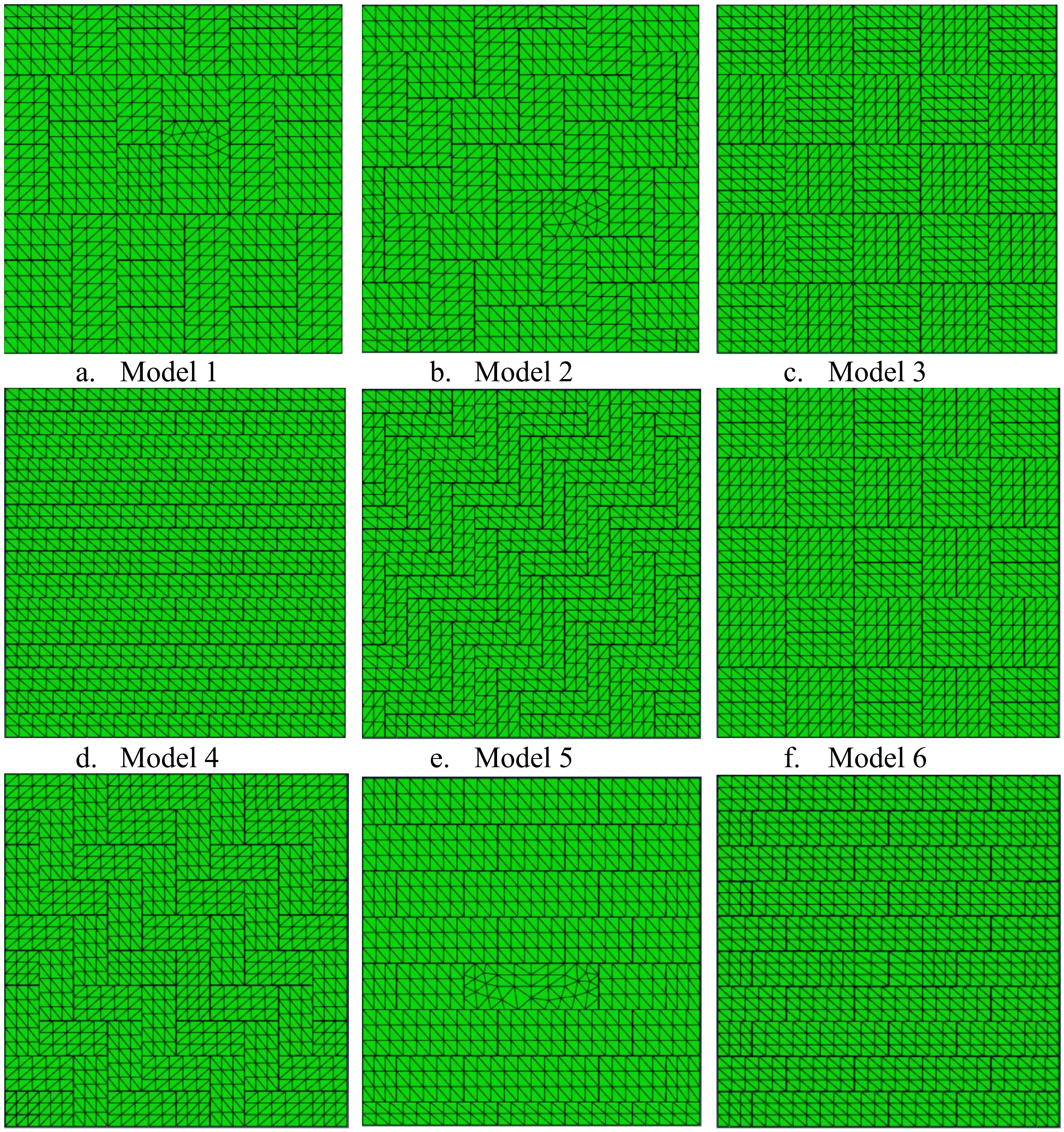

a. Model 1 b. Model 2 c. Model 3

d. Model 4 e. Model 5 f. Model 6

g. Model 7 h. Model 8 i. Model 9

Figure 5-5 The Impact of Laying Pattern on Tetrahedral Mesh Layout

The meshing details and calculation time for nine models in two mesh element types are shown in Table 5-2. Hexahedral meshed models have a much smaller number of modes and elements than tetrahedral meshed ones, and the calculation time is much shorter. For example, the calculation time of the hexahedron mesh model is only 4 minutes, which is almost 70 times less than that of the tetrahedron mesh model. Except for model 4, of which the seed size was set as 0.06 m, all the models that meshed in hexahedron that seeded at 0.05 m have almost the same number of elements. However, the calculation time of these models is varied, the same case for tetrahedron meshed models, namely the calculation time is less directly related to the number of nodes or elements as expected.

Table 5-2 Mesh Details and Calculation Time

Model #	Laying Pattern	Contacted Surfaces	Number of Nodes		Number of Elements		Calculation Time (min)	
			Hex	Tet	Hex	Tet	Hex	Tet
1	Basket Weave	110	18384	86050	11700	51003	4	278
2	Herringbone	88	18474	86453	11700	51146	4	34
3	Basket Weave	198	19140	84059	11700	48970	47	52
4	Stretcher	152	13640	91319	7778	52479	45	45
5	Herringbone	169	19230	91199	11700	52424	5	46
6	Basket Weave	133	18615	92984	11700	55020	39	45
7	Herringbone	193	18723	83721	11718	49117	5	44
8	Stretcher	103	18465	79553	11700	46982	136	194
9	Stretcher	103	18675	117632	11700	72611	48	80

Therefore, considering the complexity of mesh layout and calculation time of two different mesh techniques, the hexahedral element mesh was selected for the convenience of the result analysis.

5.3 Results and Discussion

All the above-mentioned models that considered multiple variables of materials and geometric design were calculated on ABAQUS. An example of von Mises stress and displacement calculation results for ICBP in herringbone laying pattern is presented in Figure 5-6a and b.

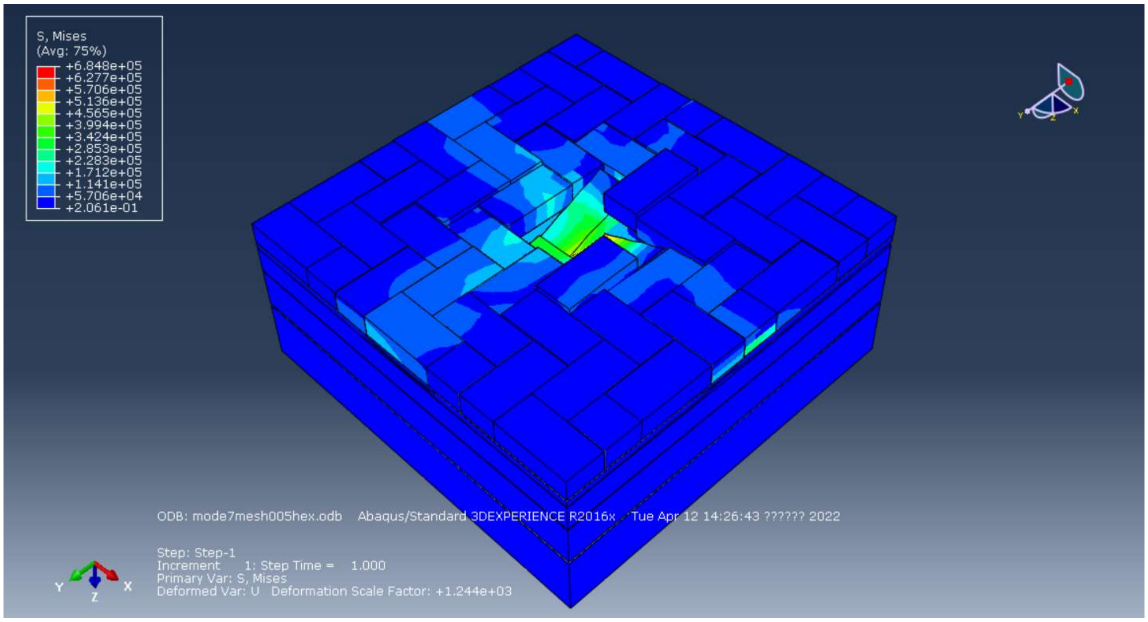

a. Von Mises Stress Result

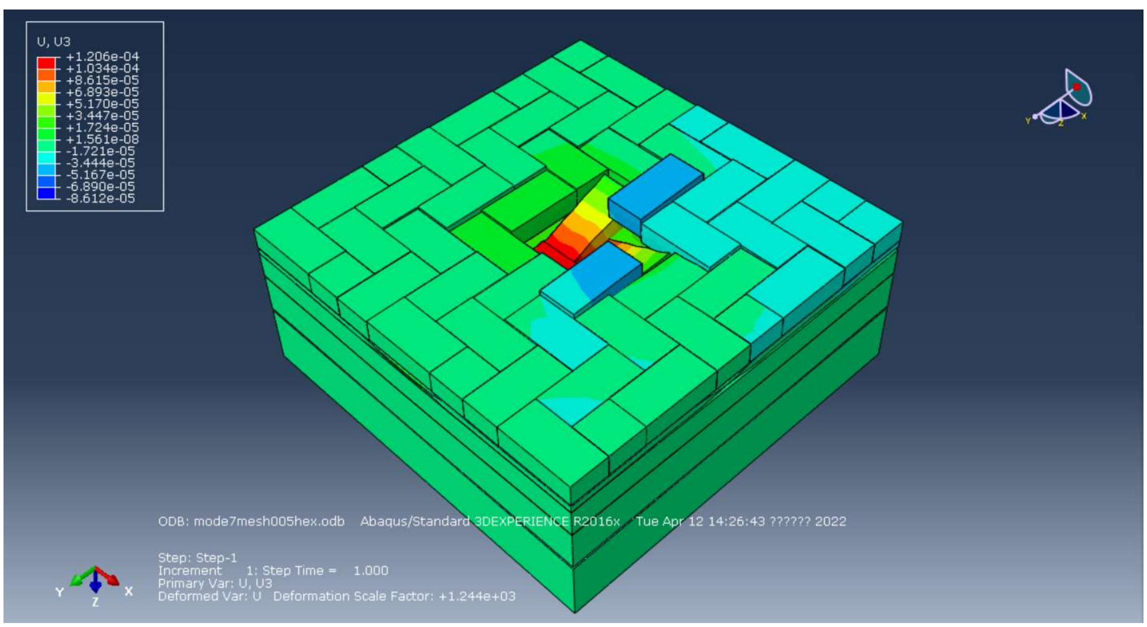

b. Displacement Result

Figure 5-6 Result of a Deformed ICBP Model in Herringbone Pattern

5.3.1 Analysis of Deflection

The deflection of the interlocking layer is the primary indicator for the whole pavement structure. In this study, the loading quantity and location were controlled the same for all nine FEM models, but the length/width ratio of interlocking, thickness, laying pattern, and the elastic modulus in three different levels was assigned to each model. In ABAQUS, the pavement deflection was reflected by model displacement U. There are four different kinds of displacements in the visualization section of the calculated model: magnitude displacement U, displacement in X-axis U1, displacement in Y-axis U2, and displacement in Z-axis U3. In this study, the deflection of the interlocking paver layer is displacement in Z-axis U3, the contour of displacement U3 for nine models are shown in Figure 5-7.

Figure 5-7 shows that the distribution uniformity of displacement is greatly affected by the abovementioned variables. It can be seen that basket weave laying pattern has the least displacement transferring effect, and namely the displacement of these three models has a concentrated loading area without expanding to a broader region from Figure 5-6a, c, and f. The reason might be, that in basket weave pattern, all the blocks can assemble into a square shape (see Figure 3-12), and these squares are not connected. Moreover, if the loading area was perfectly matched with the edges of the blocks, the loading is less likely to transfer to a further area. For example, for model 3 and model 6, each side of the square is matched with the block edge. Thus, the displacement contour is highly distinguishable from unloading areas. For model 1, model 4, model 8, and model 9, only one or two sides of the square are aligned with the block edge, so the other sides of the loading square can transfer part of the loads to a wider area.

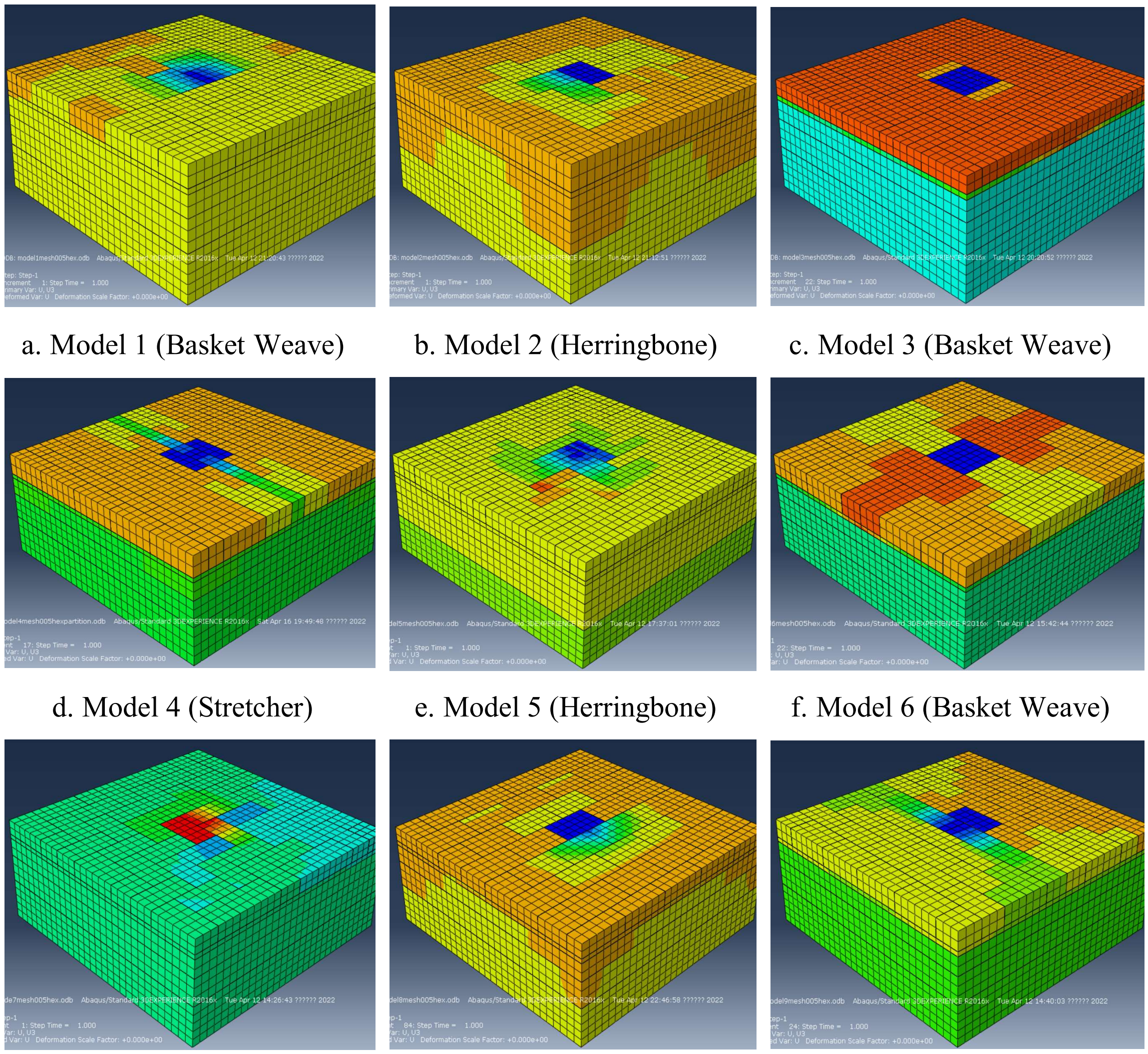

a. Model 1 (Basket Weave) b. Model 2 (Herringbone) c. Model 3 (Basket Weave)

d. Model 4 (Stretcher) e. Model 5 (Herringbone) f. Model 6 (Basket Weave)

g. Model 7 (Herringbone) h. Model 8 (Stretcher) i. Model 9 (Stretcher)

Figure 5-7 Undeformed Contour for Displacement U3

To further investigate the deflection transfer efficiency, displacement data of each model in three directions Y, X, and Z-axis were collected and drawn in Figure 5-8 to Figure 5-10.

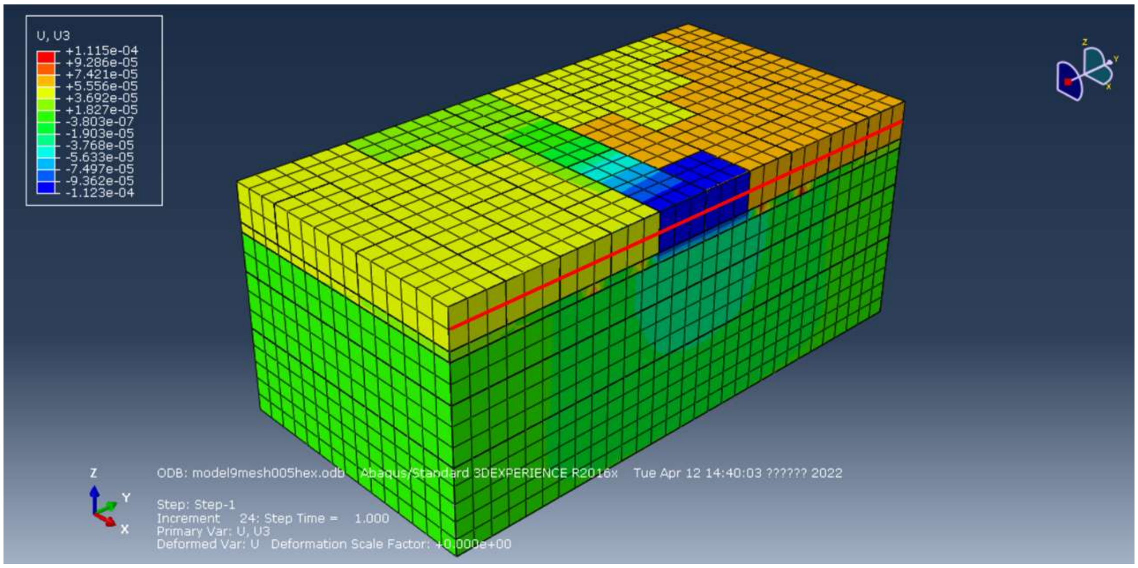

a. Collection Location of Displacement Points on Y-axis of Block Layer

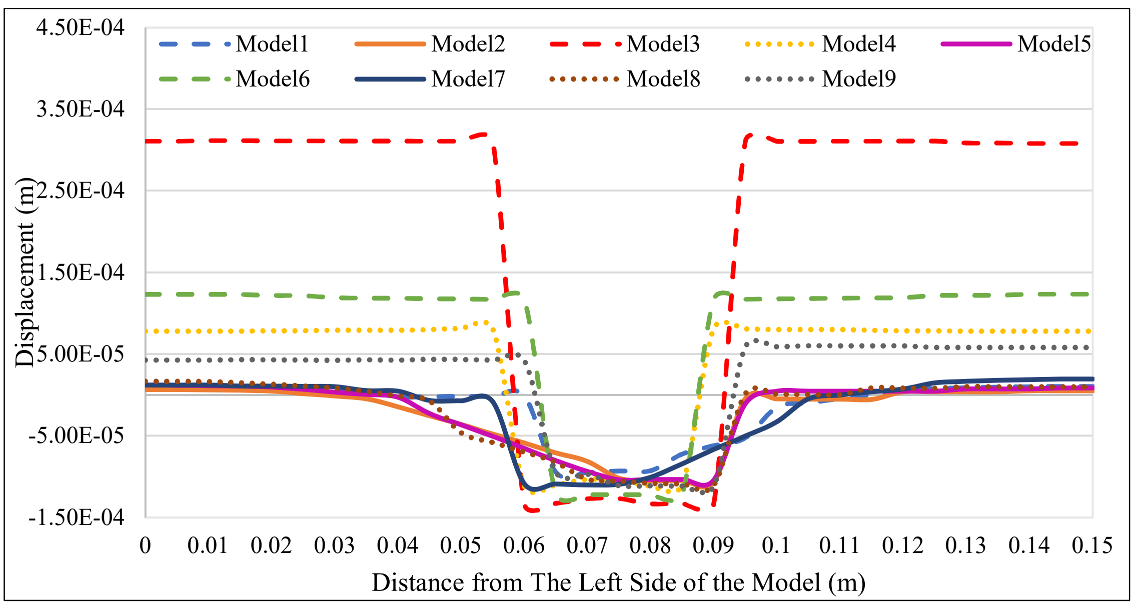

b. Deflection of Interlocking Blocks on Y-axis in the Middle of the Model

Figure 5-8 Location and Deflection Value for Block Layer on Y-axis

Figure 5-9 shows that in the Y-axis direction, during 0.06 to 0.09 m to the left side of the model. Model 3 shows the biggest deflection jump, namely, model 3 has the least deflection transfer efficiency, while model 2, model 5, and model 7 have the most uniform deflection transfer. Given that model 2, model 5, and model 7 are in herringbone laying patterns, this pattern might be better than the other two types. However, model 1 shows a similar deflection distribution trend as models 2, 5 and 7, which indicates that other factors such as length/width ratio, thickness, or elastic modulus play important roles in affecting the load transferring. Moreover, the displacement distribution of model 3, model 4, model 6, and model 9 is symmetric to the centerline as these laying patterns are symmetric to the X-axis.

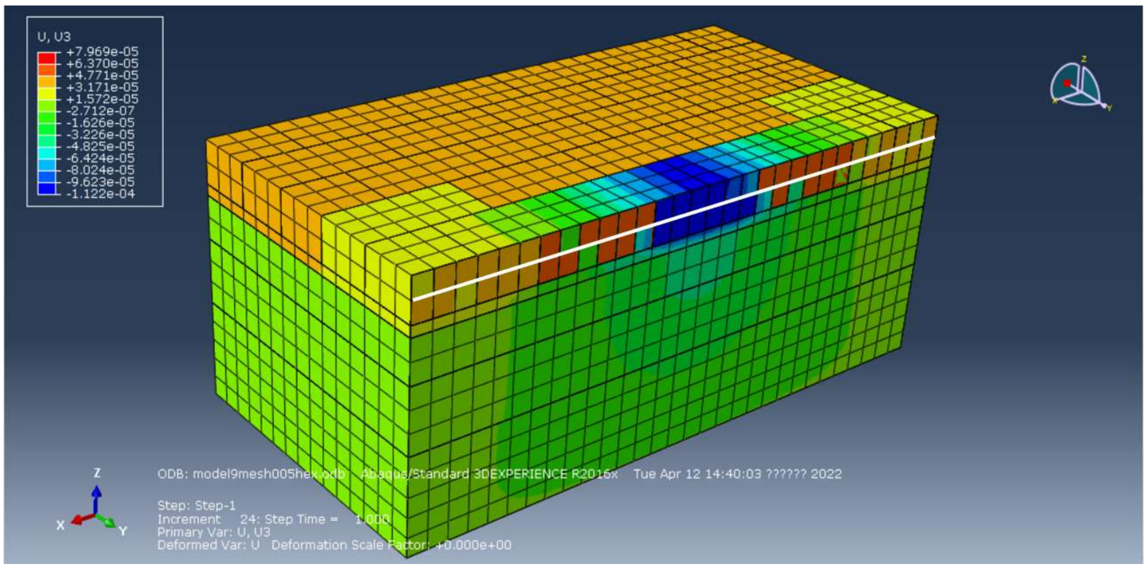

a. Collection Location of Deflection Points on X-axis of Block Layer

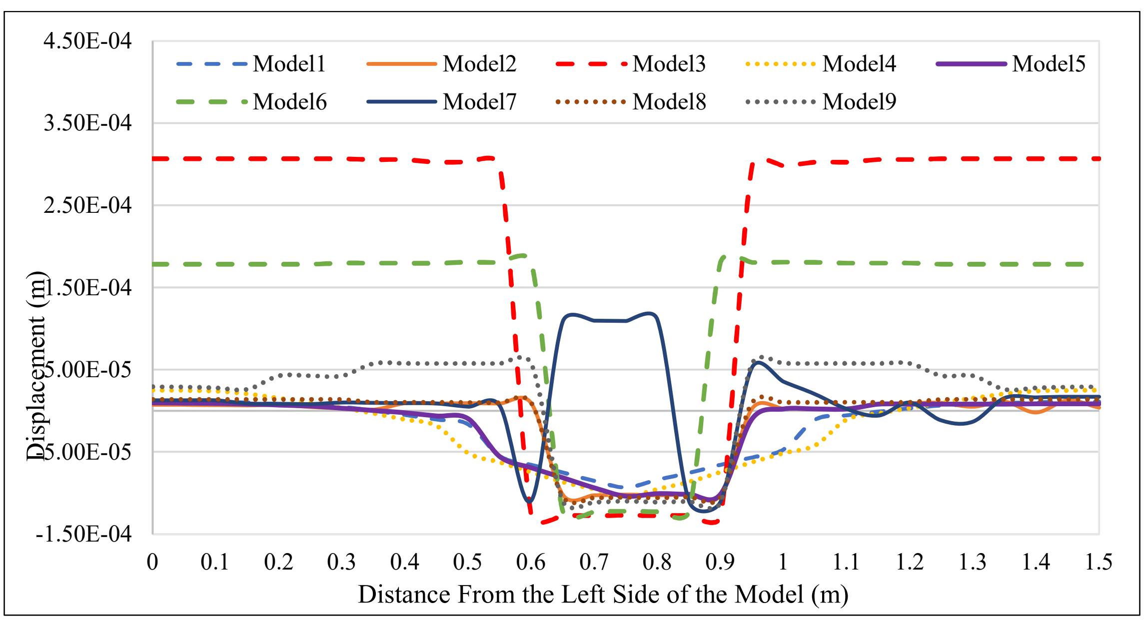

b. Deflection of Interlocking Blocks on X-axis in the Middle of the Model

Figure 5-9 Location and Deflection Value for Block Layer on X-axis

Figure 5-9 shows the deflection distribution of the center block layer in the X-axis direction, which presents a similar tendency as that of the Y-axis. It proves the findings that laying pattern might be the most important variable for load transfer.

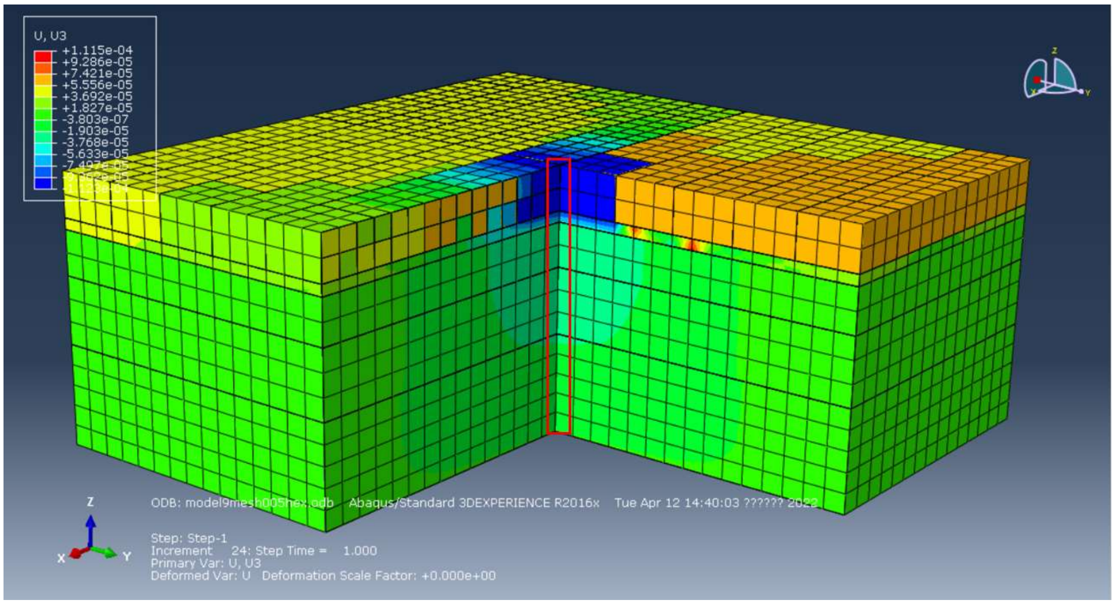

a. Collection Location of Deflection Points on Z-axis of ICPB

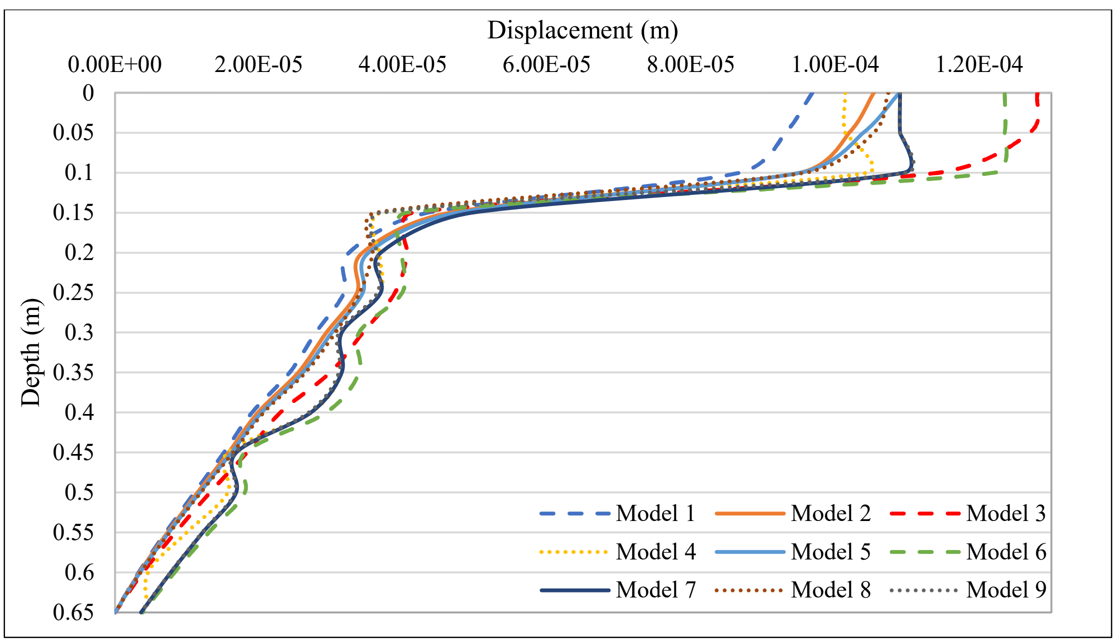

b. Deflection of ICPB on Z-axis in the Center of the Model

Figure 5-10 Location and Deflection Value for ICBP on Z-axis

Figure 5-10 presents that the displacement in the center of the model for all the nine models exhibited a similar development trend. The top layer of the model has the greatest displacement, and it decreases with the increase of depth. It shows that the most displacement or deflection occurs in the interlocking concrete block layer, the displacement drastically decreases in the bedding sand layer, approximately within depth 0.1m~0.15m.

5.3.2 Univariate Analysis of Variance for Deflection

To further investigate the influence of different variables on the deflection on the top center of the interlocking block layer, a univariate analysis of the general linear model was conducted for the performed models. The orthogonal array models input variables and observations are shown in Table 5-3. Notably, the deflection of the loading center was selected as the center block of each model, and the deflection values were probed from the four corners of the center block as shown in Table 5-3.

Table 5-3 Orthogonal Input Variables and Deflection Observations

Model #	Factors				Deflection of the Loading Center			
	R	T	P	M	m			
	N/A	m	N/A	MPa	Corner 1	Corner 2	Corner 3	Corner 4
1	3	2	3	1	8.42E-05	8.06E-05	1.94E-06	1.59E-05
2	3	3	1	2	8.28E-05	8.28E-05	1.08E-05	5.47E-06
3	2	1	3	2	1.32E-04	1.33E-04	1.34E-04	1.33E-04
4	2	3	2	1	8.30E-05	1.11E-04	1.01E-04	1.12E-04
5	2	2	1	3	1.02E-04	1.03E-04	1.01E-04	1.01E-04
6	1	3	3	3	1.22E-04	1.22E-04	1.22E-04	1.22E-04
7	1	1	1	1	1.09E-04	1.07E-04	1.09E-04	1.10E-04
8	3	1	2	3	1.01E-04	1.09E-04	1.02E-04	1.09E-04
9	1	2	2	2	1.10E-04	1.11E-04	1.11E-04	1.11E-04

The univariate analysis of variance for deflection is shown in Table 5-4. The null hypothesis of this analysis is that no statistical significance exists in a set of given observations, namely, the different factors won't affect the deflection of the ICBP center area. The significant level was chosen as 0.05.

Table 5-4 Tests of Between-Subjects Effects

Dependent Variable:	Deflection				
Source	Sum of Squares	Df [b]	Mean Square	F [c]	Sig. [d]
Corrected Model	3840.000[a]	8	480.000	288.000	0.000
Intercept	12321.000	1	12321.000	7392.600	0.000
R (Length/Width)	1578.667	2	789.333	473.600	0.000
T (Thickness)	384.000	2	192.000	115.200	0.000
P (Laying Pattern)	1322.667	2	661.333	396.800	0.000
M (Elastic Modulus)	554.667	2	277.333	166.400	0.000
Error	45.000	27	1.667		
Total	16206.000	36			
Corrected Total	3885.000	35			

Note:

a—R Squared = 0.988 (Adjusted R Squared = 0.985).

b—Degree of Freedom.

c—F value.

d—Significance Level.

Table 5-4 shows that the significance levels of all factors are less than 0.05, which means the null hypothesis was rejected and believe that these factors can significantly affect the deflection of the center area of calculated ICBP models.

5.3.3 Range Analysis of Deflection

Analysis of Variance is used to illustrate whether factors have a significant effect on the observations, while the Range Analysis can provide information like how much each factor affects the observations. The range analysis of deflection on the top center of the interlocking block layers is shown in Table 5-6. R, T, P, and M stand for factors, length/width ratio, thickness, laying pattern, and elastic modulus, respectively. The numbers in the table represent different levels as indicated in Table 3-5 in Chapter 3. The deflection results are the average value of the four corners in Table 5-4.

Table 5-5 Range Analysis of Deflection

Model #	Factors				Deflection
	R	T	P	M	
Unit	N/A	m	N/A	MPa	m
1	3	2	3	1	4.56E-05
2	3	3	1	2	4.55E-05
3	2	1	3	2	1.33E-04
4	2	3	2	1	1.02E-04
5	2	2	1	3	1.02E-04
6	1	3	3	3	1.22E-04
7	1	1	1	1	1.09E-04
8	3	1	2	3	1.05E-04
9	1	2	2	2	1.11E-04
K_1	3.42E-04	3.47E-04	2.57E-04	2.57E-04	Σ=8.75E-04
K_2	3.37E-04	2.59E-04	3.18E-04	2.90E-04	
K_3	1.96E-04	2.70E-04	3.01E-04	3.29E-04	
$\overline{K_1}$	1.14E-04	1.16E-04	8.55E-05	8.55E-05	
$\overline{K_2}$	1.12E-04	8.62E-05	1.06E-04	9.65E-05	
$\overline{K_3}$	6.54E-05	8.98E-05	1.00E-04	1.10E-04	
Optimum Level	R_3	T_2	P_1	M_1	
R_j	4.86E-05	2.95E-05	2.05E-05	2.41E-05	
Order of Effect	R > T > M > P				

Note:

K_i — The total value of observations of which the corresponding factors are in level i.

$\overline{K_i}$ — The average value of observations of which the corresponding factors are in level i.

R_j — The range of observations of which the corresponding factors are in level j.

Considering that the smaller the deflection is, the corresponding ICBP model has better deformation resistance, therefore, Table 5-5 shows that for factor R — the ratio of length and width, the level 3 (3:2) is the optimum level; for factor T — thickness, the optimum level is level 2 (0.1 m); for factor P— laying pattern, the optimum level is level 1 (Herringbone); and the factor M — elastic modulus, the level 1 (3.31E+04MPa) is the optimum level. The range value shows that the effect order of the four factors is: R > T > M > P. In other words, for the deflection of the top center of the interlocking blocks, the ratio of length and width has the greatest effect, and 3:2 is the optimum level for ratio; then comes with thickness and elastic modulus, the optimum level for the thickness is 0.1 m, and the optimum level for elastic modulus is 3.31E+04 MPa, means that higher elastic modulus has less deflection of the loading area. The laying pattern has the least effect on the deflection of the top center area, and the herringbone is the best level for reducing the deflection of the loading center.

Above all, the optimum combination for all the factors is herringbone laid blocks, of which the length and width ratio is 3:2 with a thickness of 0.1 m and elastic modulus of 3.31E+04 MPa could obtain a minimum level of deflection on the top center of the loading area.

5.3.4 Analysis of Von Mises Stress

The deflection analysis aims at evaluating the deformation resistance of interlocking block pavement, while the stress analysis focuses on the strength assessment of the pavement structure. It is widely believed that once a material's von Mises stress reaches its yield strength, the element is considered to have failed (Kuusisto 2017). Therefore, in this section, von Mises Stress was selected as the dominant stress to investigate the influence of different interlocking block factors on pavement strength.

In this section, to investigate the effect of laying pattern on the von Mises stress transferring efficiency within the interlocking block layer, nine models were divided into three groups according to their laying pattern. Model 1, Model 3, and Model 6 are in basket weave laying pattern, the von Mises stress distribution of the surface and the contour of the whole model were displayed in Figure 5-12. As mentioned previously, the laying pattern is greatly affected by the ratio of length and width of the block, especially for the basket weave pattern. Model 2, Model 5, and Model 7 are in herringbone patterns, the von Mises stress distribution of the surface and the contour of the whole model were displayed in Figure 5-13. Similarly, Model 4, Model 8, and Model 9 are in Stretcher laying pattern, the von Mises stress distribution of the surface and the contour of the whole model were displayed in Figure 5-14.

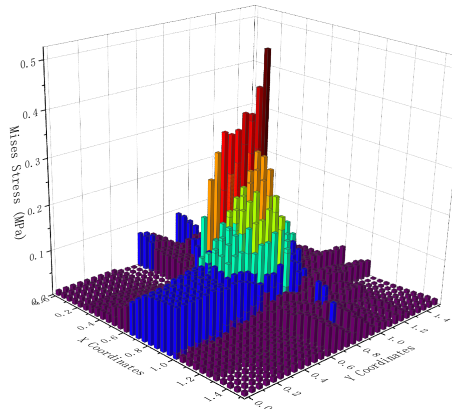

a. Mises Stress of Block Layer in Model 1

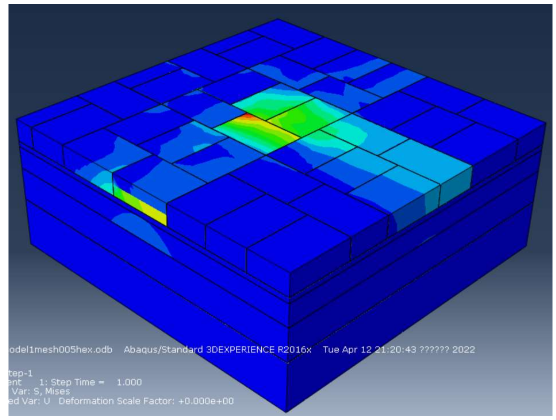

b. Mises Stress of Model 1

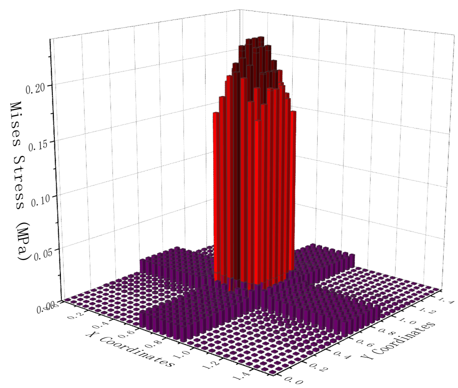

c. Mises Stress of Block Layer in Model 3

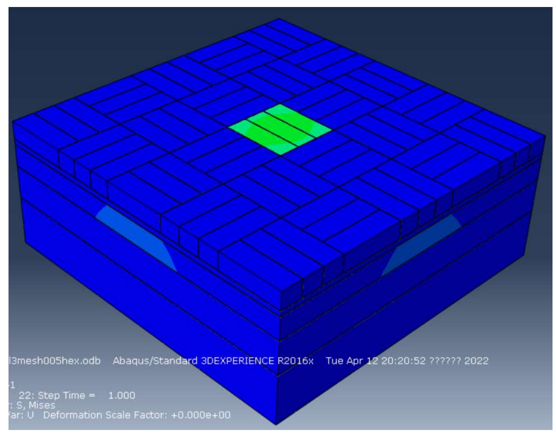

d. Mises Stress of Model 3

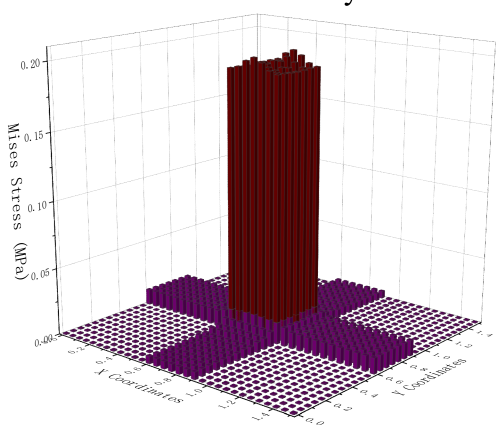

e. Mises Stress of Block Layer in Model 6

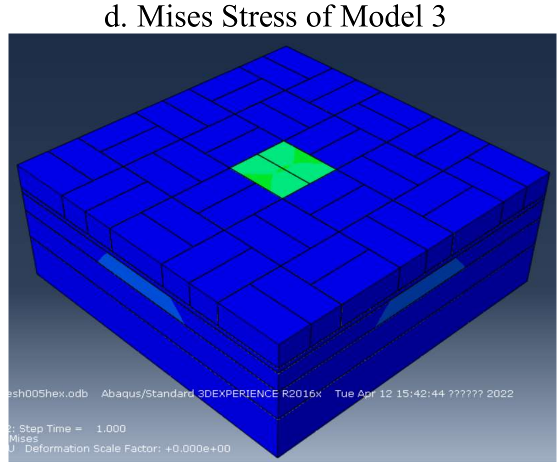

f. Mises Stress of Model 6

Figure 5-11 The Von Mises Stress of Basket Weave Models

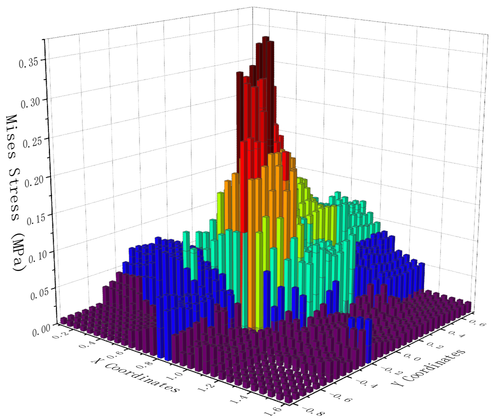

a. Mises Stress of Block Layer in Model 2

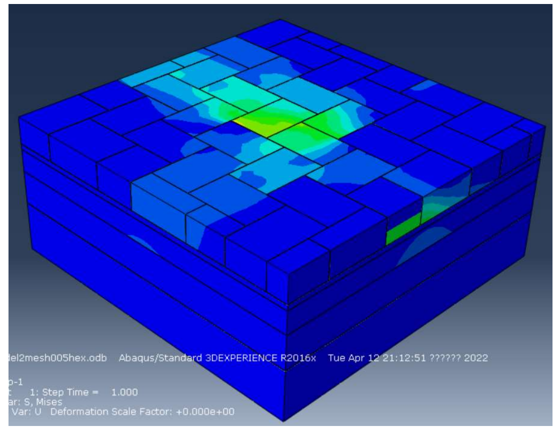

b. Mises Stress of Model 2

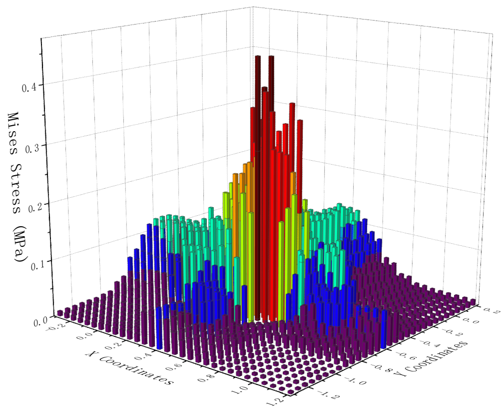

c. Mises Stress of Block Layer in Model 5

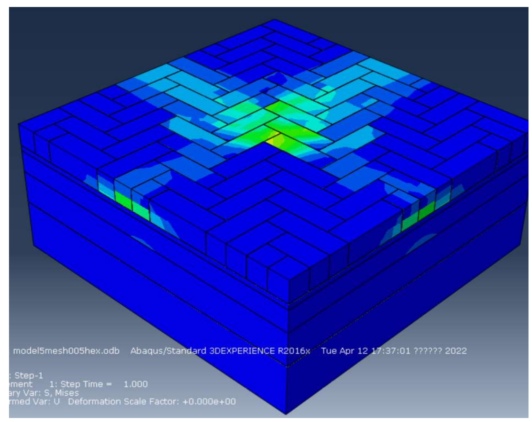

d. Mises Stress of Model 5

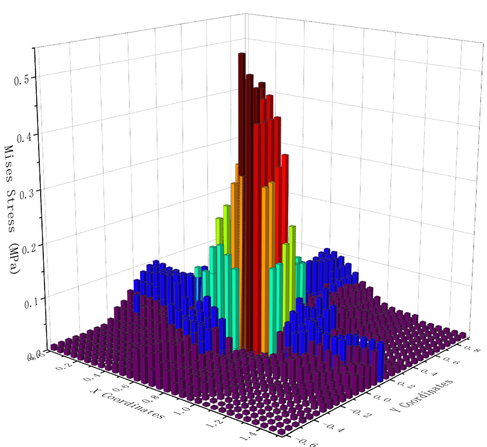

e. Mises Stress of Block Layer in Model 7

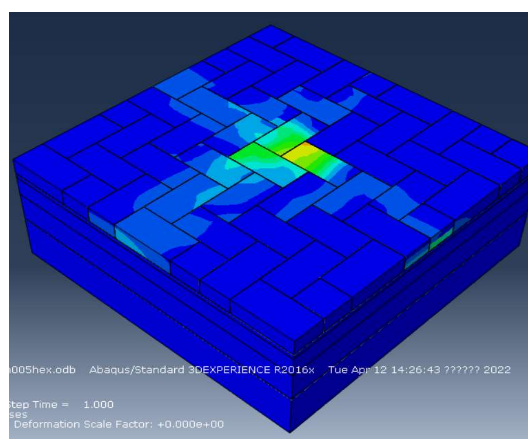

f. Mises Stress of Model 7

Figure 5-12 The Von Mises Stress of Herringbone Models

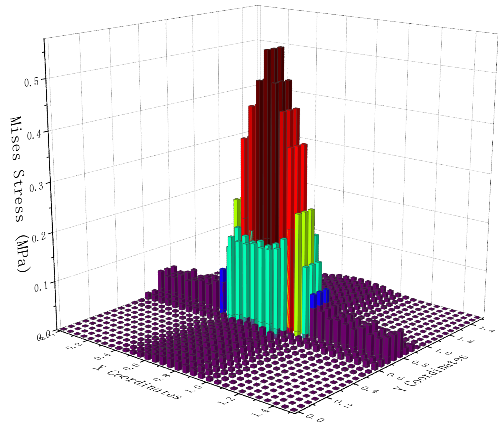

a. Mises Stress of Block Layer in Model 4

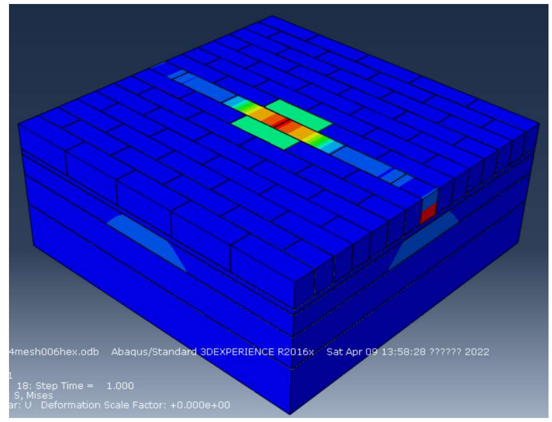

b. Mises Stress of Model 4

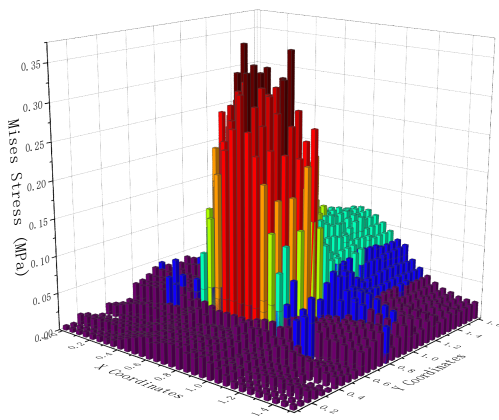

c. Mises Stress of Block Layer in Model 8

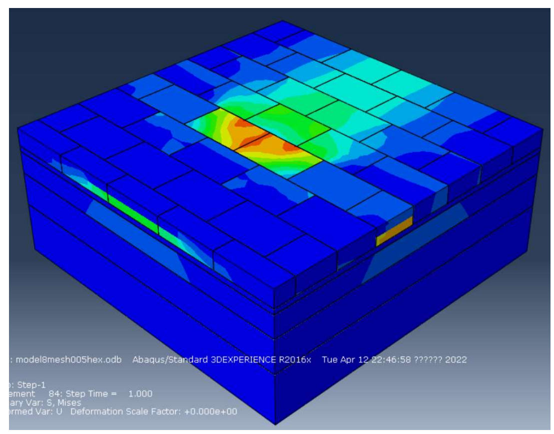

d. Mises Stress of Model 8

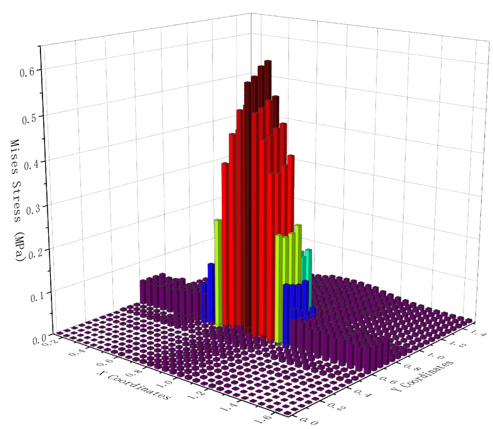

e. Mises Stress of Block Layer in Model 9

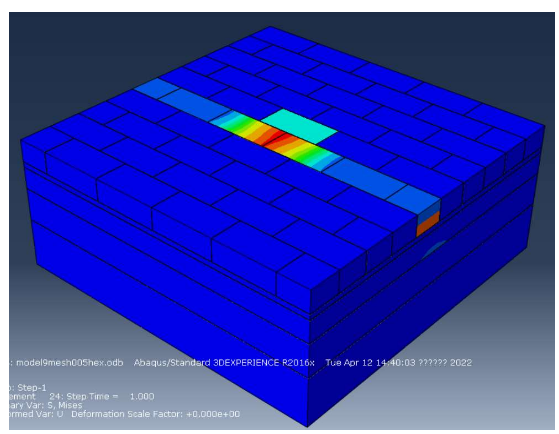

f. Mises Stress of Model 9

Figure 5-13 The Von Mises Stress of Stretcher Models

It shows from Figure 5-12 that except for model 1, the basket weave pattern has limited capacity to transfer the von Mises stress. The von Mises stress is mostly restricted with the loading area without spreading horizontally, this could be the result of the loading area being perfectly aligned with the edge of the block square in Model 3 and Model 6. However, Model 3 and Model 6 have lower von Mises stress levels than Model 1, which indicates that Model 1 might have the potential of block corner damage, while Model 3 and Model 6 could have the loading area sinking issue.

Figure 5-13 shows that the herringbone laying pattern has great load transferring. All three models show a various von Mises stress distribution within the whole surface area of each model. Compared to the basket weave pattern, the herringbone has higher maximum von Mises stress, which means the herringbone pattern is more likely to suffer from corner damage failure. From 5-13a, c, and e, it can be concluded that the maximum von Mises stress level is also related to other factors such as length/width, thickness, and elastic modulus.

Figure 5-14 shows that the stretcher laying pattern has intermediate capacity among other laying patterns in terms of load transfer. Model 4 and Model 9 has greater the maximum von Mises stress level than Model 8, this is also the result of the two sides of the loading area being perfectly aligned with the edge of the block in Model 4 and Model 9, thus the load was not able to spread to the further area. Moreover, the von Mises stress distribution for Stretcher laying patterns is highly symmetric along with the Y-axis.

To further investigate whether these aforementioned factors can significantly affect the von Mises stress distribution, a Univariate Analysis of Variance was conducted. Range Analysis was also conducted to investigate the impact order of these factors and the optimum level for each one.

5.3.5 Univariate Analysis of Variance for Von Mises Stress

The Univariate Analysis of Variance for Von Mises stress is conducted in this section to analyze whether the four factors have a significant impact on the von Mises stress distribution. The Orthogonal Input Variables and Von Mises Stress Observations were shown in Table 5-6. Similar to deflection, the significance level is determined as 0.05. The null hypothesis is that no statistical significance exists in a set of given observations, namely, the investigated factors won't affect the von Mises stress of the ICBP center area. The Tests of Between-Subjects Effects were shown in Table 5-7.

Table 5-6 Orthogonal Input Variables and Von Mises Stress Observations

Mode 1 #	Factors				Von Mises Stress of the Loading Center			
	R	T	P	M	MPa			
	N/A	m	N/A	MPa	Corner 1	Corner 2	Corner 3	Corner 4
1	3	2	3	1	0.25	0.38	0.09	0.14
2	3	3	1	2	0.33	0.37	0.20	0.13
3	2	1	3	2	0.17	0.17	0.17	0.17
4	2	3	2	1	0.43	0.43	0.43	0.43
5	2	2	1	3	0.35	0.30	0.18	0.13
6	1	3	3	3	0.19	0.19	0.19	0.19
7	1	1	1	1	0.34	0.33	0.15	0.20
8	3	1	2	3	0.33	0.37	0.20	0.13
9	1	2	2	2	0.17	0.17	0.17	0.17

Table 5-7 Tests of Between-Subjects Effects

Dependent Variable:	Von Mises Stress				
Source	Sum of Squares	Df [b]	Mean Square	F [c]	Sig.[d]
Corrected Model	3840.000[a]	8	480.000	288.000	0.000
Intercept	12321.000	1	12321.000	7392.600	0.000
R (Length/Width)	1578.667	2	789.333	473.600	0.000
T (Thickness)	384.000	2	192.000	115.200	0.000
P (Laying Pattern)	1322.667	2	661.333	396.800	0.000
M (Elastic Modulus)	554.667	2	277.333	166.400	0.000
Error	45.000	27	1.667		
Total	16206.000	36			
Corrected Total	3885.000	35			

Note:

a—R Squared = 0.988 (Adjusted R Squared = 0.985).

b—Degree of Freedom.

c—F value.

d—Significance Level.

Table 5-7 shows that the significance value of each factor is far less than 0.05, which means that all the factors significantly affect the distribution of von Mises stress.

5.3.6 Range Analysis of Von Mises Stress

Table 5-8 Range Analysis for Von Mises Stress

Model #	Factors				Von Mises Stress
	R	T	P	M	
Unit	N/A	m	N/A	MPa	MPa
1	3	2	3	1	0.22
2	3	3	1	2	0.26
3	2	1	3	2	0.17
4	2	3	2	1	0.43
5	2	2	1	3	0.24
6	1	3	3	3	0.19
7	1	1	1	1	0.26
8	3	1	2	3	0.17
9	1	2	2	2	0.20
K_1	0.65	0.6	0.76	0.91	Σ=2.14
K_2	0.84	0.66	0.8	0.63	
K_3	0.65	0.88	0.58	0.6	
$\overline{K_1}$	0.22	0.20	0.25	0.30	
$\overline{K_2}$	0.28	0.22	0.27	0.21	
$\overline{K_3}$	0.22	0.29	0.19	0.20	
Optimum Level	R_1/R_3	T_1	P_3	M_3	
R_j	0.06	0.09	0.07	0.10	
Order of Effect	M > T > P > R				

Note:

K_i — The total value of observations of which the corresponding factors are in level i.

$\overline{K_i}$ — The average value of observations of which the corresponding factors are in level i.

R_j — The range of observations of which the corresponding factors are in level j.

Like deflection, the Mises Stress in Table 5-8 is the average value of the four corners of the center block. The less von Mises stress means the structure is less likely to suffer from stress concentration. Table 5-8 shows that the optimum level for length/width is level 1 or level 3, which is 2:1 or 3:2; for thickness, the optimum level is level 1, which is 0.08 m. The table shows Basket Weave is the optimum level for laying pattern, and the optimum level for Elastic Modulus is level 3, which is 3.25E +04 MPa. It means that a smaller elastic modulus is good for reducing the von Mises stress of loading area. The order of effect for these four factors is Elastic Modulus > Thickness > Laying Pattern > Ratio of Length and Width.

Above all, the optimum combination for all the factors is basket weave laid blocks, of which the length and width ratio is 3:2 or 2:1 with a thickness of 0.08 m and elastic modulus of 3.25E+04 MPa could obtain a minimum level of von Mises stress on the top center of the loading area.

5.4 Summary

This chapter built nine 3D ICBP models considering four different geometric and mechanical variables that are directly related to the interlocking blocks: the length/width ratio, the thickness of the block, laying patterns, and elastic modulus of interlocking blocks based on the different proportions of RCA and other additives dosage. Univariate Analysis of Variance and Range Analysis was conducted for deflections and von Mises stress of the blocks within the loading area, and the results show that all the factors significantly affect the deflection and von Mises stress development, but the degree of effect is varied for deflections and von Mises stress. It was found that the optimum level for each factor is slightly different for deflections and von Mises stress as well, the combination of optimum levels for all the factors was provided at the end of each section.

Chapter 6 CONCLUSIONS AND RECOMMENDATIONS

6.1 Conclusions

The major conclusions of this research are outlined as follows:

• All concrete mixtures with the RCA replacement levels (20%, and 40%) exhibited slumps around 55 mm, and the variation was ± 5 mm.

• Mix 1 (20% RCA + 0% SCMs) had the lowest slump value of 52.9 mm among all mixtures. It can be found that the use of RCA had adverse impacts on workability.

• The water required to obtain adequate slump values also increased in general when the RCA replacement level increased. The main reason is that the residual mortar adhering to the RCA surface results in high water absorption of RCA. The pre-treatment can be used to reduce the water absorption of RCA according to other studies.

• All mixtures had air contents ranging from 4 to 7 %, and these contents fulfilled the requirement in CSA A23.2. Mix 1 (20% RCA + 0% SCMs) had the highest air content among all concrete mixtures as the porosity of RCA brings extra trapped air compared to natural aggregates. The addition of SCMs reduced the air voids of fresh concrete because of their fineness.

• The density of Mix 3 (40% RCA + 20% Slag + 10% Glass Pozzolan) was the lowest among all mixtures as Mix 3 had the highest RCA replacement level.

• The 28-day compressive strength of the Control Mix was 40 MPa and the 28-day compressive strength of Mix 1 (20% RCA + 0% SCMs), 38.5Mpa, was lower than Control Mix because the 20% RCA affected the compressive performance.

• The 28-day compressive strength of Mix 2 (20% RCA + 20% Slag) was 39.6 MPa which was slightly lower than Control Mix. Compared to Mix 1, the addition of slag improved the final compressive strength, and the development of strength happened after 7 days of curing.

• The compressive strength of Mix 3 (40% RCA + 20% Slag + 10% Glass Pozzolan) increased from the lowest on 1 day, 11 MPa, to 40.5 MPa on 28 days, which was the highest strength among all mixtures. It proved the possibility of replacing natural aggregates with RCA at a high replacement level when the SCMs are added.

• The use of RCA highly affected the density of concrete and this effect also showed in the compressive strength results. The modulus of elasticity calculated from the ACI 318-19 code was used in the finite element model as it considers both compressive strength and unit weight of concrete.

• In the Y-axis direction, the herringbone laying pattern might be better than the other two types as model 2, model 5, and model 7 have the most uniform deflection transfer.

• The top layer of the model has the greatest displacement, and it decreases with the increase of depth. It shows that the most displacement occurs in the interlocking concrete block layer, and the displacement drastically decreases in the bedding sand layer, approximately within depth 0.1m~0.15m.

• The univariate analysis of variance shows that length/width ratio, thickness, laying pattern, and elastic modulus of blocks can significantly affect the deflection of the loading area of interlocking concrete block pavement.

• Considering the deflection of the loading area of blocks, the length/width ratio has the greatest effect, then comes with thickness, elastic modulus, and laying pattern according to the Range Analysis.

• The bigger block size and higher elastic modulus of blocks could provide better performance. The combination of herringbone laying pattern, length/width ratio of 3:2, block thickness of 0.1 m, and elastic modulus of 3.31E+04 MPa is recommended with a minimum deflection on the loading area.

• The von Mises stress of models in basket weave pattern is mostly restricted with the loading area without spreading horizontally. The herringbone laying pattern has great load transferring as von Mises stress is distributed within the whole surface area of each model. However, models in the herringbone laying pattern have higher maximum von Mises stress, which means the herringbone pattern is more likely to suffer from corner damage failure.

• The univariate analysis of variance shows that all factors can significantly affect the von Mises stress of the loading area of interlocking concrete block pavement. The order of effect for these four factors is Elastic Modulus > Thickness > Laying Pattern > Ratio of Length and Width. The lower elastic modulus of blocks and thinner blocks could decrease the von Mises stress of the loading area.

• The herringbone laying pattern is recommended as the optimum laying pattern with minimum deflection under loading, and it also contributes to a better load spreading.

6.2 Recommendations for Future Work

Based on the findings of this research, the recommendations for future work are as follows:

• The blocks of ICBP can be manufactured in different shapes, such as rectangular, hexagon, unipaver, and dumble. The effect of block shape on the performance of ICBP should be studied in the future.

• A rectangular load was applied in this research to simulate traffic loads. However, the effect of loading positions should be evaluated because of the discontinuity of ICBP. Different moving loads with different moving directions should be simulated in future modelling analysis.

• New concrete mix designs with recycled materials were proposed in this research, and the compressive strength was evaluated in the laboratory. To improve the application of ICBP with recycled materials, the blocks should be industrially produced, and the mechanical properties and durability of these blocks should be evaluated.

• Filed study is necessary to understand the overall performance of ICBP. The testing road should be built under different traffic conditions, such as sidewalks, neighborhood roads, and city roads.

- Life cycle assessment should be applied to determine the sustainability of ICBP through the service life. The sustainability performance of ICBP should be compared to that of traditional asphalt pavement, which can bring a better understanding of the environmental benefits of ICBP.

BIBLIOGRAPHY

ABBO, Edward. 1985. “The Influence of Heavy Vehicle Dynamics on Rigid Pavement Response.”

Aïtcin, Pierre-Claude, and Robert J.Flatt. 2016. *Science and Technology of Concrete Admixtures*. Woodhead Publishing.

Al-bayati, Hanaa Khaleel Alwan. 2019. “Evaluation of Various Treatment Methods for Enhancing the Properties of Recycled Concrete Aggregate for Hot Mix Asphalt.” : 327.

Anike, Emmanuel E., Messaoud Saidani, Adegoke O. Olubanwo, and Mark Tyrer. 2020. “Extended Application of the Equivalent Mortar Volume Mix Design Method for Recycled Aggregate Concrete.” *World Congress on Civil, Structural, and Environmental Engineering* mix(October): 132-1-132–37.

Arjun Siva Rathan, R. T., and V. Sunitha. 2021. “Development of Deflection Prediction Model for Interlocking Concrete Block Pavements.” *Transportation Research Record: Journal of the Transportation Research Board*: 036119812110513.

Arjun Siva Rathan, R. T., V Sunitha, and V Anusudha. 2021. “Parametric Study to Investigate the Deflection and Stress Behaviour of Interlocking Concrete Block Pavement.” *Road Materials and Pavement Design*. https://doi.org/10.1080/14680629.2021.1963819.

Arjun Siva Rathan, R. T., Aravinda Sai V, and Sunitha V. 2021. “Mechanical and Structural Performance Evaluation of Pervious Interlocking Paver Blocks.” *Construction and Building Materials* 292: 123438. https://doi.org/10.1016/j.conbuildmat.2021.123438.

ASCE. 2016. *Structural Design of Interlocking Concrete Pavement for Municipal Streetes and Roadways*.

ASTM. 2001. 04 *ASTM C 936 Standard Specification for Solid Interlocking Concrete*

Paving Units.

———. 2002. 04 *ASTM C192 Standard Practice for Making and Curing Concrete Test Specimens in the Laboratory*.

Atoyebi, O. D. et al. 2020. “Effect of Curing Methods on the Strength of Interlocking Paving Blocks.” *Cogent Engineering* 7(1).

Baruah, Parinita, Sudip Basack, and Ghritartha Goswami. 2020. “Compressive Strength of Interlocking Concrete Pavement Block Influenced by Admixtures.” *International Journal of Mechanics* 14: 58–61.

CAC. 2016. *Enviromental Product Declaration (EPD) GENERAL USE (GU) AND PORTLAND-LIMESTONE (GUL) CEMENTS*.

CEMEX. 2022. “The Importance of Aggreagte Materials for Concrete.” : 2022.

del Coz Díaz, J. J., P. J. García Nieto, F. P. Álvarez Rabanal, and A. Lozano Martínez-Luengas. 2011. “Design and Shape Optimization of a New Type of Hollow Concrete Masonry Block Using the Finite Element Method.” *Engineering Structures* 33(1): 1–9. http://dx.doi.org/10.1016/j.engstruct.2010.09.012.

CSA. 2019a. Canadian standards association *CSA A23.1/A23.2 Concrete Materials and Methods of Concrete Construction/Test Methods and Standard Practices for Concrete*.

———. 2019b. *CSA A23.2-4C Air Content of Plastic Concrete by the Pressure Method*.

———. 2019c. *CSA A23.2-5C Slump of Concrete*.

CSA A231.1/A231.2. 2018. 14 *Precast Concrete Paving Slabs/Precast Concrete Pavers*.

Dahir, S. H.M., and W. G. Mullen. 1971. “Factors Influencing Aggregate Skid-Resistance Properties.” *Highw Res Rec* (37): 136–48.

Danish, Aamar, and Mohammad Ali Mosaberpanah. 2021. “A Review on Recycled Concrete Aggregates (RCA) Characteristics to Promote RCA Utilization in Developing Sustainable Recycled Aggregate Concrete (RAC).” *European Journal* *of Environmental and Civil Engineering* 0(0): 1–35. https://doi.org/10.1080/19648189.2021.1946721.

Dawson, Andrew. 2014. 204 Green Energy and Technology *Anticipating and Responding to Pavement Performance as Climate Changes*.

Domenichini, Lorenzo, Francesca L A Torre, D Ph, and Rita D Alessandro. 1998. "Experimental Concrete Block Pavement at Recoaro (Italy) 11 Years after' 2." (August 1997).

Ferreira, Luís, Jorge De Brito, and Nabajyoti Saikia. 2012. "Influence of Curing Conditions on the Mechanical Performance of Concrete Containing Recycled Plastic Aggregate." *Construction and Building Materials* 36: 196–204.

Furukawa, Aiko, Keiya Masuda, and Junji Kiyono. 2020. "Diagonal Compression Test of Mortar Interlocking Masonry Walls With Various Block Shapes and Different Support Conditions." *Frontiers in Built Environment* 6(September): 1–15.

G.P.Nikishkov. 2004. "Introduction to the Finite Element Method." *IEEE International Symposium on Electromagnetic Compatibility*.

Garilli, Erika, Federico Autelitano, and Felice Giuliani. 2017. "A Study for the Understanding of the Roman Pavement Design Criteria." *Journal of Cultural Heritage* 25: 87–93. http://dx.doi.org/10.1016/j.culher.2017.01.002.

Guan, Zhiguang, Jinxiang Feng, Qian Wu, and Peng Zhang. 2018. "Mechanical Analysis of Full-Scale Accelerated Pavement Loading Facility Based on Multi-Body Dynamics." *Systems Science and Control Engineering* 6(1): 528–36. https://doi.org/10.1080/21642583.2018.1547883.

Gunatilake, Dhanushika, and W. K. Mampearachchi. 2019. "Finite Element Modelling Approach to Determine Optimum Dimensions for Interlocking Concrete Blocks Used for Road Paving." *Road Materials and Pavement Design* 20(2): 280–96.

Hein, David K. 2016. "PAVEMENT DESIGN FOR LARGE ELEMENT PAVING SLABS." (July): 1–23.

Hengl, H. L. et al. 2018. "Horizontal Deformation Resistance of Paving Block Superstructures – Influence of Paving Block Type, Laying Pattern, and Joint Behaviour." *International Journal of Pavement Research and Technology* 11(8): 846–60. https://doi.org/10.1016/j.ijprt.2018.08.001.

ICPI. 2006. 159 Newsweek *Structural Design of Interlocking Concrete Pavement for Roads and Parking Lots*. http://www.redi-bw.de/db/ebsco.php/search.ebscohost.com/login.aspx%3Fdirect%3Dtrue%26db%3Dbuh%26AN%3D74208340%26site%3Dehost-live.

———. 2020a. "ICPI 2020."

———. 2020b. "Slip and Skid Resistance of Interlocking Concrete Pavements." (13): 1–8.

———. 2020c. "Structural Design of Interlocking Concrete Pavement for Roads and Parking Lots." (4).

IEA. 2021. *Cement*. Paris. https://www.iea.org/reports/cement.

IEEE Innovation at Work. 2020. "The Advantages of the Finite Element Method." *2020 Ieee*: 2021. https://innovationatwork.ieee.org/the-advantages-of-fem/.

Ioannides, Anastasios M., and George T. Korovesis. 1992. "Analysis and Design of Doweled Slab-on-Grade Pavement Systems." *Journal of Transportation Engineering* 118(6): 745–68.

Jafaraghaei, Usef. 2020. "2D and 3D Pavement Analysis Using the ABAQUS Program and Comparing the Results with the KENLAYER and MICHPAVE Programs همانرب زا هدافتسا اب يزاسور ی دعب هس و ی دعبود لیلحت ABAQUS همانرب اب جیاتن هسیاقم و MICHPAVE و KENLAYER ه یتعنص ناجریس ، ناجریس ، ناریا." (August).

Jamshidi, Ali et al. 2019. "State-of-the-Art of Interlocking Concrete Block Pavement Technology in Japan as a Post-Modern Pavement." *Construction and Building Materials* 200: 713–55. https://doi.org/10.1016/j.conbuildmat.2018.11.286.

Japan Interlocking Pavement Engineering Association. 2017. *Japan Interlocking Block Pavement Design and Construction Manual*. Tokyo.

Kasahara, A, and S. Matsuno. 1987. “Estimation of Apparent Elastic Modulus of Concrete Block Layer.” 2(Figure 1).

Khaki, Ali Mansour, and Ehsan Azadravesh. 2010. “Generating a 3D Model for Evaluating the Joint Opening Effects on Load Transfer Efficiency in Concrete Pavements , Using Abaqus.” (1): 1–7.

Kisku, N. et al. 2017. “A Critical Review and Assessment for Usage of Recycled Aggregate as Sustainable Construction Material.” *Construction and Building Materials* 131: 721–40. http://dx.doi.org/10.1016/j.conbuildmat.2016.11.029.

Klee, Howard. 2009. 157 Proceedings of the Institution of Civil Engineers: Engineering Sustainability *The Cement Sustainability Initiative*.

Knapton, J., and S. D. Barber. 1982. “Uk Research Into Concrete Block Pavement Design.” *Concrete Works International* 1(3): 107–11.

Kong, Deyu et al. 2010. “Effect and Mechanism of Surface-Coating Pozzalanics Materials around Aggregate on Properties and ITZ Microstructure of Recycled Aggregate Concrete.” *Construction and Building Materials* 24(5): 701–8. http://dx.doi.org/10.1016/j.conbuildmat.2009.10.038.

Kuusisto, Eric. 2017. “7 Key Concepts in Understanding Finite Element Analysis.” *Linkedin*: 1–10.

Lehne, Johanna, and Felix Preston. 2018. “Making Concrete Change Innovation in Low-Carbon Cement and Concrete The Royal Institute of International Affairs, Chatham House Report Series, Www.Chathamhouse.Org/Sites/Default/Files/Publications/Research/2018-06-13-makingconcrete- C.” : 138. www.chathamhouse.org.

Lin, Wuguang, Yoon Ho Cho, and In Tai Kim. 2016. “Development of Deflection Prediction Model for Concrete Block Pavement Considering the Block Shapes and

Construction Patterns." *Advances in Materials Science and Engineering* 2016.

Lin, Wuguang, Sungwoo Ryu, Han Hao, and Yoon Ho Cho. 2016. "Development of a Horizontal Shifting Mechanistic-Empirical Prediction Model for Concrete Block Pavement." *Construction and Building Materials* 118: 245–55. http://dx.doi.org/10.1016/j.conbuildmat.2016.04.124.

Ling, Tung Chai, Hasanan Md Nor, Mohd Rosli Hainin, and Abdul Aziz Chik. 2009. "Laboratory Performance of Crumb Rubber Concrete Block Pavement." *International Journal of Pavement Engineering* 10(5): 361–74.

Liu, Shen et al. 2019. "Compressive Performance of New Types of Load-Bearing Horizontal-Hole Interlocking Concrete Hollow Blocks." *Advances in Structural Engineering* 22(6): 1368–83.

Malahayati, N. et al. 2020. "The Effect of Water Cement Ratio (WCR) on Compressive Strength of Interlocking Bricks with Mix Design Variations." *IOP Conference Series: Materials Science and Engineering* 933(1): 3–9.

Mampearachchi, W. K., and W. P. H. Gunarathna. 2010. "Finite-Element Model Approach to Determine Support Conditions and Effective Layout for Concrete Block Paving." *Journal of Materials in Civil Engineering* 22(11): 1139–47.

Mampearachchi, W. K., and A. Senadeera. 2014. "Determination of the Most Effective Cement Concrete Block Laying Pattern and Shape for Road Pavement Based on Field Performance." *Journal of Materials in Civil Engineering* 26(2): 226–32.

Marović, Ivan, Ivica Androjić, Nikša Jajac, and Tomáš Hanák. 2018. "Urban Road Infrastructure Maintenance Planning with Application of Neural Networks." *Complexity* 2018.

Di Mascio, Paola, Laura Moretti, and Americo Capannolo. 2019. "Concrete Block Pavements in Urban and Local Roads: Analysis of Stress-Strain Condition and Proposal for a Catalogue." *Journal of Traffic and Transportation Engineering (English Edition)* 6(6): 557–66. https://doi.org/10.1016/j.jtte.2018.06.003.

Maske, Nikhil A, Anurag Anandkumar, and Abhiranjan Majumder. 2013. “Analysis of Rigid Pavement Stresses by Finite Element Method & Westergaard’s Method by Varying Sub-Grade Soil Properties.” *International Journal of Engineering Science Invention* 2(3): 1–4. https://www.ijesi.org/v2i3(version-1).html.

MasterFiber. 2021. *MasterFiber ® F 100 Enhanced Fibrillated Microsynthetic Fiber Description*.

Matar, Pierre, and Rouba El Dalati. 2011. “Strength of Masonry Blocks Made with Recycled Concrete Aggregates.” *Physics Procedia* 21: 180–86.

Mavin, K. C. 1984. “Site and Laboratory Testing of Interlocking Concrete Block Pavements.” : 55–60.

Ministry of Natural Resources. 2016. “Supply and Demand Study of Sggregate Resources.”

Miura, Yuji, Masayuki Takaura, and TOKIHIRO Tsuda. 1984. “Structural Design of Concrete Block Pavements by CBR Method and Its Evaluation.” *Ekp* 13(3): 576.

Moghadas Nejad, F, and M R Shadravan. 2010. “A Study on Behavior of Block Pavement Using 3D Finite Element Method.” *Computational Methods in Civil Engineering* 1(1): 65–71.

Mohajerani, Abbas, Jason Bakaric, and Tristan Jeffrey-Bailey. 2017. “The Urban Heat Island Effect, Its Causes, and Mitigation, with Reference to the Thermal Properties of Asphalt Concrete.” *Journal of Environmental Management* 197: 522–38. http://dx.doi.org/10.1016/j.jenvman.2017.03.095.

Mudiyono, Rachmat. 2006. “The Effect of Thickness and Laying Pattern of Paver on Concrete Block Pavement.”

Murugan, R. Bharathi, C. Natarajan, and Shen En Chen. 2016. “Material Development for a Sustainable Precast Concrete Block Pavement.” *Journal of Traffic and Transportation Engineering (English Edition)* 3(5): 483–91.

Nagakumar, M S, N Ajay, and Sharu Elishuba John. 2022. “An Analytical Approach to Analysis of Concrete Overlay (White Topping) Over Flexible Pavement (Hot Mix Asphalt) Using ANSYS Software.” In *Sustainability Trends and Challenges in Civil Engineering*, eds. Lakshman Nandagiri, M C Narasimhan, Shriram Marathe, and S V Dinesh. Singapore: Springer Singapore, 363–79.

Nejad, F.M. 2003. “Finite Element Analysis of Concrete Block Paving.” *Proceeding of the 7th International Conference on Concrete Block Paving* (October).

Nishikant, Koli, Aiwale Nachiket, Inamdar Avadhut, and Abhishek Sangar. 2016. “Manufacturing of Concrete Paving Block by Using Waste Glass Material.” 6(6): 61–77.

Nishizawa, Tatsuo, Saburo Matsuno, and Mitsura Komura. 1984. “Analysis of Interlocking Block Pavements By Finite Element Method.” : 80–85.

Noda, Esturo, Atshushi Kasahara, and Hiroshi Yaginuma. 2009. “Revised Manual for Interlocking Block Pavement Design and Construction (2007 Version).” *International Conference on Concrete Block Paving*: 1–11.

NRN. 2022. “National Road Network (NRN) - Canadian Open Data.” https://canadiangis.com/national-road-network-nrn-canadian-open-data.php.

Ontario Provincial Standard Specification. 2020. “OPSS.PROV 355 - Construction Specification for the Installation of Interlocking Concrete Pavers.” (November): 1–7.

Panda, Bikasha Chandra, and Ashok Kumar Ghosh. 2002. “Structural Behavior of Concrete Block Paving. II: Concrete Blocks.” *Journal of Transportation Engineering* 128(2): 123–29.

Permacon. 2015. *Technical Guide*.

Qiao, Yaning, Gerardo Flintsch, Andrew Dawson, and Tony Parry. 2013. “Examining Effects of Climatic Factors on Flexible Pavement Performance and Service Life.” *Transportation Research Record* i(2349): 100–107.

Rachmat, M., and T. N. Salsabilla. 2019. “Analysis of Hexagonal Paving Block as a Better Paving Shape.” *IOP Conference Series: Materials Science and Engineering* 527(1): 0–9.

Rada, By Gonzalo R et al. 1991. “STRUCTURAL DESIGN OF CONCRETE BLOCK PAVEMENTS.” 116(5): 615–35.

Raveendran Thulasibai, Arjun Siva Rathan et al. 2021. “Experimental and Numerical Evaluation of the Parameters Influencing the Shear-Stress Behavior of Interlocking Paver Blocks–Bedding Sand Interface Using Large-Scale Direct Shear Test.” *Journal of Materials in Civil Engineering* 33(6): 04021104.

RT, Arjun Siva Rathan, Sunitha V, Murshida P, and Anusudha V. 2020. “Influence of Bedding and Jointing Sand on the Shear Strength Characteristics of Interlocking Paver Blocks–Bedding Sand Interface.” *International Journal of Pavement Engineering* 0(0): 1–16. https://doi.org/10.1080/10298436.2020.1847286.

Sadiq, Noor, Miami M. Hilal, and Mohammed Y. Fattah. 2022. “Analysis of Asphalt Geogrid Reinforced Pavement Rutting by Finite Element Method.” *IOP Conference Series: Earth and Environmental Science* 961(1): 012049.

Šešlija, Miloš, Nebojša Radović, and Issa Togo. 2016. “A FEM Modeling of the Concrete Pavement Made of the Recycling Material.” *MATEC Web of Conferences* 73: 1–9.

Shackel, B. 1981. “Design of Interlocking Concrete Block Pavements for Road Traffic.” *Precast concrete* 12(7).

Shackel, B. 1988. “THE EVOLUTION AND APPLICATION OF MECHANISTIC DESIGN PROCEDURES FOR CONCRETE BLOCK PAVEMENTS B. Shackel University of New South Wales, Australia.”

Shackel, Brian. 1986. “A Review of Research into Concrete Segmental Pavers in Australia.” *1st Workshop on Interlocking Concrete Pavements Workshop on Interlocking Concrete Pavements* (1967): 11–18.

Shafabakhsh, Gholam Ali, Afshin Family, and Babak Pourzand Hossein Abad. 2014.

"Numerical Analysis of Concrete Block Pavements and Comparison of Its Settlement with Asphalt Concrete Pavements Using Finite Element Method." *Engineering Journal* 18(4): 39–51.

Skar, Asmus, and Peter Poulsen. 2015. "Modelling of Composite Concrete Block Pavement Systems Applying a Cohesive Zone Model." (September).

Tabatabaie, Amir M., and Ernest J. Barenberg. 1978. "Finite-Element Analysis of Jointed or Cracked Concrete Pavements." *Transportation Research Record* (671): 11–19.

Taheri, Vahid, Mansour Fakhri, and Parham Hayati. 2021. "Evaluation of Airfield Concrete Block Pavements Based on 3-D Modelling and Plate Loading Test." *Construction and Building Materials* 280: 122441. https://doi.org/10.1016/j.conbuildmat.2021.122441.

Tam, Vivian W.Y., X. F. Gao, and C. M. Tam. 2005. "Microstructural Analysis of Recycled Aggregate Concrete Produced from Two-Stage Mixing Approach." *Cement and Concrete Research* 35(6): 1195–1203.

Tee, Kong Fah, Ifenna F. Agba, and Abdul Aziz Abdul Samad. 2019. "Experimental and Numerical Study of Green Concrete." *International Journal of Forensic Engineering* 4(3): 238.

UNILOCK. 2019. "Design Considerations for Interlocking Concrete Pavements." : 1–31.

Weibull.com. 2012. "Taguchi Orthogonal Array Designs." (131): 1–7.

Whitehouse, Jordan. 2021. "The History of Pavers - Looking Back on the Evolution of Hardscaping in Canada." 2021(May). https://landscapeontario.com/the-history-of-pavers.

Wikipedia. 2022. "ABAQUS." *https://en.wikipedia.org/wiki/Abaqus*. https://doi.org/10.1101/2022.01.23.477440.

World Economic Forum. 2018. *The Global Risks Report 2018 - 13th Edition, Geneva, Switserland*. http://wef.ch/risks2018.

Xiao, Jianzhuang. 2018. “Recycled Aggregate Concrete Structures.” In *Recycled Aggregate Concrete Structures*, Shanghai: Springer Tracts in Civil Engineering, E1–E1. http://link.springer.com/10.1007/978-3-662-53987-3_16.